POLITEHNICA University of Bucharest
Doctoral School of Materials Science and Engineering
DEPARTMENT OF METALLIC MATERIALS PROCESSING AND METALLURGY

PHD THESIS

SUMMARY

Research on the Inoculation capacity of Lanthanum in Grey Cast Iron

---

Cercetări privind capacitatea inoculantă a Lantanului în Fontele Cenușii

Author: Drd.ing. Eduard-Marius ȘTEFAN

Scientific coordinator: Prof.dr.ing. Iulian RIPOȘAN

DOCTORAL COMMITTEE

President	Prof. dr.ing. STAN Constantin Stelian	from	University *Politehnica* of Bucharest
Scientific coordinator	Prof. dr.ing. RIPOȘAN Iulian	from	University *Politehnica* of Bucharest
Scientific reviewer	Prof. dr.ing. CHIȘAMERA Mihai	from	University *Politehnica* of Bucharest
Scientific reviewer	Prof. dr.ing. CRIȘAN Aurel	from	University *Transilvania* of Brașov
Scientific reviewer	Conf.dr.ing. KISS Imre	from	University *Politehnica* of Timișioara

BUCUREȘTI
2022

SUMMARY

INTRODUCTION

The cast iron being considered to be a natural composite metal material [14], is characterized by a high sensitivity to the conditions of production by casting (elaboration of the heat, processing and casting it), which makes very difficult the process of control of the formation of the structure, directly by casting, as well as obtaining the properties required for the cast parts. In order to know and conduct the phenomena that take place in the inoculation treatment of the castings - the procedure by which the structure and properties of the cast are improved, by introducing in the basic cast iron elements that have the role of directing the process of solidifying the cast parts - were made, in the Department of Metallic Materials and Ecometallurgy, a series of research together with Elkem, an important manufacturer [20] solutions for the production of advanced materials. Starting from that studies, the present work – through its structure and through te research programs carried out – had the objective to obtain new information regarding the effect of use of La (in classic inoculant systems, as well as in new ones, experimentally created), as an active element - added in classical inoculant systems – for treatment of experimental castings as well as the more in-depth understanding of the mechanism of nucleation of graphite in grey irons with lamellar graphite.

Keywords: grey iron with lamellar graphite, inoculation, in-mould inoculation, in ladle inoculation, La, inoculant systems, thermal analysis, chill tendency, hardness, SEM analysis, cooling module, carbides, graphite, nucleation

CHAPTER I. The study of data from literature

1.1. The place and role of inoculation in the production of grey cast irons

1.1.1. Concise history of the casting and gray cast irons

In the begining, the existence of parts of ferrous materials has been based on the discovery of the technological possibility of obtaining products through the casting procedure. From a historical point of view the oldest object produced by casting, known today, dates from approximately from 3200 BC, being a copper poured frog. [22] A major disadvantage of this procedure would be as – due to the properties of the material used and the conditions of casting and solidification – there is the possibility of not obtaining the desired properties directly from casting.[23,24]

1.1.2. The position of gray cast iron production in terms of its place in economics

- ***1.1.2.1.*** *World production of castings*

From an economic point of view the importance of cast iron products can be appreciated, knowing that: a) in 2015 the world production of cast iron (as a raw material, including pig iron and the recycled irons) was 1180 million tonne, from which China produced 710 million tonne (~ 60% of the total); and b) respectively b) in 2017, due to the reduced price and its abundance, there was (on average) in the world, in use, an amount of 2200 kg of cast iron "per capita", and in developed countries it reaches ~ 7000 ÷ 14000 kg "per capita".[28] At the same time, the amount of gross cast iron

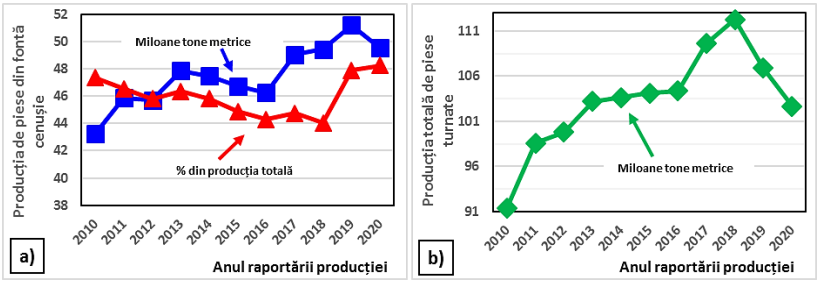

Fig. 1.2 The evolution of the reported production of the cast iron with lamellar graphite castings ***a***) in the context of the global production of castings ***b***).

and gross steel, produced in 2019 was ~ 3x109 metric tonne [29] (obtained from over ~ 2.5x109 metric tons [30] of iron ore + over 5x108 metric tonne of ferrous scrap).

Taking into account the quantity of cast parts produced worldwide and comparing it to castings produced from various types of material, the situation – published in december 2021, which refers to the production of 2020 – shows that the first place is taken by grey cast iron castings with almost 49% of the total production, followed by ductile iron castings (23.25%).[31]

From *Fig. 1.2. a,b* it is observed that the positive trend of the world production of parts made by casting - from the last 10 years - is also supported by the high level of production of grey cast iron. This aspect is underlined mainly in the last 3 years (2018-2020) – a period when the world production of castings has decreased – when the production of gray cast iron, compared to the global amount of cast products, has increased.

1.1.2.2. *Production of cast parts in Romania*

In Romanian's foundries, according to 2020 WFO Global Foundry Report[32] (for 2019), there were 80 active foundries, which produced parts of various sizes. According to statistical data[31], the structural changes in the production of metal materials consist of: a) a dominant position of the parts produced from non-ferrous materials (70.3% aluminum) while b) the production of iron alloys decreases at values ~ 23.5%, of which 17.6% gray cast iron, 4.1% steel and 1.75% cast iron with graphite nodular.

1.1.3. Current problems in the field of cast iron industry and possible solutions

D.M. Ştefănescu dedicates a large work to this situation [33], problematic for the cast iron industry, in which he summarized the possible causes that generate the present state.

1.1.3.1. *Problematica deplasării spre utilizarea altor materiale pentru fabricarea pieselor*

Due to the development of the new advanced fields of use of materials - electronics, computers, optics, space vehicles, etc - and of the investments made in their research, which resulted in technological discoveries and a special technological leap, other materials emerged in the field of activity of the parts produced traditionally from ferrous materials by metallurgical methods. There is even a phenomenon of mutation of the production of parts, from the family of ferrous (cast irons) in that of the non -ferrous. The problems arise when decision, to adopt one solution or another, is not based on sufficiently analyzed and well understood conclusions but on obtaining various advantages. That is why it is necessary to carry out a profound research and good knowledge of the materials but also to make a detailed comparison, of the various existing materials. [34]

1.1.3.2. *The specificity and consequences of generalizing the way of melting the charge materials in CIF*

A. <u>CIF advantages</u>

The new generation of acid-lined medium-frequency coreless induction furnaces (CIF) revolutionized the iron foundries, by: a) high melting speed, so high production rate at lower furnace capacity; b) no heel required (100% solid charge); c) larger furnace availability; d) reasonable stirring ability (high steel scrap charge + carbon raiser—lower cost); e) higher iron quality for larger scale production.[46,48,49]

B. <u>Effects on the chemical composition of the melt</u>

The competitive performance of these melting furnaces leads to increasing production tonnage of grey (lamellar graphite) iron at low sulphur (< 0.03%S) and residual aluminium (< 0.003%Al) levels at higher overheating ([1500ºC), characterized by higher eutectic undercooling solidification and consequently high chill (carbides) and unfavourable undercooled graphite morphologies sensitiveness.[47]

1.1.3.3. *Limits of scientific knowledge & technology in the foundry industry*

The cast iron, probably the most complex alloy, includes in its chemical composition many elements (over 30), even more than super alloys (15 elements). The effects of many of these elements on the properties

and microsctructure of the castings are known, but others remain undiscovered, and it is necessary to be studied. [33,49] In the foundry industry there are difficulties that have origin in various sources: a) the high complexity of the production process that leads to a high final price of some raw materials, b) the negative effect of the casting technology on the environment, and the environmental regulations introduced by the environmental control institutions for reducing this effect, c) the multitude of areas in which these raw materials, already of strategic level, are used, d) the correlation between request and offer (which determines the emergence of competition in order to obtain them) but also e) the economic game of the great financial powers.[33]

1.1.3.4. Use of La (RE) in producing parts from ferrous alloys (cast iron and steel)

In metallurgy, the introduction of use at (RE) occurred late, by the scientific advance in the field of introducing different elements in order to improve the quality of the poured ferrous parts, undivulged knowledge by the foundry industry until the beginning of the XX century BC.[55] According to Kanetkar et. al, and other researchers, the use of RE has evolved most in the range of production of parts casted from steel and cast iron with nodular graphite[64,65]. The occurrence, in China, of a monography on the use of RE in cast irons indicates the sustained efforts made in the direction of fruitfully maximising (words of chinese President Xiaoping being famous: "While the Middle East Has Oil, China Dominates Rare Earths" [66]) of huge deposits of RE which it holds.[67] Regarding the grey cast iron with lamellar Graphite, the studies on the use of RE in the treatment of lamellar grey cast irons in the liquid state are more recent, those efforts are sustained by the foundry academic group within the SIM-UPB Faculty, starting in 1998, through collaborations - with the Norwegian producer, recognized at a global level, Elkem - within numerous research projects materialized by unpublished and published works. [68-75]

1.1.3.5. The issue of obtaining and using RE (La)

The special properties of RE have made them usable in a large number of industry branches [77], this influencing the evolution of RE production in unexpected ways, for cast iron foundries. The increasing of demand, combined with global political developments, produced a major deficit of RE on the global market so that prices have undergone significant increases. At the same time, the regulations introduced by the environmental legislation in the economically advanced countries have determined them to outsource the production of RE in regions with more relaxed regulations. For the next period the situation of RE resources, it is announced to be even harder, due to the fact that prices have increased [84] and most of the supplies companies [85], report the existence of low stocks (between 5-14.25%) of raw materials.

1.1.4. Typologies, characteristic properties and ways of obtaining gray iron castings

1.1.4.1. Typologies of gray cast iron

The most used criterion, for the classification of castings, is that of the chemical composition, namely the presence of carbon in the structure. [23] The second classification criterion is represented by type of morphology adopted by graphite, in the free state, during the solidification process - form that can be lamellar, compact/vermicular or nodular -, from this point of view, the gray cast irons being generally classified according to the type of graphite formed (cast iron with lamellar graphite, compact/vermicular and nodular respectively).[86]

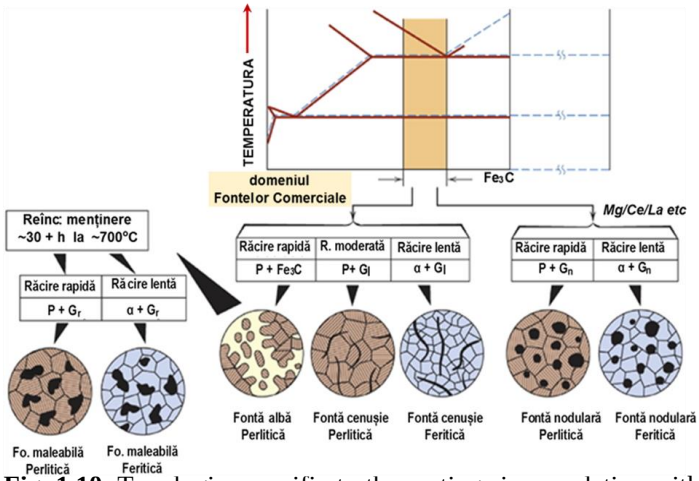

Fig. 1.10. Typologies specific to the castings in correlation with the main characteristics of their classification: chemical composition, cooling speeds and microstructures formed. [87]

In *Fig. 1.10* [87] are represented the general types of cast irons and the relationships between composition, structure and influence exerted by temperature, through cooling speeds and thermal treatments.

1.1.4.2. Characteristics specific to gray cast irons

Based on the metallurgical scientific experience and statistical studies but also on the analysis of the specialized literature can be presented *typical values* of the characteristics of the various types of metals, and these metals can be (on this basis) grouped according to the metallurgical and physical similarities. In general, however - according to Total Media™ [90] and the AFS Association [91] - these *typical values* are estimative and can be used in carrying out calculations that offer approximate results, and not exact, categorical values. At the same time, the determined properties obtained are specific, they can only characterize materials that are analyzed under the same conditions, on the same types of samples or (if other types of samples are used) on samples for which they have been compatible. In addition, it will be taken into account that a high value of a property, for a certain type of cast iron (used under certain conditions), does not involve a higher quality compared to another type of cast iron (used under other conditions).[93]

A. From the point of view of the chemical composition

Regarding the influence of the chemical composition on the solidification process, the most important influence over structure is exerted by the amount of C in the liquid cast iron, but the structure of the cast iron can be major changed and by the accompanying elements. The effect of the elements in the composition of the cast iron is dependent on their power and orientation (in a positive or negative direction, from the point of view of the analyzed characteristic), which are specific to each element. Thus the position of the cast iron on the solidification diagram - signaled by the equivalent carbon - in relation to the eutectic point, is influenced.[86]

B. From the point of view of the morphology of graphite and metal matrix

Another type of influence on the properties of the castings (tensile strength, for example), is exerted by the different morphologies of graphite formed in cast iron and by the constitutional composition of the metal matrix under the influence of the chemical composition and by the speed at which the solidification process is performed, respectively.

C. From the point of view of carbides formation processes

From the point of view of avoiding the process of carbides formation, in the critical sections of the cast parts - provided that the cast iron falls into the desired standards and it is desired to obtain certain tensile strength - it is necessary that the value of the ratio between the maximum whitening width (determined before the inoculation) and the maximum width of the bleaching (determined after inoculation) to fall into a certain area of values. [86]

D. From the point of view of the determined properties and of the type of analyzed sample

Traditionally the property used to characterize the castings was the tensile strength[95], but later various other properties were added to facilitate a faster classification in a certain mark and even to distinguish and describe more precisely the properties of the parts delivered. to the beneficiary [86]. Regarding the gray cast iron one of the most important and representative property, compared to other materials, is the capacity to attenuate vibrations, for which it holds the best capacity [96], this is why they are recommend for use in the production of machine frames, plates for sustaining of foundations and other components that require this type of property.

1.1.4.3. Mode of producing gray cast iron castings

The cast iron can be considered as one of the materials with the highest susceptibility to the action of the phenomena that take place during its elaboration, casting and solidification. These are the reasons that make it indispensable to know and acquire the control capacity over the technological factors that influence a certain structure, which produces the final properties of gray iron castings. [23]

A. Technological elements that changes the structure and properties of castings

a. The effects of chemical composition on cast iron castings

The cast iron castings from foundry industry have in the chemical composition a large number of elements [33,49] which are classified in several important groups: 1) elements that are part of the

basic chemical composition (C, and, Mn, P and S); 2) gases, (O, N, H); 3) the accompanying elements (Cr, Ti, Al, Pb, Bi, Sn, As, etc.) and 4) the alloying elements (Ni, Cr, Cu, Al, Mo, etc.).

The result of the action exerted by these elements on the cast iron, manifests on the carbon in the cast iron in the solidification process, so that it will be forced to solidify in free (graphite) or linked (cementite) form, in this respect the elements being graphitizing or anti -graphitizing. [98, 99]

b. The effects produced by the intervention over the thermal regime at solidification. Cooling rates

The thermal regime at the solidification proccess of the melting is mainly determined by the speed of heat transmission (in both directions: loss or accumulation in melted iron), which is being dependent on a complex of factors, which refers to both the construction of the piece (wall thickness, geometric configuration , etc.), to the form in which the casting takes place (regarding the thermophysical properties of the mould), as well as to the characteristics and parameters of the casting technology.[102]

b.1. Configuration of castings

The construction (configuration) of the cast parts largely influences the cooling speed, through a complex of factors, the cooling conditions (taking into account the fact that obtained castings have a complex configuration, with variable wall thicknesses and different geometries) being more rigorously expressed through cooling module (Z) or the equivalent thickness (Re), defined by the ratio between the volume of the piece (V) and its surface (F) [102]:

$$Z = R_e = V/F \quad (1.1)$$

-where: R_e – conventional (equivalent) thickness, [cm]; F – the total cooling surface of the part, [cm^2]; and V – the volume of casted part, [cm^3].

b.2. Thermophysical characteristics of the mould

The thermophysical characteristics of the mould, influence to a high extent the capacity to transmit the heat during the process of solidifying the cast iron, through: the thermal conductivity (λ), the thermal diffusivity (a) and the specific heat (c_p). Commonly is used the heat accumulation coefficient (b_f) expressed by relation[102]:

$$b_f = \sqrt{\lambda \times c_p \times d}, \ [J/m^2 h^{0,5} K] \quad (1.4)$$

- where: λ – thermal conductivity of the mould, in W/mK; c_p – specific heat, in J/kgK; d – relative density, in kg/m^3.

b.3. The influence of the temperature of the melt and of the speed of pouring

Highlighting the influence of the casting temperature on the cooling speed is difficult - taking into account the fact that in the solidification process of cast iron also intervenes the effect of melt overheating (previously applied), which is more complicated - so that the data from the literature is contradictory in this regard.[102] Maintaining the cast iron in the liquid state, until casting, has an influence but this is limited and, therefore, in this way the results obtained are less influenced. The increase of the casting temperature has the effect of reducing the cooling speed.

B. Possibilities of production of iron castings

Taking into account the aspects mentioned related to the influences of the technological factors on iron castings, the modes of obtaining the iron castings were (and continues to be) varied, each foundry, according to the local conditions, trying to adopt proper technology.

a. Directly by casting (chemical composition and technological process verified as effective)

In the past (~ 1920 AD) there was the practice in which, immediately after melting, at the exit of the molten cast iron the desired pieces was poured, but it was not a general practice used due to the difficulty and insecurity in obtaining the desired type of cast iron, as well of incertainty in resulting the fluidity required to obtain an iron casting free from defects.[103] The most used procedure became that of remelting the pig iron and the use of synthetic cast iron.[104] But only by this method, parts with advanced performance features cannot be obtained.

b. Technological procedures for obtaining specific properties

In view of the aspects mentioned at pct. a, have been sought, and discovered over time, practices that allow to achieve some performance improvements. Additional operations have been applied knowing that the properties of castings can be modified through: cooling speeds; thermal treatments performed after pouring the parts; or through the intervention - on the liquid cast iron - with various active chemical

elements, introduced in small quantities in melted cast iron. Recently, studies have begun to be carried out in order to obtain cast iron parts from semi-solid state (under pressure and at low temperatures).[105]

b.1. Increased/reduced cooling rates during cooling process

The use of moulds made from materials with thermal coefficients that ensure the obtaining of the desired properties, as well as of elements that, placed in various critical points (chillers), produce controled changes in the solidification parameters..[107-109]

b.2. Thermal treatments subsequent to the solidification of castings

Because sometimes, after casting, the cast iron parts do not meet the requirements (mechanical, technological properties, etc.) for operation and those regarding the processability, the castings can be subjected to thermal treatment operations. These can be of several types: normalizations, quenching, annealing, thermochemical treatments, etc..[102]

b.3. Processing of cast iron in the liquid state

Some of the most convenient procedures in order to treat the cast iron in the liquid state are: a) of thermal nature (overheating and maintaining it in the elaboration aggregate); b) of a mechanical nature (by vibrating the cast iron, the treatment with ultrasound or by bubbling) or c) of nature to modify the processes that take place by acting through the chemical composition by: vidification of the liquid cast iron; or by the addition in the melt - in various quantities and modalities - of active elements that have the ability to make major transformations in the way of achieving an sounding solidification process (method called modification or inoculation).[23,46,102]

C. Technological process of obtaining cast iron parts

The gray cast iron parts can be produced by a variety of technologies, but, generally, the essential technological process in order to obtain them includes: the melting of the charging; obtaining of the desired composition (the content in C, Si, Mn, etc); the treatment of the melt - the flows (for refining the melting) or modification (nodulisation and/or graphitisation); realization of the pattern, of the mould and of the feeder and, finally, the casting process.[110,111]

1.2. Liquid state processing: Inoculation

All the operations that participate in obtaining the castings are important, but, without knowing and conforming to the way of behaving of the melt during the solidification process, the desired characteristics of the material, from the quality point of view, cannot be obtained. Once known, by the foundrymen's, the processes that take place during the solidification these can be used so as to (with the help of acquired knowledges - of which those related with the modification of the cast iron play a very important role today in the foundry's) perform the technological process in order to obtain the desired quality for cast iron castings.

1.2.1. Thermodynamic elements of the solidification processes of cast irons

The equilibrium state is reached if the Gibbs free energy is minimal. Although in the real systems, in fact, there are no equilibrium conditions, however - by using the presumption of the presence of a local thermodynamic balance - this presuppostion allow to determine the liquid and solid composition of the metal alloys using the phase balance diagrams. [27]

The undercooling

The generator of any phase transformation that includes solidification - reverse process of melting, transformation from liquid into a solid state - is the variation of free energy. The free energy of any phase is a function, which is dependent on pressure, temperature and composition. The steady state is reached when Gibbs' free energy is (becomes) minimal, which makes as a condition for achieving balance (for a multiphase system) to be that the chemical potential of each component to be the same in all phases. At this temperature, there can be no more transformations (the melting for the process of accumulation of heat or the solidification for the process of cooling; when the heat is transferred), this being the balance temperature. Thermodynamics cannot contribute to obtaining additional clarifications in relation to the nature of the undercooling process. However, it is very important that thermodynamics has the power to reveal the connection that exists between the solidification process and the conditioning of the existence of this process by occurence of the undercooling process.[27]

1.2.1.1. *The thermodynamics of compounds formation based on standard state of components*

From the data present in the analyzed literature[46,72,114,115] it turns out that diametrically opposite positions of metals are found - if we refer to the standard enthalpia (ΔH^o298) or to the free energy (ΔG^o1723) of the formation of the compound at high temperatures - the values ΔG^o_{1723} being low for all the 4 types of compounds (oxides, sulphides, nitrides and carbides).

The classification of the elements according to the standard enthalpy (ΔH^o298) for the formation of oxides, sulfur and nitrides denotes a position of La in the optimal area of the group, with La in forehead, as one of the most reactive elements. And in the case of arranging that have as reference the free energy (ΔG^o1723), lanthanum it is positioned in the first places, in terms of the affinity of the formation of sulphures and nitrides [72,114]. Regarding the potential for the formation of oxides, Lanthanum is positioned at the forefront of the elements of compounds forming, also, compared to the potential for carbide formation is at an average level of formation of these types of compounds.At an overall look both the standard enthalpy and the free energy needed for compounds formation, they decrease from oxides to sulphures, then to nitrides and lastly to carbides.[114]

1.2.1.2. *The effect of temperature on the thermodynamic capacity of compounds formation*

The real measure of the affinity of the metallic elements for non-metals (as O, S, N, C), is rendered by the value with which the thermodynamic capacity of a system is reduced when transfering from a (reference) state to another state (an equilibrium state). A higher value of ΔG^o (more negative value), makes the affinity of a metal for a non-metal (O, S, N, C) to increase, proportional. It was observed [67,116] that, at an increase in temperature, arised an increase of $\delta g^o t$ and of the capacity of carbide formation (CO and CS).

1.2.1.3. *The dissolved components and thermodynamics of the formation of their compounds from liquid state*

After the analysis [72,114,117] of Free energy values (ΔG^o_{1723}) capable of forming and developing compounds from components (free or dissolved in the melt), the following can be said: a) for compounds formed from components dissolved in the liquid, free energy of formation is considerably more reduced, comparatively with free energy of formation necessary for obtaining compounds from free components, probably due to the energy needed to dissolve the components in the liquid, thus, their stability (for pure compounds) in the solution is lower; b) for the formation of the compounds based on the components dispersed in the melt, the order of the active elements - according to the free energy (ΔG^o1723) - is, with few deviations, in the analogous tendency with that of the compounds formation on the basis of the free components present in the liquid under standard conditions; c) the limits of the temperatures at which the formation of compounds can occurre are narrower for the formation of oxides and carbides, compared to those of sulphures and nitrides; d) according to the current data for free energy of formation of sulphures and carbides from the dissolved elements, can be estimated a tendency to reduce the free energy in the order : oxides → sulphures → nitrides → carbides.

1.2.1.4. *Complex compounds and the thermodynamics of their formation*

The ability to form complex compounds in melted cast iron is important, in particular, in terms of high compatibility of their crystallographic structure - most of them falling into the hexagonal crystallographic system - with that of the structure of the graphite crystallographic lattice (hexagonal). [114] The proportion of complex compounds that can be formed is dependent of numerous factors [72]: a) on the removal of oxygen from the liquid, during its processing; b) of the reaction force of the component elements in relation to oxygen; c) of the basic chemical composition of the elaborated, processed and casted alloy; d) of the type of refractory materials used to build the aggregate; e) of the particularities of the pouring ladles and of the moulds; f) of the processing and solidification time of the alloy, etc.

Regarding the germination of the graphite, a special interest can be granted to the complex compounds - particularly silicates - formed on the surface of the primary micro-inclusions (oxides,

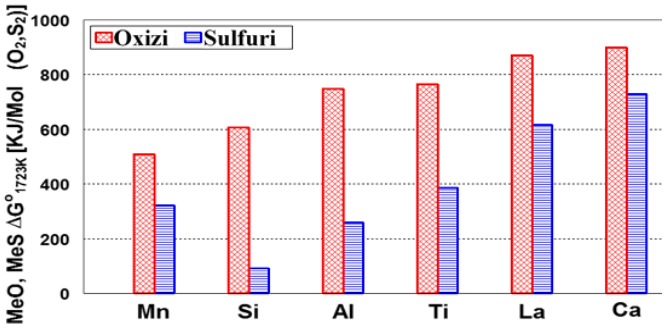

Fig. 1.33 Gibbs free energy (ΔG°1723) and the ability to form the oxides and sulfides (Mn, Si, Al, Ti, Ca) [75]

sulphides) in the form of very small layers, which facilitate the precipitation of the graphite during solidification.[114] In *Fig. 1.33.* [75], an arrangement of the elements used in the foundries for the treatment of cast irons is presented, which reveal the very high capacities of the elements as Ca, La, Ti, Al - compared to those of Mn and Si - to form oxides and sulphides, which recommends them for their use (in the process of treating and casting of the cast iron) for the purpose of controlling the formation of the compounds that can be use as support for nucleation of graphite.

1.2.1.5. The formation of graphite and other constituents of gray cast iron

The final structure of the castings, obtained at solidification, is a result of a process of creating stable nuclei of solid inclusions in the liquid (by nucleation) followed by a process of their growth. By nucleation and growing of the inclusions is determined the morphology and degree of finishing of the microstructure of the cast piece, besides the phases it contains.

A. Nucleation

The types of nuclei that are formed in the melt, in the process of its solidification, have been classified so that the inclusions formed are considered to be the result of homogeneous germination and/or heterogeneous germination.

a. Homogeneous nucleation

When the equilibrium temperature of transformations is exceeded, significant fluctuations in density, atomic configurations or heat content, etc., occur in the liquid. These make possible the formation of tiny particles of crystalline solid (with long-distance order) called embryos.[27]

b. Heterogeneous germination

Solidification may also be induced by pre-existing corpuscles of some crystals or by oxide films, mould walls or even by small quantities of chemical elements added for this purpose. This type of nucleation, in which the growth of the crystal is carried out on the supports "foreign" of the molten alloy, is called heterogeneous germination. The mechanisms specific to homogeneous germination are different from heterogeneous ones.[123] Heterogeneous germination is strongly dependent on the interface energy of the solidified nuclei (solidified metal). The value of this energy depends on the crystalline structure of the two phases.

c. Conditions for graphite nucleation

According to heterogeneous nucleation theories in the field of solidification, the inclusions must meet specific conditions in order to act as supports for nucleation, such as:

- the substrate must be: (a) solid, into the melt, (b) its melting point has to be greater than that of the melt, and (c) it must not dissolve in the melt;
- between the nucleation support and the metal melt must: a) there should be a low contact angle or/and b) there should be a high surface energy between the liquid and the support (to meet the energy requirements at the included interface-support/graphite;
- the nucleation substrate must have a large surface area of contact with the melt;
- there should be a high similarity between the crystalline network of the substrate and the crystalline grid of the solid phase (resulted after solidification of the atoms attached to the substrate);
- inclusion-support should have the ability to carry out nucleation at as low as possible undercooling.

B. The process of growing of non-metallic inclusions

Once the distribution of deoxidants no longer allows the saturation growth required for the nucleation process, the process of germination of the oxidative phases in the melt ceases. Subsequently, the mechanism of the process of precipitation of deoxidation products is taken over by the nuclei already formed, which will develop further.[121]

1.2.2. Inoculation of cast irons

Inoculation – currently, considered a usual method – is used for melt treatment in all commercial cast irons (gray, compact and nodular), while the compacting modification is essential for the production of cast iron with compacted/vermicular graphite (intermediate level of compactness) and nodular graphite cast iron (maximum compactness). Inoculation is the process of directing the structure and characteristics of the cast alloys by reducing the degree of undercooling and increasing the number of inclusions (intended to be supports of nucleation) to achieve an controlled graphitization process, during solidification of the melt. The inoculant is the material (or alloy) added to the melt in order to activate the process of achieving the desired phase to be obtained, by triggering and controlling of the nucleation of graphite during the solidification of the melt.[130,131]

- ***1.2.2.1.*** *Grey cast irons and inoculation*

The effects of inoculating treatment are manifested on[23,46,102,130]: 1) *graphite*, resulting in a change in: a) the number of nucleation centers; b) the shape of graphite; c) the distribution of graphite; d) the size of graphite particles; 2). (avoidance of the occurence) of *defects*: a) gas bubbles (hydrogen, nitrogen); b) abnormal graphite lamelles; c) microshrinkage formation; d) intercellular carbide formation; e) steadite formation; f) undercooling graphite formation; g) C-type graphite formation. In addition, inoculation can also be carried out, within various limits, for the control of: a) the formation of austenite; b) the formation of eutectic cells and c) the formation of metal matrix.

For specific conditions in the case of different types of moulds used in foundries, ***the structural characteristics of melted iron*** are essential and they force the cast iron to partake a certain type of solidification model. The state of the charge evolves, immediately after its melting, from a state ***1***) of colloidal liquid, ***2***) through a quasi-homogeneous solution, and up to ***3***) that of a quasi-ideal solution.[133] In the process of inoculation, the evolution of the metal charge is taken into account, toghether with changes of the temperature of the metal bath, during the preparation of the melt in general (from the evacuation out of the elaboration aggregate up to the solidification).[46]

A. Theoretical models of graphite formation

With regard to the mechanism of graphite formation, it consists of two stages: 1) the creation of core nuclei, 2) the precipitation of graphite on nuclei (new or existing in liquid).[46,72]

The compound MnS manifests itself as an inclusion with average nucleation capacity of graphite, but there is a possibility that other types of sulphides have a greater potential than MnS to nucleate graphite. Silicates of inoculation elements added [used in industry] (Ca, Sr, Ba) also have a good ability to act as nuclei for graphite. It has also been found that elements like Ca, Ce, La, Pr, Nd, Sr can be present in MnS nuclei and can form complex sulphides (Mn, X)S, the latter achieving a better match with the graphite lattice and becoming the most efficient sources of nuclei (from all types of supports created to cause heterogeneous germination).[130] According to these hypotheses, research has been carried out on the gray cast irons after which a three-stage model of graphite nucleation was proposed.[136] The stages of this model are shown in *Figure 1.41.*[130]: (1) small (0.1-3µm, usually less than 2.0 µm) oxidative-based areas are formed in the melt; (2) complex compounds nucleated on these microinclusions (~1-10µm, usually below 5.0 µm) of type (Mn,X)S, where X = Fe, Si, Al, Zr, Ti, Ca, Sr, P; (3) and (due to the smaller crystallographic difference between them and graphite) graphite germinates on the facets of compounds (Mn,X)S. [120,127,136-140]

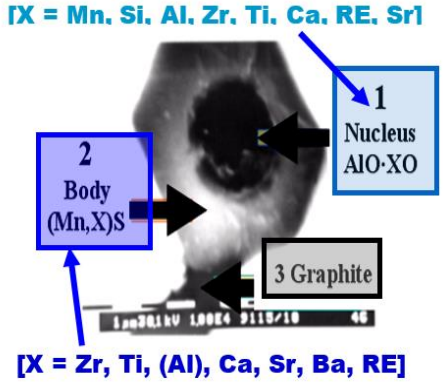

Fig. 1.41. Compounds (Mn,X)S typical involved in nucleation of various castings inoculated: three-stage nucleations model [130]

1.3. Conclusions. The objective of the thesis. Research directions and proposed experimental programs

Despite competition from newer materials, gray cast iron is still used in those areas where its properties have designated it as the most suitable material. This is because gray cast iron possesses a number of specific characteristics, and at the same time has the lowest production price of ferrous materials, and can be produced in almost any foundry.[179] This paper aims to explore the possibilities that rare earth (RE) additions can provide to the inoculating alloy systems, aiming to determine their potential to produce improved results in the field of processing of cast iron with lamellar graphite. Taking into account previous experiences acquired during the production of nodular graphite castings – through the procedure of modifying the liquid cast iron with RE-based modifiers – that cause technological reconsiderations (positive after all) in this field[180,181] it is proposed to carry out research in order to test the possibility of making such positive reconsiderations also in the field of cast iron with lamellar graphite castings. The domain of cast irons still is holding many mysteries that have not yet been discovered, the only obstacle to their revelation – according to Prof. Doru M. Stefanescu[33] – being only the true will, seriousness and involvement in carrying out these researches.

In order to achieve the proposed objectives, a complex experimental program – comprising three experimental programs – was developed, presented systematized in Chapter III.

CHAPTER II: Methods, equipment and experimental conditions of research

Taking into account the conclusions resulting from the analysis of the current state of research in the field – in order to achieve the intended purpose – a series of specific techniques, devices, tools, procedures and analyzes were used that define both the research method and the conditions and character of the experimental programs.

2.1. Processing the cast iron in the liquid state

In terms of the requirements imposed in the working-out of the cast iron, the most important aspects that were considered were: the type and quality of charge materials casted.

2.1.1. Aggregates, charging materials and smelting of the metal charge

2.1.1.1. *Aggregates used for smelting the charge*

In order to carry out the experiments, the INDUCTRO type medium frequency coreless induction furnace (C.I.F – 380V supply at 50Hz) was used with acid lining and with capacity of 80 kg, at working frequency 2400 Hz and average power frequency 100 kW. Also, is used the electric oven with medium frequency induction (380 V, supply at 50Hz) with crucible, working frequency 8 kHz and maximum power 28kW, and with a graphite crucible with capacity of 10kg is used.

2.1.1.2. *Charge materials and smelting of the metal charge*

Depending on the experimental program, cast iron waste from the Câmpina foundry (for Program I) and waste from previous experiments (for Program III) were used as charge, which were re-melted in a furnace (C.I.F.), with a capacity of 10 kg, as well as synthetic cast iron (for Program II) which was introduced into the 80kg acid-lined induction electric furnace in order to be remelted and to obtain the experimental cast iron.

2.1.2. Preparation of the melt in order to carry out the treatment with inoculant alloys

2.1.3.2. *Control of the thermal regime of the elaboration*

A. <u>The thermal regime of the elaboration</u>

The thermal regime of the inoculation consisted of: heating the charge, melting, overheating and maintaining the overheating temperature. The overheating temperature - depending on the degree of

eutecticity of the cast iron - was calculated, being established separately, for each experimental program, taking into account other factors such as the temperature of the inoculant treatment, the pouring temperature, as well as other elements of influence over the parameters of the casting process (such as casting mould, sample size, place and time of inoculation, etc.).

B. Mobile device for temperature measuring

The monitoring of the thermal regime of the cast irons, during their elaboration, was carried out with the help of the portable digital instrument - with immersion lance - "Digilance IV Memory" [183]. This portable instrument is equipped with a lance at the end of which is placed a transducer thermocouple, which is immersed (being protected by a quartz sheath) in liquid cast iron, and the determined temperature can be displayed on the digital screen of the device or stored in its memory and subsequently transferred to a PC drive.

2.1.3.2. *Controlul compoziției chimice a topiturii*

A. The importance of the chemical composition for liquid treatment

This stage considers the evolution and preparation of the melt in terms of chemical composition, so that it responds as effectively as possible to the treatments that will be performed later. Thus, after melting, the chemical composition was corrected, in terms of C and Si content. For this purpose, a chemical analysis was performed to determine the compositional state of the melt and then proceeded, when necessary, to the introduction of the necessary correction materials.

B. Determination of the chemical composition of the elaborated cast iron

In the experiments performed, the analysis of the chemical composition of the elaborated and casted irons was performed in two ways. A primary, rapid estimation was performed by the thermal analysis method (Quick-Lab method), and the second method, used at the end of the melt correction process, was that of optical emission spectrometry (OES), in for the precise determination of the chemical composition.

2.1.2.3. *Determination of the complete chemical composition*

Disc-type samples were taken - in cylindrical SaF-DO moulds, called "OES samples" (Optical Emissions Spectrometry) - which were rectified on one sides, after which the chemical analysis was performed at the spectrometer. The results obtained are presented, in the form of concentration, in percentage units.[184]

2.1.2.4. *Chemical composition of experimental cast iron*

In order to carry out the reporting of inoculated cast iron to a reference, the chemical composition of the base cast iron used as charge was determined for all experimental programs, but - where possible - the composition was also determined for the treated cast iron studied.

2.1.2.5. *Chemical analysis and study of chemical composition in the solidification research of cast irons*

The results that are obtained through the various equipments provide a precise picture of the specific state of the final material elaborated, as well as in various stages of its processing. This information can be detailed and analyzed in depth through the mathematical apparatus provided by the related sciences from the fields of chemistry, physics, etc. Among them, the mathematical apparatus and the relations used in this paper to deepen the chemical information obtained are further mentioned.

A. Analysis by reference to specific chemical parameters

An analysis of the influence factors of the chemical composition and of the various descriptive parameters (CE, Cc, Sc, Px, F, K'gr, K "g, ΔMn, Mn/S, MnxS) of the cast iron was performed. [23,130]

a. Analysis in terms of the amount of sulfur that could be bound - by means of the added inoculant or the basic cast iron - in the final, inoculated cast iron.[185]

For the purpose of the inoculant equivalence calculation, the amount of sulphides resulting from the interaction of the inoculant with the molten alloy is determined. Premises underlying the calculation consist in: a) determining the chemical composition of the inoculants; b) it is assumed that the inoculants are fully assimilated (the inoculant is completely dispersed, during casting, in the entire

volume of the part and is fully assimilated); c) the properties of the resulting compounds (atomic weight, density, etc.) are used (from the literature). [186]

b. Analysis from the perspective of the actual consumption of the inoculant added in the experimental cast iron

In order to determine the actual amount of inoculant consumed in the process of solidification of the cast iron, there is no mathematical solution that takes into account all the factors that influence the inoculant consumption, which is why the use of empirical solutions or tests carried out in the particular context of each foundry is used.[187] For this reason, in this paper, for the calculation of the actual consumption of the inoculant ($C_{real.inoc.}$), will be used the relationship [187]:

$$C_{real.inoc.} = \frac{G_{p.t.} \times 100}{C_{inoc.\,ad.}}, \% \quad (2.23)$$

- where: a) $G_{p.t.}$ is the weight of the castings, and b) $C_{inoc.ad.}$ it is the amount of inoculant added.

2.1.3. Tratamentul fontei în stare lichidă

2.1.3.1. *The selected method for liquid state processing:*

From the treatment methods currently applied to liquid cast irons - inoculation, preconditioning, potentiators - in order to determine and control the realization of the graphitization process in the experimental cast irons, in the present paper, the inoculation method was chosen which consists in the insertion into the melt of some active elements (Ca, Ba, Sr, La etc) able to interact with S and/or O from cast iron, forming solid compounds with the role of graphite nucleation.

2.1.3.2. *Inoculants used:*

The inoculants that were used in the experiments came from a major manufacturer of inoculation material, being used as such. In addition, specially prepared alloy systems of inoculants were used to study the influence of La, in association with various other inoculating elements, on the inoculation efficiency.

2.1.3.3. *The approach used to perform the inoculating treatment*

A. The moment and the place to accomplish of inoculation process

In the case of Experimental Program I, the inoculation was performed by inserting the inoculant in the pouring ladle, just before the moment of pouring into the molds. For Experimental Program II and III, a late inoculation was chosen, performed by introducing the inoculants even in the casting moulds.

B. The temperature of inoculation

Because, in Experimental Program I, the inoculation was performed - using a cast iron with medium graphitization potential - in the casting ladle, a temperature value of ~ 1430^{o}C was selected to perform the inoculation. For the Experimental Program II, it was taken into account that the inoculation is performed in ceramic cup moulds, exactly at the time of casting so that the inoculant treatment was established to be performed at a temperature of ~ 1400^{o}C. For the samples casted within the Experimental Program III, being without thermocouples and with a large amount of inoculant, it was established to perform the treatment of the graphitization modification at a temperature of ~ 1450^{o}C.

2.2. Casting of cast iron and analysis of solidification process

2.2.1. Thermal regime and control of specific temperatures of casting (evacuation, inoculation, casting)

2.2.1.1. *Stand for processing, control and supervision of molten cast iron*

A complex monitoring device was made: the fixed stand, adapted in order to supervise the thermal process on the flow of elaboration and casting of the cast iron through the stand provided with two control stations of the cast iron evacuated in the casting ladles. Each control post is equipped with: a place for the temporary arrangement of the pouring ladle, supports holders for OES sampling devices

as well as for an immersion temperature lance. The lance has attached a K-type thermocouple, which is immersed in molten cast iron in order to monitor, the evolution of the temperature of the cast iron discharged into the ladle, on a control screen. In this way, the operator, upon reaching the temperature established by the Experimental Program Project, proceeds to perform the operations provided in the experiment plan: inoculation process, OES sampling, casting in moulds, etc.

2.2.2. Types of samples, molds and analyzes. Methodology for performing analyzes

2.2.2.1. *Thermal analysis of the solidification process*

A. Types of samples for thermal analysis

The first type of samples used to research the proposed theme, for the first two experimental programs, were ceramic cup samples (QuickCup™). The samples have a cooling module of ~ 0.75cm and are used for thermal data collection and analysis. Test specimens of this type are adapted to be used in multiple contexts and to multiple device genres. Specifically, they are used on simpler devices that only perform a fast melt evaluation process, or in more sophisticated systems with the help of which more extensive studies are carried out – for the computerized analysis of cooling curves in order to perform determining of the characteristics that was unknown in the solidification process of materials[188] – after the processes of the elaboration of the material and of the castings.

B. Preparation of samples for thermal analysis

After casting, in the case of all the samples obtained in the experimental programs, it was started the development of a sample coding system, followed by the determination of physical characteristics (such as weight, dimensions, etc.), and by the recording of all these data into the databases corresponding to each experimental program.

C. Analysis equipment. Complex system (made by Faculty SIM-UPB) for the acquisition, storage and analysis of thermal data

In-depth analyzes of thermal data were carried out using the thermal acquisition and analysis line made within the FAC cast iron collective. - S.I.M from U.P.B. It features a fixed stand (with 15 quick cup ceramic cup mounting locations), a mobile stand (with another 15 ceramic cup mounting posts) and a data acquisition block with 32 acquisition channels and a specialized software for thermal analysis.

D. Theoretical principles and useful relationships. Analysis of cooling curves

a. Descriptive parameters of cooling curves

After registration, each recorded cooling curve was reopened in the same program - in the dedicated analysis module - and specific parameters[188,189] of cooling curves were identified and extracted, with which they can be performed studies – according to current scientific standards[189] – on how the cast iron solidify. The information obtained at this stage shall then be analyzed in a comparative and/or integrative manner, taking into account the other types of analysis carried out.

b. Relative performance of inoculants

In order to identify the behavior of the inoculars, from the point of view of efficiency, a separation of them will be carried out according to the relative performance, calculated according to *eq. 2.30*[192]

$$PR_i = \frac{\sum_K (X_{iK} - CL_K)}{S_K} \quad (2.30)$$

- where: a) X_{ik} – the measured value of parameter K, considered - using the inoculant i -, from the analyzed data set; b) CL_k - the average calculated value of the parameters K, from the analyzed data set; c) S_k - the standard deviation of the parameters K, of the analyzed data set.

2.2.2.2. *Analysis of the tendency to form carbide (chilling tendency)*

A. Samples for chilling tendency analysis

Another type of samples - made within the experimental program I - were those specific to the study of the chilling tendency, respectively those of wedge type, corresponding to the ASTM A367 standard.

Samples of this type are used because with their help can be made the most efficient simulations - of the behavior that could be developed, by a casted iron with a certain wall thickness, during solidification - in order to determine the response capacity to the formation of cementite.

B. Preparation of wedge samples for analysis

The wedge samples - cooled slowly, in moulds - were knocked-out of mould, cleaned, marked and then determined their dimensional characteristics, in order to make the calculation of the real cooling module. Later they were broken so that the rupture (broken area) was located in the middle of the samples.

C. The technique of evaluating the chilling tendency of cast irons

The last operation performed consisted in measuring the whitening tendency - on the broken surface -, in *Fig. 2.13* being presented the typical whitening areas (chilling zones) of the samples.

D. Macroscopic analysis (on the fracture)

The size of the chilled surface (whitened) on the samples is expressed in absolute values (mm), according to the measurements made on the cast wedge samples, as follows: a) absolute clear chill - ACC, mm, measured on the sample; b) Absolute total chill - ATC, mm - measured on the sample

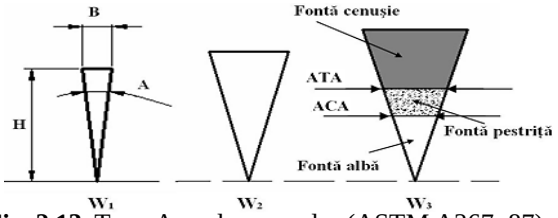

Fig. 2.13. Type A wedge samples (ASTM A367–87): CC - clear chill, TC - total chill.

2.2.2.3. *Microscopic analysis (optical metalography)*

A. Samples performed for optical metallographic analysis

The samples used, in the case of experimental programs I and II, for the metallographic structural analysis are, ceramic cups type, which have been used to carry out the thermal analysis of cast iron. In the case of the experimental program III, the cast cylindrical samples are used.

B. Preparation of samples for microscopic analysis

For microstructural analysis, the Quick-Cup™ ceramic cups have been cut, then rectified for further grinding and polishing operations. The rectification operation was also performed to obtain the surface flatness and the parallelism between the two opposite surfaces of the sample. Because the quality metallographic analysis was performed, along the entire height of the sample, the metallographic preparation operations were performed manually, in order to avoid sectioning the samples.

a. Preparation for metallographic analysis of graphite

The metallographic preparation of the samples consisted of an initial grinding stage, performed on SiC-type abrasive discs, of 80 µm, 180 µm, 220 µm, 500 µm and 1000 µm. In stage 2, the MD-largo diamond disc was used for which the MD-largo diamond solution was used as a lubricant. During the polishing phase, the discs were used: MD-DAC with DiaPro DAC diamond solution; MD-NAP with DiaPro NAP-B diamond solution and MD-Chem disc with the solution of OP-S NonDry – colloidal silica in suspension – for the final polishing.

b. Preparation for the metallographic analysis of the base metal matrix

For the analysis of the basic metal matrix, the samples were attacked with a 2% concentration Nital solution, for ~ 30 sec. - by diving in the attack solution - after which the solution was removed.

c. Preparation for metallographic analysis of eutectic cells

For the analysis of eutectic cells, an attack was made, with a mixture of 50% Nital 3% solution and 50% solution made from 5g $CuCl_2$+ 40ml HCL+30 ml H_2O+ 25 ml ethyl alcohol, for ~40 sec., by immersion, followed by removal of the attack solution.

C. Instrument for optical analysis

The samples, prepared for each type of analysis, were studied using a metalographic analysis line consisting of: optical microscope, PC and image analysis software "Analysis Five 5" ®.

D. The principles, methodology and types of optical metallographic analysis

Two methods of study were used to verify and select an effective method to be applied in the next phase (Program II) research, namely qualitative and quantitative methods. For the first method

the analysis of the sample as a whole was considered and for the second the analysis of the sample was carried out at 10 mm – as indicated by ATAS-Novacast™[194] – as reference taken the insertion area of the thermocouple in the ceramic cup.

a. Qualitative optical analysis

According to those presented above, in order to carry out the qualitative analysis, first structural images were acquired, from field to field, along the entire axis length (Fig. 2.16,a) for all types of microstructural analysis after which was performed the analysis, by using the classical metallographic method, for all acquired images.

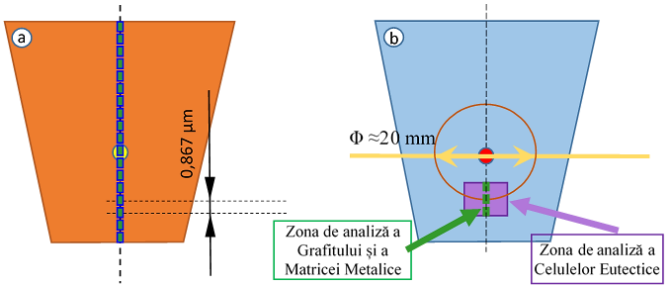

Fig. 2.16. Image acquisition scheme to perform metallographic analyzes: a) qualitative; b) quantitative (made so that images are acquired to comply with ATAS-Novacast recommendations)

b. Quantitative optical analysis

The analyzes performed for the study of the particularities of the graphite were made on the basis of the images made at the x100 magnification. For the analysis of the graphite (morphology, distribution, dimensions), the automatic software module, *Cast Iron*, was used, which was configured so that a comparative analysis between all the analyzed samples using, for all samples, the ISO-945 standard. In the case of the analysis of the basic metal matrix, for the samples was used the method of visual comparison of the images purchased with the ISO-945 standards-printed on physical support-to determine the ferrite/pearlite ratio, and to estimate the presence of the other constituents (carbides, phosphorous eutectic, etc.). For the analysis of eutectic cells, after the chemical attack for grains detection (eutectic cells), images were purchased at x20 magnification, which were automatically analyzed by the technique of the grains interception lines.

2.2.2.4.*Scanning electron microscopy with energy dispersive X-ray spectroscopy (SEM/EDX)*

A. Performing samples for SEM metallographic analysis

In order to achieve the objectives of experimental program III, samples were casted into cylinder shapes, with dimensions of ϕ=30mm and length 100mm. The mold flask frame, pattern plate and the pattern were designed and manufactured. The casting moulds were made of furanic resin.

B. Preparation of samples for SEM analysis

The cylindrical samples were cut, rectified, so that later to carry out the grinding and polishing operations, in order to study them under the SEM microscope according to those mentioned. In addition, they were prepared for SEM analysis by placing into an ultrasound alcohol bath and then was deposited a carbon band, for signal conduction.

C. The equipment of analysis[197]

The actual research of the samples was carried out using the electronic scanning microscope produced by FEI, model QUANTA 450 FEG. It has a minimum resolution in secondary electron imaging at 30kV: of 1 nm (even better in high vacuum mode) and of 5 nm (even better in low vacuum mode).

D. Principles and methodology for conducting SEM analysis on experimental samples

I. **what?**

a. a. contact area with unassimilated inoculant
b. b. the contact area with the assimilated inoculant
c. c. the beginning area of graphite formation (the border between the assimilated inoculant and the graphite structure)
d. d. inclusions/compounds/metal matrix

II. **how?**

e. e. determination of the composition of the elements at points of interest
f. f. mapping
g. g. "manual" measurements of the dimensions of inclusions
h. h. line of analysis

2.2.2.5. *Hardness analysis*

A. Samples for hardness analysis

The selected samples in order to carry out the hardness analysis are those cast in order to carry out the thermal analysis of the cooling curves, at solidification, using the opposite halves of those used for structural analysis. The preparation consisted in: a) achieving the flatness of the outer face of the cup type sample, b) then the cutting, at the middle of the samples. After cutting the samples were rectified, in order to achieve the parallelism of the opposite faces.

B. The methodology of determination applied

The impressions were made on the height of the samples at a distance from the small sample base of 3 mm and then further – on the sample axis – from 3 to 3 mm, except that the central area (where thermocouples were installed) was avoided. (v. *Figure 2.19*). Then the measurement of impressions diameter, at two directions (perpendicular to each other), was made.

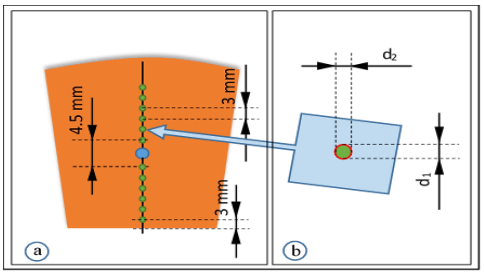

Fig. 2.19. The diagram for making traces at the hardness tester, a) way for achieving the impressions; b) way of determining of the dimensions of impressions

CHAPTER III
SYSTEMATIC PRESENTATION OF EXPERIMENTAL PROGRAMS

3.1. Experimental programs accomplished

The general experimental program designed was made up of three stages, which led to the formation of 3 experimental programs. They analyzed the following aspects: A) the study of the influence of addition of La (to the classic inoculant FeSiCaAl) on the efficacy of the inoculation process; b) the study of effects of La in association with other active elements (Ba, Sr, Zr,) on the effectiveness of the inoculant treatment; (c) the study, by SEM analysis, of the mechanism of nucleation of graphite by the treatment with various inoculant systems, with La or Mg.

3.2 Method of carrying out the proposed experimental programs

3.2.1. Experimental Program 1. *The study of the effect produced by the addition of La, in the commercial inoculant FeSiCaAl, on the efficiency of inoculation of hypoeutectic gray iron with medium nucleation potential of the graphite*

The program proposes the study of the effect produced by the addition of the active element La – in the commercial/reference inoculant of the type FeSiCaAl – on the efficiency of treatment of a hypoeutectic grey cast iron, with a medium nucleation potential of graphite (~0,5% S and the Mn*S corelation of ~0,2-0,3), in order to identify the opportunity to use La in the production process of gray cast iron castings with lamellar graphite.

Tabelul 3.4. The standard and real chemical composition of used inoculants

Nr. crt.	Added Inoculantsi	Standard Composition,%					Real Composition, %				
		Si	Al	Ca	La	Zr	Si	Al	Ca	La	Zr
1.	LaCaAlFeSi	-	-	-	-	-	67.0	0.961	1.198	4.0	0.0048
2.	CaAlFeSi	72-75	1.0-1.5	0.5-1.0	-	-	75	1.25	0.75	-	-

Figure 3.1 shows the general diagram for the implementation of the experimental program 1, from the loading stage of the experimental cast iron into furnace until to the last one, that of the types of analyzes carried out. Two batches were developed, into C.I.F. type furnace, with a capacity of 10 kg. After the casting of the

samples, the physical data of the samples were recorded (tabulated) after which the samples where prepared for specific analyzes.

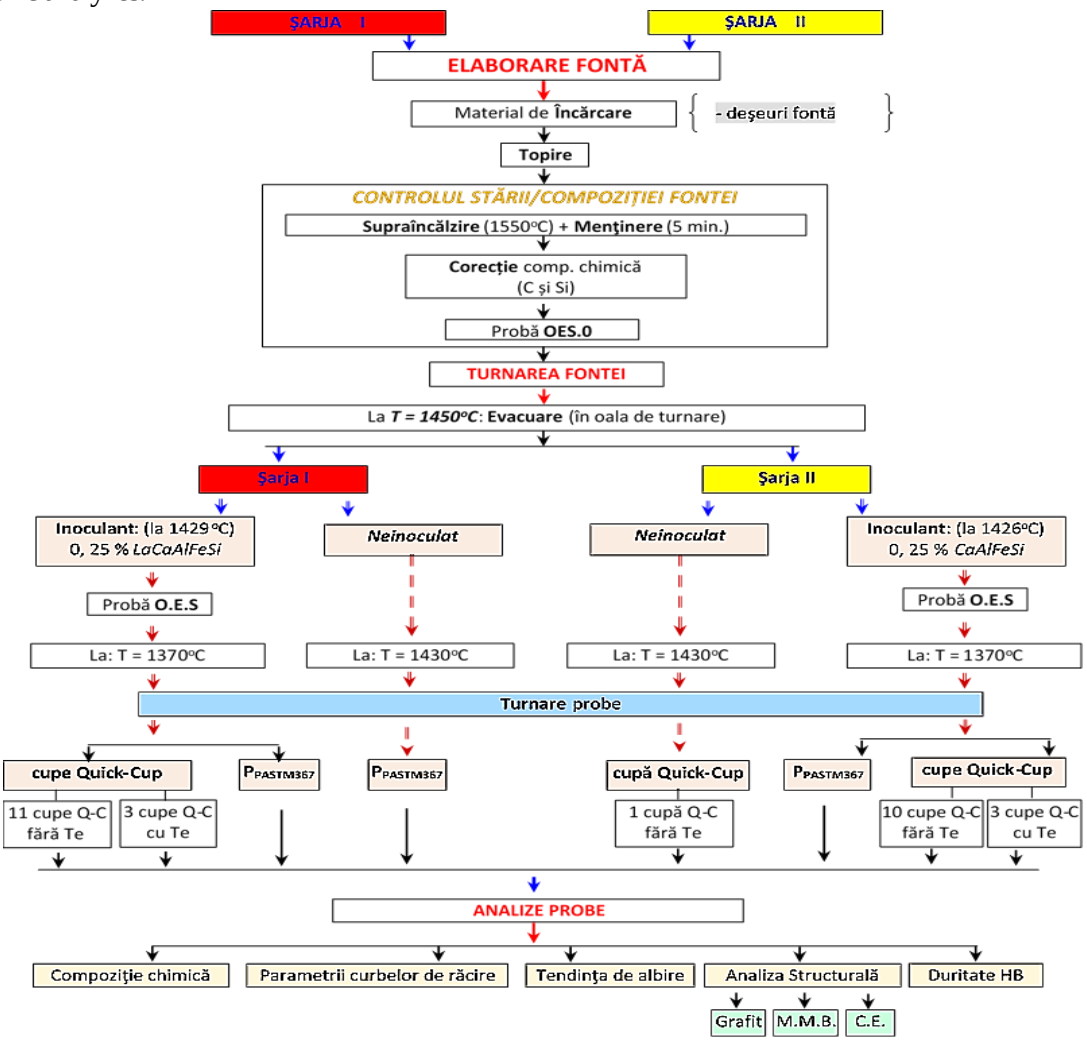

Fig. 3.1. Diagram of Experimental program I (OES sample – samples for determination of chemical composition by optical emission spectrometry method; Q-C cups – casted samples in ceramic cup mould for thermal analysis; $P_{PASTM367}$ – Standard ASTM A367 wedge sample

3.2.2. Experimental Program 2. *Research on the modification produced on the solidification process of the hypoeutectic gray cast iron, by inoculants containing La in association with various other active elements (Ba, Sr, Zr)*

The second stage aims to carry out research on the changes produced in the solidification process - in the hypoeutectic gray cast irons with critical conditions of graphite solidification - by the inoculants containing La together with other accompanying active elements of the type: Ba, Zr or Ti. The aim is to try to identify the particular mode of action of La - within the solidification process - by comparison with the effects introduced by the other additional active elements.

Figure 3.2 shows the general diagram of implementation of the Program II, from the stage of loading the experimental cast iron into furnace until to the last one, that of the types of analyzes carried out. A heat has been conducted and after melting of the base cast iron (in the 80 kg induction furnace, synthetic cast iron being used as charging), the cast iron condition is controlled by means of thermal processing and an treatment with various inoculant systems whose composition is shown in **Table 3.10**.

Tabelul 3.10. Compoziţia chimică finală a inoculanţilor utilizaţi în experimentările efectuate

Amestecul de inoculant obţinut	Compoziţia chimică, % gr.							
	Si	***Al***	***Ca***	***Ba***	***La***	***Zr***	***Ti***	***Fe***
La	67.0	0.96	1.20	-	4.00	0.005	-	26.84
LaZr	69.4	1.48	1.27	-	3.70	3.10	-	21.05
LaBa	65.8	1.44	1.33	1.35	3.62	-	-	26.46
LaBaZr	67.6	1.46	1.30	0.68	3.66	1.55	-	23.76
LaZrTi	65.8	1.40	1.21	-	3.51	2.94	5.10	19.98
LaBaZrTi	65.8	1.42	1.27	0.66	3.56	1.51	2.62	23.14

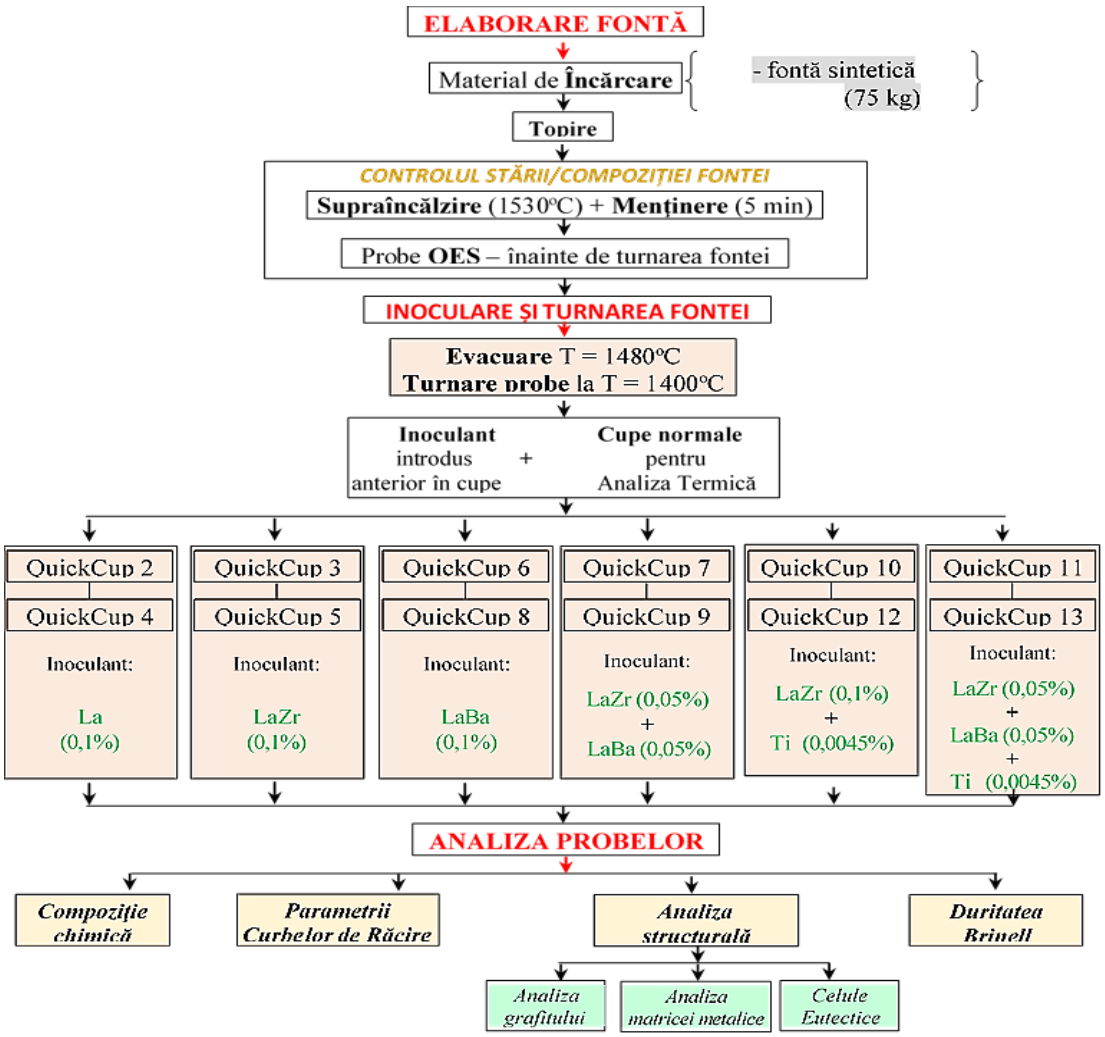

Fig. 3.2. The diagram of the project for accomplishing of the Experimental Program II

3.2.3. Experimental Program 3. *Research, carried out by the SEM-EDAX method, on the nucleation and solidification of the overinoculated hypoeutectic gray iron castings, in the case of the use of different inoculant systems, with and without La, in order to highlight the action of La during the formation of the solidification structure.*

The third program focuses on the deepening of the study - by SEM/EDAX research method - regarding the nucleation and solidification of the hypoeutectic gray cast iron in the case of the use of the different inoculant systems. A number of 4 inoculation systems were used, with and without La or Mg, in order to discover the particular action mode of La (during the formation of the solidification structure) by path of comparison with the action mode of Mg - as a replacement element of La - in combination with other specific active elements (Sr, Ba, Ca, Al, Ti, etc.). *Figure 3.3* presents the general diagram for carrying out the experimental program, the details related to the process of elaboration, inoculation and casting of the experimental cast iron, respectively the types of analyzes carried out within this experimental program. After charging the C.I.F. furnace (with, 9 kg, cast iron scrap) and the melting of the charge, the liquid cast iron is processed - by thermal processing and the correction of the chemical composition - after which it is evacuated (at 1480ºC) in the casting ladle. Then OES samples are taken, to determine the detailed chemical composition, and the cylindrical samples (established by the experimental project) are casted. Inoculation is done at the time of casting, being performed directly in the cylindrical moulds, made of furan resin.

In order to obtain them, new inoculants are created by the mixing of commercial inoculants produced by the company Elkem was done. In **Table 3.18.** the chemical elements identified in the compositions of the final mixed inoculants are presented. After obtaining the inoculants and completing the casting of the samples, they were knocked-out of mould and then cleaned.

Subsequently, the physical data of the samples were determined and then recorded and later on they were prepared for the analyzes of optical spectrometry (SEM and EDAX).

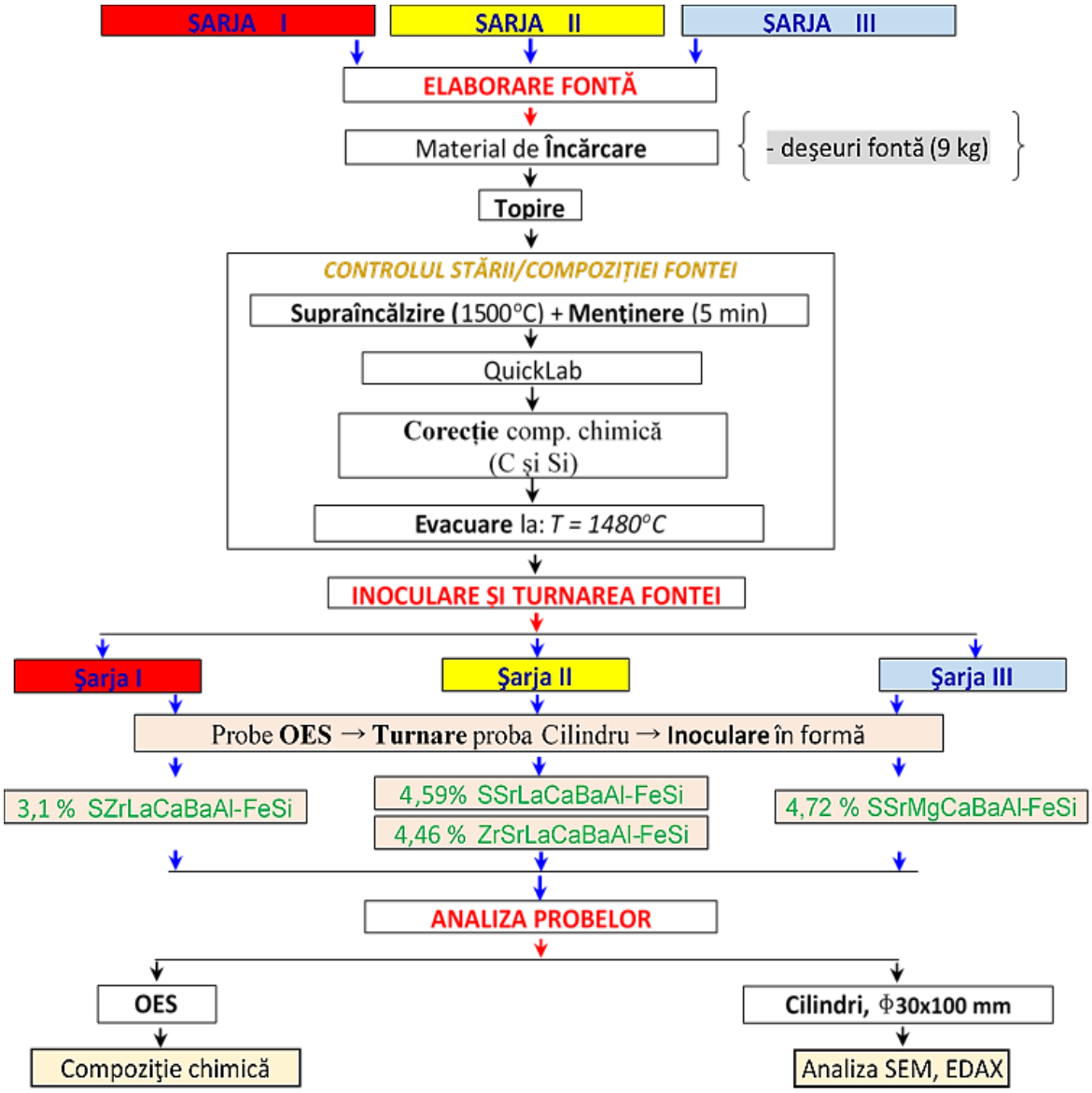

Fig. 3.3. The diagram of the project for accomplishing of the Experimental Program III

Tabelul 3.18. Chemical composition of inoculating mixtures used in Program III.

Heat		**I**	**II**		**III**
Mixed inoculant notation		***3***	***5***	***6***	***11***
Mould Notation		***F4***	***F6***	***F7***	***F12***
Chemical elements and percentage amounts, introduced into the mix of experimental inoculants used in the study. [%]	**Si**	70.0595	70.4628	73.0333	70.1545
	Al	0.7295	0.9693	1.168	1.4161
	Ca	0.6115	0.4221	0.4563	1.0696
	Ba	0.4818	0.3349	0.3433	0.4036
	La	1.7828	1.3007	1.2333	-
	Mg	-	0.0163	0.0167	0.65691
	Zr	1.4937	0.0081	1.04	0.3448
	Sr	-	0.3284	0.3367	0.3185
	Ti	-	0.0163	0.0167	0.0158
	S	1.9348	1.3057	-	0.4158
	Mn	0.0009	0.0006	-	0.0002
Total amount of inoculant introduction	[%]	**3.1**	**4.59**	**4.46**	**4.72**
	[g]	**15.67**	**23.17**	**22.5**	**23.82**

CHAPTER IV
EXPERIMENTAL RESULTS, ANALYSIS AND CONCLUSIONS

4.1. The study of the produced effect, by the additional addition of La in the commercial inoculant of the FeSiC, on the efficiency of inoculation in the hypoeutectic gray cast iron with medium nucleation potential of the graphite [Experimental Program I]

4.1.1. Preparation of batches, types of samples and analysis

The data recorded during the elaboration and casting of the samples showed that the limit values of the thermal regime of the batch and casting comply with the design prescriptions to a high degree.

1Tabelul 4.2. The work plan schematization of the Experimental process for the purpose of carrying out the research

Cast Iron state*		Comp. Chim.	Thermal Analysis					Wedge samples [chilling tendency]	Hardness [HB]	Metallographic Analysis		
			Temp.–Timp	*Subrăcire*	*Tst*	*Tmst*						
					Calculat [Si]	*Calculat* [Si]	*Măsurat* [Te]			*Gf.*	*MMB*	*CE*
A	*U.I.*	X	X	X	X	X	-	X	X	x	x	x
B.1	*Inoc 1*	-	X	X	X	X	-	X	X	x	x	x
B.2	*Inoc 1+Te*	-	X	X [$\Delta T_{(1-3)}$]	X [B.1=B.2]	X [B.1=B.2]	X	-	-	-	-	-
C.1	*Inoc 2*	-	X	X	X	X	-	X	X	x	x	x
C.2	*Inoc 2+Te*	-	X	X [$\Delta T_{(1-3)}$]	X [C.1=C.2]	X [C.1=C.2]	X	-	-	-	-	

* U.*I.*: uninoculated; *Inoc 1*: inoculated (cu 0.25wt% inoculant type LaCaAlFeSi); *Inoc 2*: inoculated (with 0.25wt% inoculant type CaAlFeSi); *Te*: addition of Telurium in ceramic cups, before casting the cast iron

Regarding the analyzes performed after obtaining and preparing the samples, according to **Table 4.2.** it is observed that the thermal analysis is more in-depth realised - using mathematical relations, for calculating the parameters of eutectic transformations in the stable system (Tst) and metastable (Tmst) from several sources - with the aim to achive more varied modeling that can bring some more detailed observations by which to profoundly detect the behavior of the cooling curves.

4.1.2 The physical characteristics of casted samples

Next, using the results recorded after measuring the wedge samples (see **Table 4.6.**), the values of the cooling modules of the obtained specimens were calculated (see **Table 4.7.**), these – compared to the values of the american standard ASTM A367 – are within the standardized limits.

4.1.3 The chemical composition of the processed castings and the control parameters of the structure

With the help of chemical composition data, obtained after analysis, the determination of the specific parameters of the chemical composition for the complete characterization of the obtained cast iron is carried out (see **Table 4.12**).

Tabelul 4.12. Parametrii specifici ai fontei inoculate conform compoziției chimice pentru Programul Experimental I

Inoculant Sistem *	Perlitisation Factor	Ferritisation Factor	Corelations between Mn and S			Graphitisation constants		Degree of eutecticity	
	Px	*F,%*	*Mn/S*	*(%Mn) x (%S)*	*ΔMn*	*K'gr*	*K"gr*	CE [%]	Sc
LaCaAlFeSi	4.76	8.26	9.514	0.0294	0.1345	0.919	1.226	3.7679	0.87
CaAlFeSi	4.48	10.88	11.453	0.0243	0.1496	0.9936	1.325	3.7633	0.87

According to the given data, both tested castings have a close chemical properties, including the equivalent carbon (CE = 3.76 - 3.77%) as well as the specific control factors, namely those related to the

sulfur and manganese content (0.046 - 0.055%S. , 0.52 - 0.53%Mn, 9.5 - 11.5 Mn/S, (%Mn) x (%S) = 0.021 - 0.03, ΔMn = 0.13 - 0.15). According to the obtained chemical composition, the inoculated experimental charges are characterized by: a) an average hypoeutectic position on the Fe-C diagram, b) a good ratio of manganese and sulfur content and c) by a low level of active elements and minor elements.

4.1.4 Thermal analysis of cooling curves

Table 4.13 centralizes the data regarding the localization of the cast iron on the FeC diagram from the point of view of the Tst and Tmst equilibrium temperature values. For this purpose, various calculation solutions have been used to determine the reliability of the behaviour of the registration and analysis system (SIM-UPB Faculty) - using the solutions proposed by: Sillen-Novacast, Kanno and UPB - by the method of mathematical relations (to avoid achieving an appreciation through the statistical methods that would involve processing with large databases and with extensive statistical relationships that cannot have their place in this work).

Table 4.13. Calculated and measured eutectic temperatures, (Tst) and (Tmst), of casted irons

Inoculant Type		Tst, °C	Tmst, °C		ΔTs (= Tst – Tmst), °C		
	0	*1*	*2*	*3*	*(1) - (2)*	*(1) - (3)*	
	Methode	*Calculated*	*Calculated [Si]*	*Measured [TEU=TER] =[Te]*	*Calculated*	*Measured*	
Range	S	1163,79 ÷ 1164,73	1126,00 ÷ 1127,68	1116,58 ÷ 1119,08	36,11 ÷ 38,72	45,64 ÷ 47,20	S
[Difference]		[-0,94]	[1,68]	[2,50]	[2,62]	[1,56]	
{Average}		{1164,26}	{1126,84}	{1117,83}	{37,42}	{46,42}	
	K	1149,88 ÷ 1150,77	1116,05 ÷ 1117,30		34,72 ÷ 32,58	31,69 ÷ 33,30	K
		[-0,89]	[-1,25]		[-2,14]	[1,61]	
		{1150,33}	{1116,68}		{33,65}	{32,49}	
	UPB	1151,48 ÷ 1160,71	1124,80 ÷ 1125,75		26,68 ÷ 34,96	32,40 ÷ 44,13	UPB
		[9,22]	[-0,95]		[8,27]	[11,72]	
		{1156,10}	{1125,28}		{30,82}	{38,26}	

Table 4.14 summarizes the values of the main parameters of the acquired cooling curves (as mean values of the recorded curves, the range of the maximum and minimum values and the difference between the minimum and maximum values) while *Figure 4.2* shows the positions of the representative parameters of the cooling curves, for all recorded curves. **Table 4.15** summarizes the results (in the form of mean values of recorded curves, the range of maximum and minimum values and the difference between minimum and maximum values) – obtained by calculation using for ΔTm the 3 established methods, namely: Sillen, Kanno and UPB — for the degrees of undercooling (ΔTm, ΔT_1, ΔT_2, ΔT_3) reported to the previously determined metastable eutectic system temperatures.

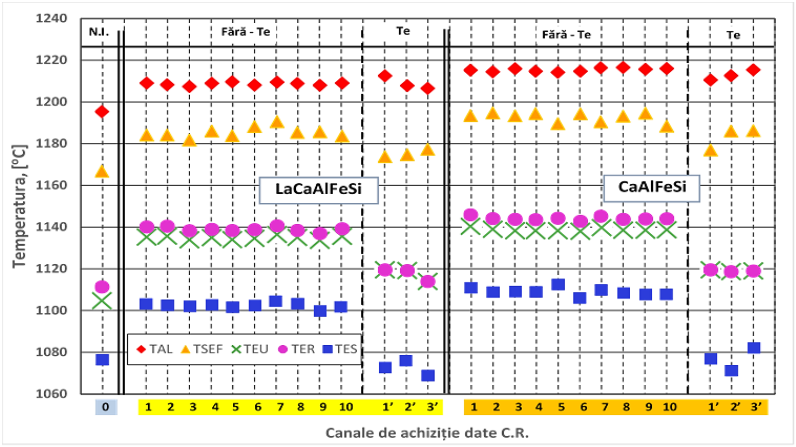

Fig. 4.2. Position of the representative parameters of the cooling curves in the experimental cast iron

From *Fig. 4.2.*, the positive effect produced on the main parameters of the cooling curves, with the upper position of the Ca-FeSi inoculant, is observed compared to the reference (non-inoculated) cast iron. *Fig. 4.4.* shows the position of parameter ΔT1 for non-inoculated and inoculated cast irons as well as for that of Te added after the moment of inoculation. For the representation of the position of the parameter ΔT_1 – as for the undercooling that will be analyzed further – the actual (measured) value of the temperature Tmst, determined using the cup with Te, was used as a reference. In the case of both inoculant systems used, the process of inoculation of the melt performed before the solidification

Table 4.14. Representative Parameters of Cooling Curves

Nr. Crt.	Inoculation state*	Added quantity %	Representative Parameters of Cooling Curves, [°C]						Eutectic Recalescence
			TM	*TAL*	*TSEF*	*TEU*	*TER*	*TES*	*ΔTr =TER - TEU*
	U.I.	-	1366.5	1195.4	1166.8	1104.8	1111.4	1076.4	6.59
Range	LaCaAlFeSi	0.25	1261.51 - 1309.01	1207.4 - 1209.7	1181.8 - 1190.6	1133.7 - 1136.5	1137.0 - 1140.6	1099.8 - 1104.5	3.34 - 4.88
[Difference]			[47.5]	[2.3]	[8.8]	[2.8]	[3.6]	[4.7]	[1.54]
{Average			{1286.44}	{1208.7}	{1185.3}	{1134.9}	{1139.0}	{1102.4}	{4.10}
		0.25 + Te	1222.25 - 1235.59	1206.51 - 1212.56	1173.8 - 1177.3	1114.0 - 1119.5		1068.9 - 1076.0	-
			[13.34]	[6.05]	[3.5]	[5.5]		[7.1]	
			{1228.42}	{1209.0}	{1175.2}	{1117.6}		{1072.5}	
	CaAlFeSi	0.25	1255.35 -1290.47	1214.2 -1216.5	1188.38 - 1194.73	1138.0 - 1140.4	1142.8 - 1146.0	1106.1 - 1112.5	4.77 - 6.04
			[35.13]	[2.3]	[6.35]	[2.4]	[3.2]	[6.4]	[1.26]
			{1272.01}	{1215.4}	{1192.6}	{1138.8}	{1144.2}	{1109.0}	{5.39}
		0.25 + Te	1233.33 - 1235.6	1210.5 - 1215.4	1177.0 - 1186.2	1118.7 - 1119.6		1071.2 - 1082.1	-
			[2.27]	[4.9]	[9.2]	[0.9]		[10.9]	
			{1234.18}	{1212.8}	{1183.1}	{1119.1}		{1076.7}	

* *U.I.*: uninoculated; ** *Te*: addition of Te in the ceramic cups, before casting the cast iron

Table 4.15. Representative undercooling parameters for the solidification process, related to the various solutions proposed for the calculation of eutectic equilibrium temperatures

Inoc Type.	Result	Inoc	ΔTm/°C			ΔT1/°C				ΔT2/°C				ΔT3/°C			
		%	Sillen	Kanno	UPB	Sillen	Kanno	UPB	Te_real	Sillen	Kanno	UPB	Te_real	Sillen	Kanno	UPB	Te_real
U.I.		U.I.	59.95	46.00	46.71	-21.23	-11.28	-20.03	-14.31	-14.64	-4.69	-13.44	-7.72	-49.57	-39.62	-48.37	-42.65
LaCaAlFeSi	Range	0.25	27.30 ÷ 30.13	13.40 ÷ 16.22	24.23 ÷ 27.05	5.98 ÷ 8.80	16.36 ÷ 19.18	7.91 ÷ 10.73	17.08 ÷ 19.90	9.32 ÷ 12.93	19.70 ÷ 23.30	11.25 ÷ 14.85	20.42 ÷ 24.02	-27.89 ÷ -23.19	-17.52 ÷ -12.81	-25.97 ÷ -21.26	-16.80 ÷ -12.09
			[2.82]							[3.60]				[4.70]			
			{28.86}	{14.95}	{25.78}	{7.25}	{17.63}	{9.18}	{18.35}	{11.35}	{21.73}	{13.28}	{22.45}	{-25.29}	{-14.91}	{-23.36}	{-14.19}
	[Difference]	0.25+Te	44.27 ÷ 49.80	30.36 ÷ 35.89	41.19 ÷ 46.72	-13.69 ÷ -8.16	-3.31 ÷ 2.22	-11.76 ÷ -6.23	-2.59 ÷ 2.94	-13.69 ÷ -8.16	-3.31 ÷ 2.22	-11.76 ÷ -6.23	-2.59 ÷ 2.94	-58.79 ÷ -51.66	-48.41 ÷ -41.28	-56.86 ÷ -49.74	-47.69 ÷ -40.56
			[5.53]											[7.13]			
			{46.23}	{32.32}	{43.15}	{-10.12}	{0.26}	{-8.19}	{0.98}	{-10.12}	{0.26}	{-8.19}	{0.98}	{-55.14}	{-44.76}	{-53.21}	{-44.04}
CaAlFeSi	{Average	0.25	24.31 ÷ 26.70	10.36 ÷ 12.75	21.57 ÷ 23.96	12.02 ÷ 14.42	21.97 ÷ 24.37	13.22 ÷ 15.61	18.94 ÷ 21.33	16.79 ÷ 19.96	26.74 ÷ 29.91	17.99 ÷ 21.16	23.71 ÷ 26.88	-19.94 ÷ -13.50	-9.99 ÷ -3.55	-18.75 ÷ -12.31	-13.03 ÷ -6.59
			[2.39]							[3.17]				[6.44]			
			{25.94}	{11.99}	{23.20}	{12.79}	{22.74}	{13.98}	{19.70}	{18.17}	{28.12}	{19.37}	{25.09}	{-16.99}	{-7.04}	{-15.79}	{-10.07}
		0.25+Te	45.15 ÷ 46.07	31.20 ÷ 32.12	42.41 ÷ 43.33	-7.34 ÷ -6.43	2.61 ÷ 3.52	-6.15 ÷ -5.23	-0.43 ÷ 0.49	-7.34 ÷ -6.43	2.61 ÷ 3.52	-6.15 ÷ -5.23	-0.43 ÷ 0.49	-54.82 ÷ -43.92	-44.87 ÷ -33.97	-53.62 ÷ -42.73	-47.90 ÷ -37.01
			[0.92]											[10.90]			
			{45.64}	{31.69}	{42.90}	{-6.92}	{3.03}	{-5.72}	{-0.00001}	{-6.92}	{3.03}	{-5.72}	{-0.00001}	{-49.28}	{-39.33}	{-48.08}	{-42.36}

process leads to a visible improvement - by the fact that ΔT1 increased from a negative value (-14°C) to positive values (17-20°C) - of the quality of the cast iron. Inoculation thus stopping free carbide formation and promoting the creation of favorable conditions for graphite nucleation, for the solidification conditions used: ceramic cup moulds and casted samples having a cooling module of 7.3mm.

The addition of Te to the ceramic cup, before casting cast iron, contributes to a significant decrease in the values of parameter ΔT_1, of the inoculated cast iron, respectively up to values between -2.5 - +2.5°C. Thus, the formation of carbides was promoted, the solidification process being moved into the carbiding system.

Fig. 4.5 shows the positions of the undercooling ΔT_3 in the case of cast experimental cast iron. The uninoculated cast iron (U.I.) has solidified at a very low temperature, since TES is more than 40°C below the value of Tmst (ΔT3 = -42.5oC). Inoculation significantly (positively) influences the last part of the solidification process – by the fact that the treatment reduces undercooling (ΔT_3 = -5 – -15°C) – to a greater extent for the Ca-FeSi inoculated castings. The addition of Te (antigraphitizing element) before solidification drastically affects the moment of the end of inoculation, which is illustrated by the value of ΔT_3 showing an increase (in negative values) to values between -40 – -47°C.

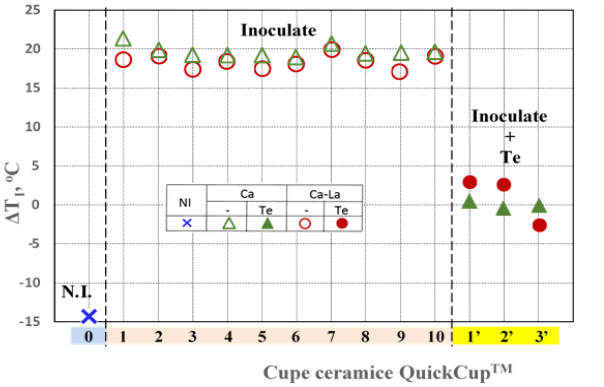

Fig. 4.4. Undercooling (ΔT_1 = TEU – Tmstreal) at the point of the lower threshold of the temperature of the eutectic reaction (TEU) taking as reference the actual metastable eutectic temperature ($Tmst_{real}$) [0: Non-inoculated; 1–10: Inoculated; 1'– 3': Inoculated + added Te]

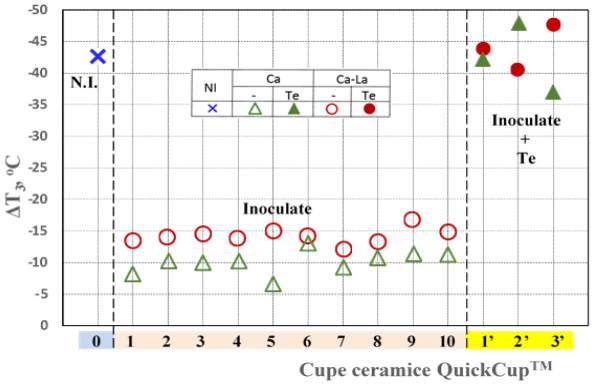

Fig. 4.5. Undercooling at the end of solidification taking as reference the actual metastable eutectic temperature ($Tmst_{real}$) [0: Non-inoculated; 1 – 10: Inoculated; 1' – 3': Inoculated + added Te]

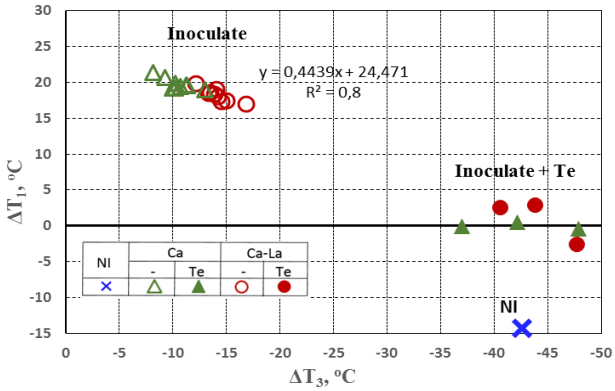

1**Fig. 4.6.** The relationship between undercooling at the end of solidification (ΔT_3) and undercooling in the first part of the eutectic reaction, corresponding to the lower threshold of the eutectic temperature (ΔT_1) for uninoculated (U.I.), inoculated and inoculated +Te, respectively.

Figure 4.6 shows the relationship between end-of-solidification undercooling (ΔT_3) and undercooling in the first part of the eutectic reaction, corresponding to the lowest eutectic temperature (ΔT_1). In the case of base iron, both parameters of undercooling have negative values, which correspond to the highest undercooling for the entire solidification process, a process that took place at a temperature below the value of the metastable eutectic temperature, promoting the appearance of carbides instead of graphite (including at the interface between the eutectic cells) and contraction defects in the space between the eutectic cells.

Inoculation affects both of the undercooling parameters considered, resulting in a ΔT_3 not lower than -17°C and a ΔT_1 greater than 17°C. The higher the value of ΔT_1 (the lower the undercooling at the beginning of the eutectic reaction, respectively), the lower the undercooling (with less negative values) will also occur at the end of the solidification, this is true for both inoculation systems, there is a good correlation between them.

Table 4.16 shows the values of the parameters specific to the first derivative of the cooling curves, which mainly influence the end of the solidification of the melt. A higher GRF1

value means that nucleation and eutectic growth manifest in longer times, resulting in the formation of a larger amount of graphite.

Table 4.16. The representative parameters of the first derivative of the cooling curve (FDES, TEM) and the graphitization factors GRF1 and GRF2

Nr. Crt.	Aquisition Channel Notation	Inoculant Type	Inoculant Quantity, %	FDES	TEM	GRF1	GRF2
				[°C/sec]	[°C/sec]	[sec]	[∠]
Range [Difference] {Average		*N.I.*	-	-2.30	0.20	25.50	31.08
		LaCaAlFeSi	0.25	-3.5 ÷ -3.27	0.17 - 0.24	43.6 - 50.5	16.74 – 19.38
				[0.24]	[0.06]	[6.9]	[2.64]
				{-3.4}	{0.2}	{47.4}	{17.68}
			0.25 + Te	-3.03 ÷ -2.85	-0.04 ÷ 0.03	21.5 -30.5	30.5 - 39.17
				[0.48]	[0.065]	[5.3]	[4.74]
				{-2.95}	{0.0041}	-27.40	{34.09}
		CaAlFeSi	0.25	-3.55 ÷ -3.07	0.26 - 0.32	40.7 - 46.0	17.0 - 20.7
				[0.48]	[0.065]	[5.3]	[3.68]
				{-3.41}	{0.28}	{43.7}	{18.56}
			0.25 + Te	-2.99 ÷ -2.84	-0.03 ÷ -0.01	21.0 ÷ 24.6	31.6 ÷ 45.5
				[0.15]	[0.018]	[3.6]	[13.9]
				{-2.91}	{-0.0228}	{23.3}	{37.775}

Figure 4.8 makes a comparison between the values of the eutectic recalescence (ΔTr) and the maximum recalescence speed (TEM) for the case of the two inoculated castings. It is visible that inoculation with Ca,La-FeSi results in lower values of the recalescence (ΔTr = 3 − 5°C) and of the maximum recalescence speed (TEM = 0.18 − 0.24°C/s) – compared to the Ca-FeSi commercial inoculant system (the values obtained in this case are: ΔTr = 5 − 6°C, TEM = 0.26 − 0.34°C/s) – on average 25 − 30%. Treatment with strong anti-graphitizing Te leads to the avoidance of the appearance of graphite, so that all the undissolved carbon content in austenite has formed carbides.

According to *Figures 4.9* and *4.11*, the inoculation contributed to increasing the ability of the cast iron to form graphite during solidification, because the value of the parameter GRF1 increased, from a level of its value of 25.5 in the noninoculated castings to the value of 43.7 for inoculation with Ca-FeSi and for the inoculated castings with Ca,La-FeSi, to the up to the value of 47.4. Inoculation with Ca,La-FeSi leads to a higher value of the GRF1 factor than the value obtained for Ca-FeSi inoculation (respectively values between 43.6-50.5, in the first case, compared to 40.7-46.0, in the second case). As expected, the addition of Te after inoculation, canceled the graphitizing effect of this metallurgic treatment, so that the GRF1 factor returned to the initial values of the base cast iron.

The lower values of the parameters GRF2 and FDES denotes a better cast iron quality. In this case the inoculation reduced the value of the GRF2 parameter from $GRF2_{nein.}$ ~ 31 to values situated in the range 16 − 20, in the case of both inoculants; and from the point of view of perfomance the inoculant Ca,La-FeSi, ranks better with an interval of values between 16.7−19.38 (and an average of 17.68) versus the value range 17.0−20.7 (with the average 18.56) of the inoculant Ca-FeSi. The addition of the tellurium, after inoculation, increased the value of the GRF2 factor to a level just above the interval obtained by the noninoculated cast iron (30−45). A similar behaviour was also recorded for the FDES parameter. Thus, if the noninoculated cast iron is characterized by a FDES = -2.30°C/s, the inoculation process moves the value of this parameter to values between -3.3 − -3.6 °C/s, while the addition of Te after inoculation leads to an interval with intermediate value limits (-2.8 − -3.0°C/s).

It is noted that the performance of the Ca,La-FeSi alloy – compared to the inoculant Ca-FeSi – is better in the assessment carried out by the GRF1 parameter (which seems more sensitive to the variations of melting that solidifies), compared to the one noticeable through the parameters GRF2 or FDES. The inoculant's ability to act is manifested not only in conditions where only the inoculant acts on the melt, but also in the case of the manifestation of a strong antigraphitization factor, such as that of the addition of Te, although in these conditions the inoculating capacity has a lower level of efficiency.

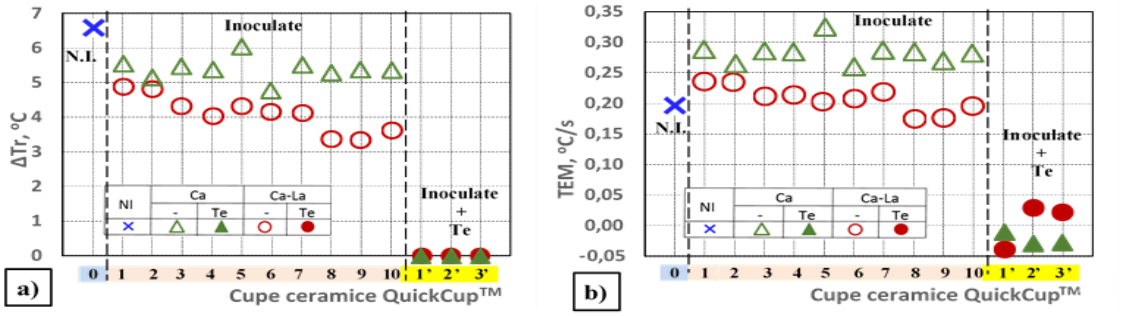

Fig. 4.8. The variation in eutectic recalescence, ΔTr (**a**), the maximum recalescence velocity (eutectic reaction) TEM (**b**) and their position, as absolute, mean and deviation from mean of the actual values obtained (**c**) in the case of the two inoculated cast irons [U.I. – uninoculated cast iron]

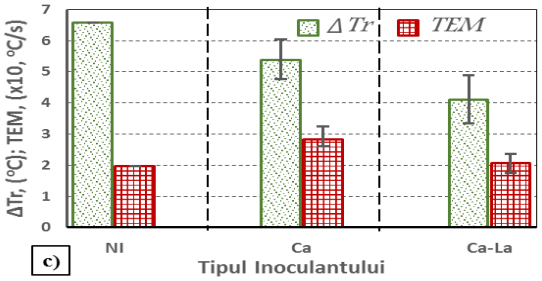

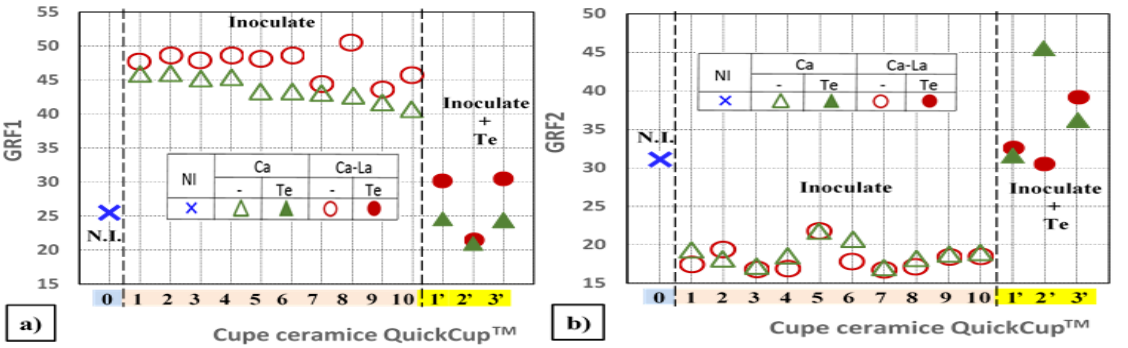

Fig. 4.9. Graphitizations factors GRF1 (**a**, seconds) and GRF2 (**b**, angular measurement), and the value of first derived of cooling curves at the end point of the solidification of FDES (**c**, °C/s)
[U.I.. – uninoculated cast iron]

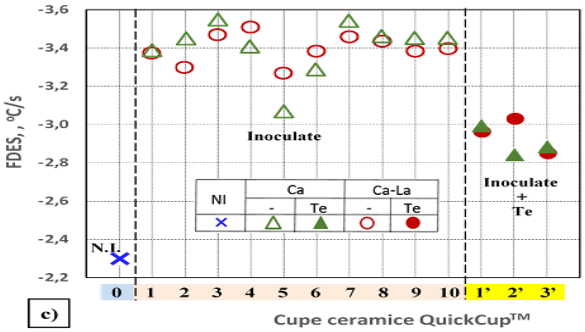

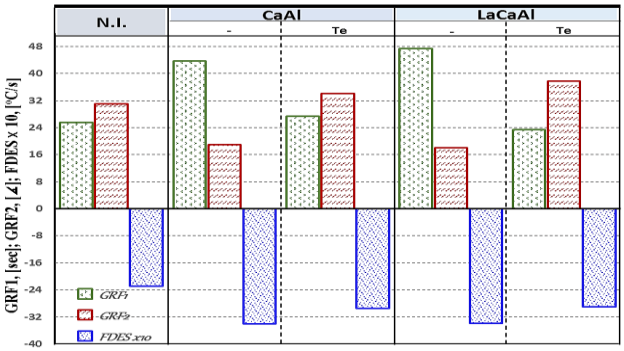

Fig. 4.11. The average value and the limits of the graphitization parameters GRF1 (seconds), GRF2 (angular measurement) and the value of first derived of cooling curve at the end of the solidification (°C/s) of the uninoculated castings (U.I.) and inoculated (Ca, Ca-La), [Te - addition of Te after inoculation]

4.1.5 Chilling Tendency

Following the control of the solidification - by means of the method of determining the tendency to form the carbides (whitening) - it is presented, in *Fig. 4.14. a*, the results obtained, for the inoculated castings from cast iron, in the form of relative total chill parameter (RTC),

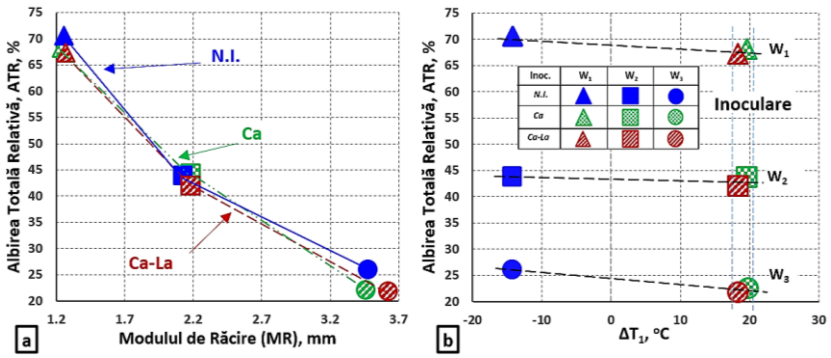

Fig. 4.14. Relative total chill, RTC related to (cooling modulus) CM, (**a**) and the relationship between RTC and the undercooling parameter (**b**) at the end of solification (ΔT_1) [W_1, W_2, W_3- types of wedge samples]

which is influenced by the cooling rate of the solidification – expressed by the cooling module of the castings – as well as by the system of inoculant used (in the present case: Ca,La-FeSi, versus Ca-FeSi). The decrease of the cooling rate of the solidification – achieved by increasing the cooling module – leads to decreasing the incidence of carbides formation, expressed by decreasing the value of relative total chill. This effect is valid for both inoculation systems, of which more efficiently (with ~ 20%) is the system Ca,La-FeSi. The superior inoculation capacity of the alloy Ca,La-FeSi is more visible – taking into account the real value of the cooling module – in the case of wedge samples type W_1 (solidification at the highest cooling speed). This capacity is very important for the category of castings that have thin walls (walls smaller than 5mm).

In *Fig. 4.14. b*, are illustrated the effect and importance of inoculation for the control of the chilling tendency (RTC) and also the relationship between the chilling tendency of the gray cast irons and the eutectic undercooling ΔT_1 (regarding the lower threshold temperature of the eutectic reaction, TEU, correlated with the eutectic metastable temperature, Tmst).

4.1.6 Structural analysis

4.1.6.1 Qualitative metallographic optical analysis

The method set out in Chapter II (Research method) was used as a working principle to carry out qualitative microstructural analyzes. Compared to the presented ones, it should be mentioned in addition to the fact that, after the analysis and obtaining the conclusions - in order to present the results in the work - the following systematizations were made.

After the image acquisition, a calculation was made to determine the distances at which each photo is located on the actual sample. The locations of the images on the analyzed sample do not match exactly with the distance of 10 mm from the center of the thermocouple (these being located at a distance of 9.76 mm) but - yet from the point of view of the observed structure and also from the point of view of the difference from the recommended value (by ATAS-Novacast) - the analyzed structure falls within the structural appreciation mentioned by ATAS, confirming them. In *Fig. 4.15.* the real positions of the images acquired under the microscope are graphically shown and analyzed – for the samples studied – in order to establish the microstructural characteristics of the graphite and the metal matrix.

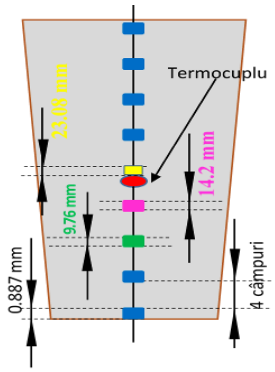

Fig. 4.15. The actual layout of microstructural images analyzed in the inoculated samples investigated

A. The graphite

The *reference* (uninoculated) cast iron has a typical structure of gray iron with undercooled lamellar graphite (type D, according to ISO 915), except for the center of the sample, where the structure evolves to interdendrytic lamellar graphite type E. Also, in the area of the thermal center of the sample and on large surfaces above the thermocouple, areas with shrinkages are present. The sample inoculated with *the classic inoculating system* (CaAlFeSi) has an interdendritic lamellar graphite (type E) structure in most of the sample, except for the central area where – under the influence of the Ca and of temperature from the thermal center of the sample – the graphite lamellae evolved into well-developed type A graphite. In the upper part of the sample (at the large base) – where the influence of the end zone is manifested – graphite has a development toward the lamellar

undercooling graphite (type D). With regard to the sample inoculated with the LaCaAlFeSi *complex system*, it mainly has an interdendritic lamellar graphite (type E) structure, except for the upper part of the sample (at the large base) where the formed graphite is a D-type undercooled lamellar graphite. As with the other two samples, a better development of graphite slides is observed in the central area of the LaCaAlFeSi inoculated sample. Comparing inoculated samples, it is observed in CaAlFeSi-treated sample that graphite lamellae are numerically less, but in terms of lamellae growth they are better developed. The LaCaAlFeSi system has a higher number of graphite particles, their length and degree of development being lower than the classical inoculant. Inoculated cast irons do not have any areas of shrinkages, which confirms the positive effect of inoculation in both cases.

B. Metal matrix

The analysis of the basic metalic mass of the uninoculated cast iron reveals a pearlitic structure, at the bottom (small base) of the sample. In the area of the small base there is a larger amount of carbides (~ 3 –5%), while in the upper area of the sample - above the thermocouple area - a carbidic structure (ledeburite, steadite) is present and phosphide eutectic is also present. Regarding the inoculated castings, in general - on the largest surfaces - both experimental castings have a pearlite-ferrite structure, with ferrite contents at values below 2%. In their case, the amount of ferrite is more pronounced in the lower area (towards the small base ~ 3-5% ferrite) and also in the upper area of the samples (large base), with ~ 2 –4% ferrite in the case of LaCaAlFeSi and ~ 3-5 % in the case of CaAlFeSi. And in the case of castings treated with inoculant, areas with phosphide eutectic were identified.

C. Eutectic cells

In the analysis of eutectic cells, the uninoculated sample shows – in the lower part of the sample – a small number of eutectic cells, which are of the largest size compared to inoculated samples. Compared to the uninoculated sample, inoculated samples formed a large number of eutectic cells, with the best positioning being of the sample inoculated with the classical system, CaAlFeSi.

D. Final conclusion

Following the qualitative evaluation of the metallographic structure, it was found that the samples have certain areas characterized by a structural constant. These surfaces are located in two characteristic areas of the samples, i.e. approximately halfway between the thermocouple and the small base of sample, and halfway between the thermocouple and the large base of sample. Following these observations, it was decided that quantitative analyzes should only be carried out at the lower surface of the samples at a distance of ~ 9−10 mm from the small base of the QuickCupTM samples.

4.1.6.2 *Quantitative metallographic optical analysis*

According to the ones mentioned in the qualitative metallographic analysis (subchapter 4.1.6.1) at quantitative structural metallographic analysis of the samples, images located at distances of 8,87−9.76 µm from the small base and approximately 9 µm from the thermocouple were used (for analysis of graphite and for base metal matrix). For the analysis of eutectic cells, images situated at a distance of 6,66-9.98µm from the small base of sample were selected.

A. The graphite

After the automatic image analyzes, the results obtained for them were tabulated. *Fig. 4.16.* shows the results of the graphite analyzes, presented graphically, namely: the area occupied by graphite; the shape, distribution, nodularity and dimensions of graphite together with its morphological characteristics.

The generated report presents a position in which the graphite, formed in the uninoculated sample, is the most deficient, a situation illustrated by: a) the large number of particles detected, b) the smallest graphite separation area, c) the predominant graphite shape being the compact one and e) the graphite size being small all this generating a large nodularity (~24%) for a gray cast iron.

For the sample treated with the LaCaAlFeSi complex system nucleated a number of 249 inclusions (approximately 25% more inclusions than to the classical inoculant), but the area occupied by them (14.55% of the microstructural area analyzed) is very close to that resulted from the treatment with the classic inoculant. Over 60% of the particles are small in size, between 15−30µm – and about ~37% between 60−250µm – but the degree of nodularity is almost 2 times

lower than that of the uninoculated cast iron (~13%), their shape being predominantly type II and I (according to ISO 945). The sample inoculated with the clasical inoculant, CaAlFeSi, has the lowest number of inclusions formed (189) but the largest area occupied with graphite (~15,9%). The preponderent form of graphite is type I (~54.6%, followed by type II with ~ 30%) and ~49% of the graphite lamellae have dimensions between 60−250µm, the nodularity (the smallest) reflecting also a good development of graphite lamellae (~8.8% nodularity).

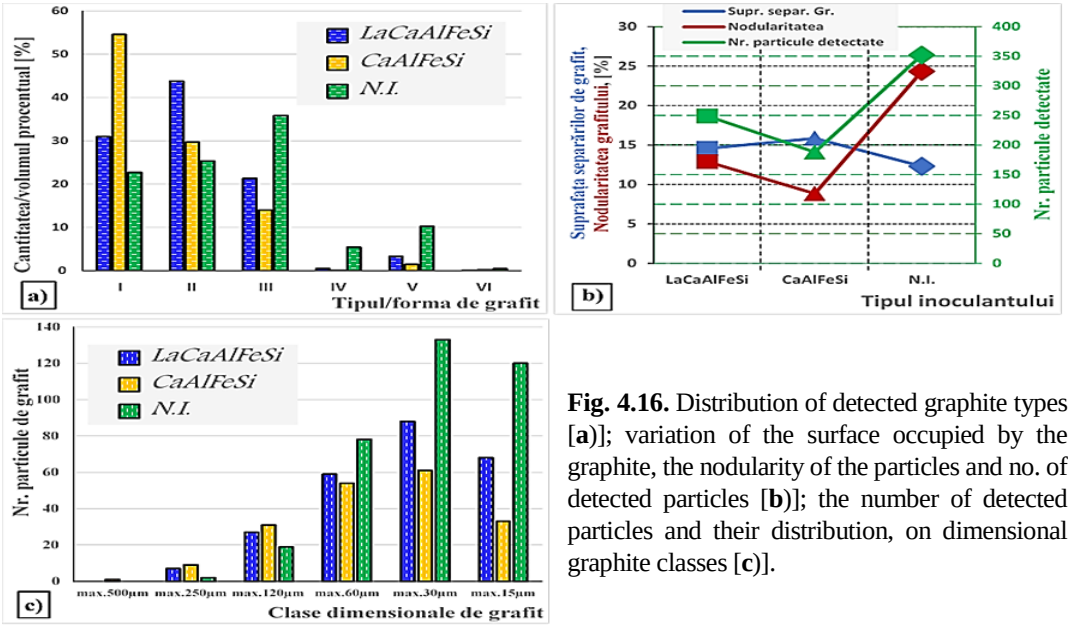

Fig. 4.16. Distribution of detected graphite types [**a**)]; variation of the surface occupied by the graphite, the nodularity of the particles and no. of detected particles [**b**)]; the number of detected particles and their distribution, on dimensional graphite classes [**c**)].

The results obtained in the case of the microstructural analysis of the graphite - from the point of view of the number of graphite particles formed - are confirmed by the thermal analysis of the cooling curves, through the parameters GRF1 and GRF2 (which show a superior graphitizing position of the inoculating with LaCa), while those regarding the formed graphite surface are confirmed by the graphitization constants (K'gr and K "gr) obtained in the case of preliminary chemical analysis.

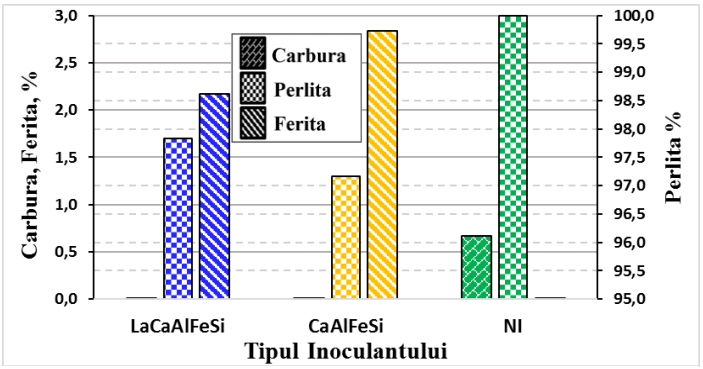

Fig. 4.17. The characteristics of the base metal mass (ferrite, pearlite, carbides) depending on the type of inoculant used

B. The analysis of the base metal mass

Data of the analysis of the basic metal mass (see *Fig. 4.17.*) reveals that the experimental castings have a pearlitic structure. The uninoculated cast iron has a pearlitic matrix but presents, in the analyzed area, carbures (with values of 0.67%, from the surface). The inoculated cast iron have a pearlite-ferrite metal mass, with pearlite of ~97.8%, for the inoculated cast iron with the complex system, and ~97.2%, for the one treated with the classic inoculant. Consequently, the average amount of ferrite is at values of ~2.2% (more advantageous, in terms of efficiency) for the inoculant LaCaAlFeSi and 2.8% respectively for the inoculant in the CaAlFeSi system, results that confirm the results obtained in the preliminary chemical analysis - by the parameters of pearlitization (Px) and ferritization (F/%) - but also the analysis of the graphite, by the fact that an increased capacity for the formation of the ferrite is specific to graphite inclusions with the greatest dimensions (obtained, as seen, in the case of the system CaFeSi).

C. Analysis of eutectic cells

The results of the automatic analysis (using 2 cross-intercept lines - arranged at a distance of 1700 µm - each with a length of 4434.37 µm) of the structural images are rendered in **Table 4.25**.

Table 4.25. Characteristics of eutectic cells detected in experimental cast irons

Nr. Crt	Inoculant type	Total size (length) of the analysis line, [µm]*	The number of grains, 1/cm	The average grain size, [µm]
1	***LaCaAlFeSi***	8868,45	19	466,77
2	***CaAlFeSi***		21	422,32
3	***N.I.***		17	521,69

According to them – compared to the reference sample – both of inoculated castings have a greater number of eutectic cells, which confirms the inoculation action of the graphitizing modifiers. Regarding the positioning of the two inoculants used, although the complex LaCaAlFeSi has produced, compared to the reference sample (uninoculated, 17 cells 1/cm), a better degree of cell finishing with ~ 10% (a number of 19 grains , 1/cm) it is surpassed – as a level of performance – by the classic inoculation system, CaAlFeSi, with which a degree of cell finish (compared to the uninoculated sample) was obtained with ~ 20% (a number of 21 of cells, 1/cm), respectively a dimension of cells of 422 m compared to 522 m in the case of untreated sample.

4.1.7. Brinell hardness

For the determination of Brinell hardness, and for the realization of impressions, the halves opposite to those used for metallographic analysis were selected for the analysis. After their preparation, the impressions were made using force (178.5kgf) applied to a steel ball with a diameter of 2.5 mm, for a period of 5 sec.

The results obtained - determined at a distance of 9 mm from the small base of the samples, as well as those of the average hardness (for each sample) - after determining the dimensions of the impressions, and transforming them into Brinell hardness values, are rendered in *Figure 4.21*.

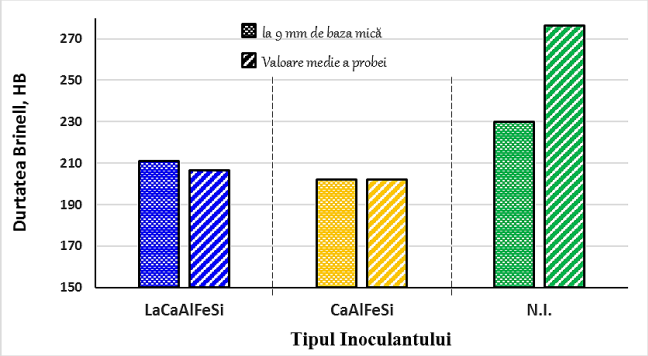

Fig. 4.21. Corelația între valorile durității Brinell de la înălțimea de 9mm față de baza mică și cele obținute pe toată înălțimea probelor, pentru fontele experimentale analizate

The analyzes performed previously as well as the present ones highlight that the treatment process applied to the experimental cast iron has removed the phenomenon of carbides formation (present in the case of uninoculated castings) so that, in the inoculated cast irons, the variation of the hardness values is due – and in association with other factors – the variation of the pearlite-ferrite ratio (highlighted and previously within the chemical analysis, indirectly through the pearlitisation factors, *Px*, and by the ferritisation ones, *F*) as well as the dimensions and type of the formed graphite (highlighted by the structural analysis of the graphite in the microstructure of the cast iron). Regarding the inoculated castings, in the case of the clasical treatment (with the CaAlFeSi system), its lower positioning is visible, compared to the treatment performed with the complex system LaCaAlFeSi, through which a more efficient control over the amount of ferrite formed and the removal of carbides has been achieved.

Comparative analyzing the two sets of data obtained - the averages of the hardships on the entire sample and the values of the hardness obtained at a distance of ~ 10 mm from the small base (see fig. 4.21) - for the inoculated cast irons with the two inoculant systems, it is noted that there is a good correlation between them, the differences between these data sets not essentially influencing the ability to characterize the properties of hardness in the sample analyzed. In conclusion, the data set obtained from the analysis performed (at the height of ~ 10mm from the small base) can be used in the study of the subsequent experimental program, in order to carry out a classification of treated cast irons and in order to establish their performance level.

Following all the analyzes designed and realized for experimental Program I, a comprehensive analysis was carried out in order to be able to give an overall conclusion on the performance of the studied

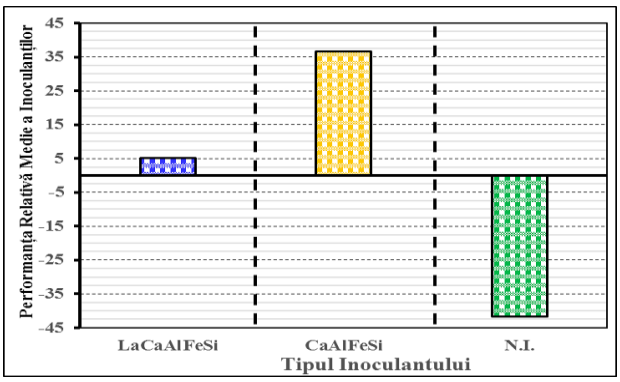

Fig. 4.22. The average relative performance of the inoculants, obtained from the realization of various types of analyzes (thermal, microstructural and hardness), for the analyzed experimental cast irons

cast irons. From the average performance data, corresponding to the inoculated experimental cast irons - analyzed compared to the uninoculated cast iron - it is observed that the inoculant treatment applied to the experimental castings had a positive effect on the properties of the cast samples, so that the characteristics of the inoculated tests have been improved to a considerable extent: from a (negative) performance level of ~- 41% of the uninoculated cast iron there was a significant change in the quality of the castings, which show increases of ~ 78% (for the cast iron treated with the inoculant CaAlFeSi, to an average relative performance obtained of 36,68%) and ~ 47% respectively, for the case of treatment performed with the complex inoculant system LaCaAlFeSi (at an average relative performance obtained of 5.12%).

4.2 Research on the modification of the solidification process of hypoeutectic gray cast irons, by inoculants containing La in association with various other active elements (Ba, Zr, Ti), [Experimental Program II]

4.2.1. The parameters of the experimental program

From the point of view of the main practical implementation coordinates of the elaboration and casting of samples, within the thermal ratio, the furnace discharge (after the processing of cast iron) and the casting of samples in molds was made at temperatures very close to those established by the experimental program, also, 12 samples were obtained in ceramic cup molds – duplicated with the same inoculant in 2 ceramic cups to ensure certainty of data acquisition – and an OES type sample, with no missed samples during casting.

4.2.2 Physical characteristics of casted samples

After knocking-out of mould of the samples and obtaining their characteristics, the data obtained were analyzed in order to select - from each type of experimental inoculant - of one of the 2 cast samples that correspond at the best qualitatively (in terms of their characteristics: the quality of the registered cooling curve, casting defects, filling degree, etc.) to the research objectives.

4.2.3 The chemical composition of the elaborated castings and control parameters

Since the inoculation process was done in moulds it was no longer possible to take OES samples before inoculated samples were poured, thus limiting the analysis of the composition of the experimental cast iron to the results obtained after the correction of the composition of the processed cast iron. These data were used for the determination of specific parameters of the chemical composition and detailed characterization of the obtained cast iron.

Table 4.32. Specific parameters of experimental cast iron, determined on the basis of chemical composition, for experimental Program II.

Heat	Perlitization Factor	Feritization Factor	Corelation between Mn and S			Graphitization Constants		Eutecticity Degree		Elem. chim.
	Px	*F/%*	*Mn/S*	*(%Mn) X (%S)*	*ΔMn*	*K'gr*	*K"gr*	*CE [%]*	*Sc*	*Si*
I	7.28	0.67	24.17	0.00825	0.1017	0.75	1.00	4.11	0.965	1,11

The elaborated cast iron is (see **Table 4.32**) in the range of hypoeutectic cast irons, with CE <4.3% and Sc <1.0 corresponding to a specific range of gray cast iron, namely type 250. [200] Intentionally the composition contains a very small amounts of sulfur (<0.02%S) and residual Al (<0.002%), as well as

control parameter values (%Mn)x(%S) < 0.008, Mn/S< 25 and ΔMn <0.15, all of which are adapted to the creation of critical conditions for the solidification process, from the point of view of the eutectic undercooling. In this way it becomes possible to evaluate more accurately and to distinguish more precisely the effectiveness of each system of inoculant variant tested.

4.2.4. The actual consumption of inoculat

Since an essential parameter for the properties of the treated cast iron is the degree of assimilation of the inoculant introduced into the melt, by calculus, the actual consumption of inoculant was determined.

Table 4.33. Actual inoculant consumption of the samples casted with inoculated experimental cast iron

Nr. Crt.	INOCULANT				
	Inoculant system	*Active element*	*Theoretical quantity*	*Percentage*	
				Theoretical	*Real**
			[g]	*[%]*	*[%]*
1	**La**	***La, Ca***	0,37	0,10	0,10017
2	**LaZr**	***La, Ca, Zr***	0,37	0,10	0,10004
3	**LaBa**	***La, Ca, Ba***	0,37	0,10	0,10620
4	**LaBaZr**	***La, Ca, Ba, Zr***	0,38	0,10	0,09273
5	**LaZrTi**	***La, Ca, Zr, Ti***	0,39	0,1054	0,11097
6	**LaBaZrTi**	***La, Ca, Ba, Zr, Ti***	0,4	0,1054	0,10758

* - without Titan addedt; with Ti added.

Analyzing these results – although the variations are quite small – it is noted that the samples inoculated with La and LaZr are very close to the projected values, while for the inoculants of LaBa, LaZrTi and LaBaZrTi the values are higher (with differences from the reference of about 0,6; 0,5 and 0,2% respectively). In contrast, the LaBaZr inoculant system has the biggest difference from the reference one, which is about -0,8% (being underinoculated).

4.2.5 Thermal analysis of cooling curves

The careful measurement and analysis of representative temperatures (TAL, TSEF, TEU, TER, TES) led to the identification of specific effects produced by the various variants of inoculant systems tested. The first derivative of the cooling curve also provides other information through the TEM, FDES, GRF1 and GRF2 parameters.

Table 4.34. The representative parameters of cooling curves, the specific parameters of their first derivative and the graphitic factor (GRF1)

Inoculant type	Parameters of cooling curves [°C]						Parameters of first derivative [°C/s]		GRF_1 [sec]	GRF_2 [∠]
	TM	*TAL*	*TSEF*	*TEU*	*TER*	*TES*	*TEM*	*FDES*		
La	1288.2	1162.3	1157.1	1145.3	1147.6	1110.6	0.094	-5.2	74.5	9
LaZr	1295.3	1161.8	1156.0	1145.1	1147.3	1108.7	0.101	-4.7	66.2	11,25
LaBa	1293.9	1161.8	1155.5	1144.8	1147.5	1107.7	0.123	-5.2	64.2	8
LaBaZr	1278.2	1162.5	1156.4	1145.1	1146.8	1104.3	0.092	-4.6	62.9	10,25
LaZrTi	1264.3	1162.3	1155.2	1144.8	1147.2	1105.8	0.095	-4.7	59.6	10
LaBaZrTi	1261.3	1163.3	1154.7	1144.9	1147.5	1109.6	0.114	-5.1	60.8	8,5

The optimum capacity to increase the value of the TAL parameter, and respectively to promote the formation of austenite dendrites, was obtained by treatment with the inoculant of the LaBaZrTi complex system followed by LaBaZr inoculant. Active elements such as Ba, Zr and/or Ti, seem to increase the capacity of the inoculants based on La to promote the early nucleation of austenite, thus improving the quality of castings.

Generally high values of TEU and/or TER parameters, especially when there are critical solidification conditions, lead to improved structural properties, by preventing carbide formation and promoting the graphite formation of type A. The effects exerted on the castings of the various variants of compared inoculants are characterized by very close values – for parameter TEU =1144.8-1145.3°C (with a maximum variation of 0.5°C) and for TER = 1146.8-1147.6°C (with a maximum variation of 0.8°C) – but which presents specific positions that allow to establish the effects they have on the eutectic reaction. For the beginning of the eutectic reaction, the inoculating system La, is the most effective

while, for the end of the eutectic reaction the alloys in the LaBaZr system have optimal effect. A special mention can be made about the element of Zr, which has the ability to improve the entire visual spectrum - corresponding to the cooling curve - of the eutectic reaction.

Taking into account all the representative parameters of the cooling curve positively influenced by inoculation, an overall performance level of the inoculants tested could be established: the FeSi-based alloy with La being in this respect in the best position. Inoculants of different compositions can also be considered, on the basis of the specific beneficial effects obtained, such as: promotion of solidification of dendritic austenite (by the inoculant LaBaZrTi) or the lowest degree of eutectic realescence (ΔTr, obtained with inoculant LaBaZr) (see *Fig. 4.26.*).

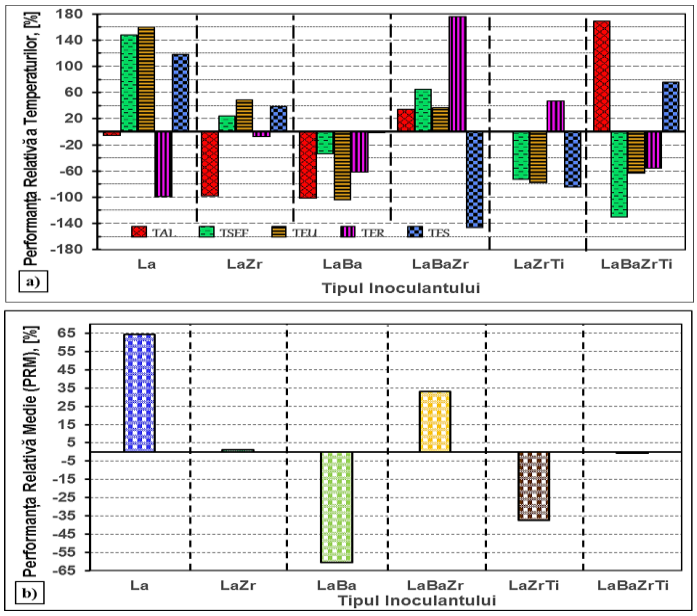

Fig. 4.26. Variația performanței relative a inoculanților experimentali în funcție de parametrii reprezentativi ai curbelor de răcire (**a**) și variația performanței relative medii (PRM) pentru fontele inoculate (**b**)

Obtaining additional data on the characteristics of the solidification of the cast iron (by means of thermal analysis) – specifically related to the eutectic reaction and the conditions existing at the end of solidification – requires reporting of the temperatures of the TEU parameters, TER and TES at equilibrium eutectic temperatures in the stable system (Tst) and the metastable system (Tmst), respectively (see *Fig. 2.9. a.*). The new resulting parameters are referred to by the term "degree of undercooling at solidification" for the different solidification moments, which are shown in **Table 4.36.** and *Figure 4.27*. In this way, it is possible to carry out a more accurate assessment and to obtain direct information on the sensitivity of carbides formation and also to assess the possibility of unexpected events which could occurre when the solidification process is in evolution.

Table 4.36. Representative parameters of undercooling in inoculated experimental cast iron

Inoculant system	Representative arameters of undercooling							
	ΔTm	***Tst***	***Tmst***	***ΔT₁***	***ΔT₂***	***ΔTr***	***ΔT₃***	***ΔTs***
La	15.13	1160.4	1133.7	11.66	13.92	2.26	-23.09	26.8
LaZr	15.36	1160.4	1133.7	11.43	13.67	2.24	-24.97	26.8
LaBa	15.67	1160.4	1133.7	11.11	13.82	2.71	-25.92	26.8
LaBaZr	15.38	1160.4	1133.7	11.40	13.18	1.78	-29.36	26.8
LaZrTi	15.62	1160.4	1133.7	11.17	13.53	2.36	-27.89	26.8
LaBaZrTi	15.59	1160.4	1133.7	11.20	13.80	2.60	-24.10	26.8

As a general situation, all experimental cast irons (treated with tested inoculants and casted) are susceptible to graphite solidification, with favorable conditions for carbon precipitation in the form of graphite and not of carbides during solidification, which illustrates the effectiveness of all tested inoculants. Also on this type of parameters can be applied the mathematical processing specific to the determination of relative performance (using the *relation 2.30*), for each type of inoculant used (see *Fig. 4.29.*). According to the performance analyzes, the reference inoculant, with La, has the best performance in terms of the parameters ΔTm and ΔT_1, followed by the LaBaZr inoculating system, and then by the LaZr system, in terms of relative average performance. Unfavorably placed systems being, in order, LaBaZrTi and LaZrTi, while the system with the worst results being the one with LaBa.

The parameter GRF1 provides information about the graphite formed immediately after the maximum of the realescence (TER) is reached – expressed by the time recorded from the time when the maximum value of the eutectic recalescence is reached to the time when the maximum value of TER decreases by 15°C – a high value of this parameter indicating the fact

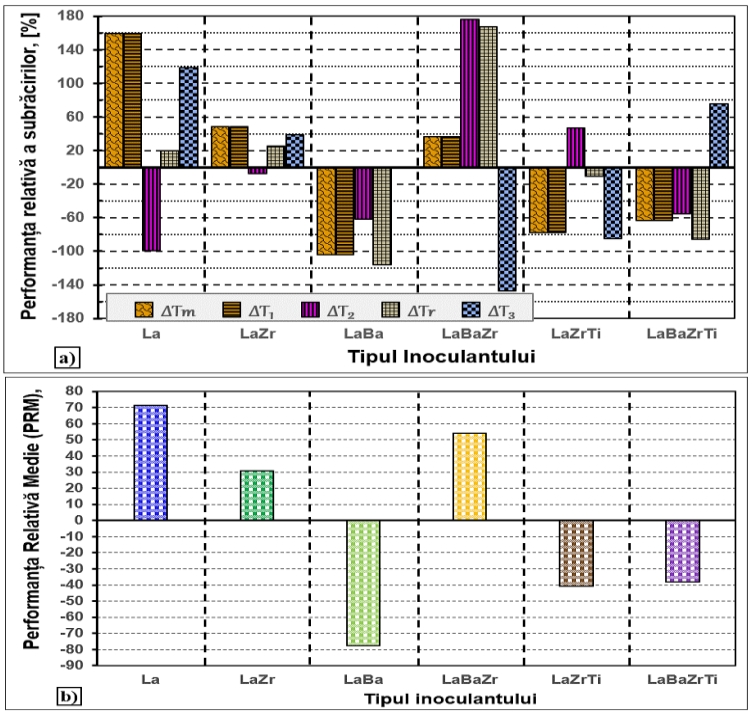

Fig. 4.29. Relative performance of inoculating systems tested in terms of degree of the undercooling parameters (**a**); and average relative performance of the undercooling parameters for experimental inoculants (**b**)

that nucleation and eutectic growth, respectively, have been manifested for a long time, lead to the formation of a larger amount of graphite. The GRF2 graphitization factor is the speed at which the cast iron crosses the complete solidification area, being measured with reference to the FDES point (of the first derivative) and the angle formed by the sides of this lower pick. Low values of this factor indicate the formation of a large amount of graphite at the end of the eutectic solidification process.

The TEM parameter ([-C/sec], being the maximum speed of the recalescence, determined on the first derivative of the cooling curve) forms an overview of how graphite formation proceeds at the beginning of solidification. From this point of view, a high value of the maximum speed of the recalescence designates the amount of graphite formed at the stage of the eutectic transformation. A very high TEM value, however, can also mean the formation of too much graphite at the eutectic transformation, which could be negative (possibly manifested in the case of the LaBaZrTi and LaBa inoculant systems). According to the results obtained, TEM it is situated in a low range (0.0926−0,123 ºC/s), which indicates a low sensitivity, but also (see *Fig. 4.32.*) the fact that the lowest speed of the maximum recalescence – so positive effect – has the inoculant LaBaZr followed by La, the inoculant LaBa having the worst effect (highest value).

The results obtained for parameter GRF1 – for all inoculating experimental systems – are situated in a high values range and appear to be quite sensitive, compared to the active elements introduced into the inoculating systems used. From this perspective, the inoculant LaCaAl has the best inoculation ability and is recommended to be used for general applications.

The graphitization factor GRF2 and the value of the first derivative at the end of the solidification (FDES) illustrate the behavior of the cast iron at the end of the solidification, these parameters being in close connection. The high thermal conductivity causes more reduced (more negative) values for FDES (which also indicates the possibility of avoiding shrinkage) but also lower (therefore optimal) numeric values for the GRF2 parameter. From *Fig. 4.32.* it is noted that the effect of inoculation, in the case of the GRF2 factor, is the best for the case of the inoculating system LaBa, followed by LaBaZrTi and then by the reference inoculant, with La. The weakest positioned is the LaZr system, followed (almost at equality) by LaBaZr and LaZrTi. Regarding the FDES factor, the best results were almost equal for inoculating systems La, LaBa and LaBaZrTi, and the most inefficient (from this point of view) being LaBaZr. Thus, through the similar results between FDES and GRF2, the large amount of graphite obtained at the end of the solidification (of the studied experimental cast iron) is confirmed.

An additional observation, drawn from *Fig. 4.32*, would be that although the speed of recalescence (TEM) in the case of the inoculant system of reference (with La) is close to those of the LaBaZr and LaZrTi systems – and the amount of primary graphite solidified (determined by the parameter GRF1) is the highest in the case of the La system – the system position at the end of solidification (FDES) is negative of higher value compared to the other two systems. Which means that although most graphite is formed at the beginning of the solidification process – in a fairly long period of time (but with the highest efficiency, given that the LaBaZr and LaZrTi inoculating systems

formed, in about the same period, less graphite) however, there remains a large amount of active nuclei in the cast iron so that it forms, and in the end of solidification process, carbon in free state.

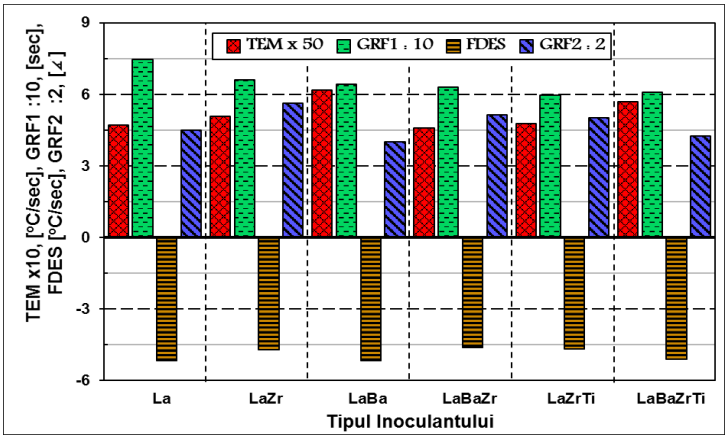

Fig. 4.32 Representative parameters (TEM x 10, [°C/s]; FDES, [°C/s]) of the first derivatives of cooling curves and graphitization factors (GRF1 : 10 [sec]; GRF2 : 2 [∠], for inoculated experimental cast irons.

The results confirmed the efficiency of the thermal analysis method (of cooling curves), which contributes to the assessment of the capacity of the active element lanthanum, introduced into gray cast iron, to promote the formation of graphite under critical solidification conditions; conditions commonly encountered – in the case of various types of gray cast iron castings – in industrial production processes such as: high melt overheating values and low active elements content (such as S and Al) in the formation areas of graphite inclusions.

4.2.6. Metallographic structural analysis

4.2.6.1. Quantitative structural analysis: Principles

This analysis is carried out in the light of the recommendations of the manufacturer of the cooling curve analysis software, ATAS-NovacastTM [194], namely that the properties of the cast material in this type of mould (if investigated at a distance of 10 mm from the thermocouple) they are similar to ones of a cylindrical sample with a diameter of 30 mm. So that, following their verification – carried out in experimental Program I – it was decided to abandon the use of the analysis variant shown in *Fig. 4.33.a* (respectively the structural analysis in the 3 areas of the sample) and to adopt the use of the method shown in *Fig. 4.33.b*, because they provide sufficient quantitative and qualitative results, these presenting a high level of confidence.

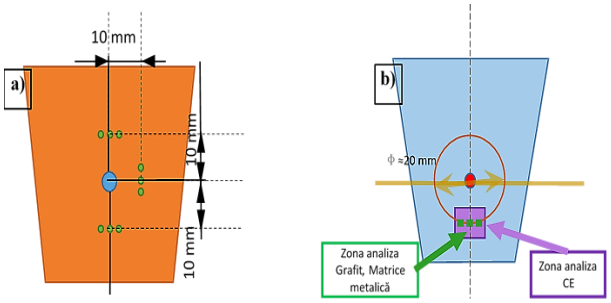

Fig. 4.33. The diagram of the principle applied to quantitative analysis which has been performed: **a**) so that images are acquired in order to comply with the recommendations made by ATAS-Novacast; and **b**) the work variant selected after testing the ATAS recommendations

4.2.6.2. Microstructural analysis of graphite

The results of the microstructural analyzes of graphite – the mean values of the 3-point analyzes performed out on each sample – respectively for: the determination of the graphite occupied areas (from the total surface of the analyzed area, from the sample), of the morphology and of the dimensions of the graphite, which are presented in **Table 4.39**. Relative to the size class distribution of particles detected in automatic image analysis, most particles (~73% to 83% of the total particles identified) are those positioned within the small size range (between 30µm and 15µm) that was expected. However, an appreciable amount of graphite formed is within the lamellae lengths range of 60-250µm: in the case of LaBaZr inoculated iron is ~20 % of the total particles detected, for LaZrTi inoculation is ~26 %, while the best positioned is the LaZr inoculant (with ~27 %).

In order to establish the general positioning of the inoculants, in terms of graphite analysis, the relative performance method shall be used. Thus, using the results obtained in: a) determining the total area of graphite, b) the sum of the distribution of forms I and II of graphite, as well as c) of the

number of particles that have dimensions between 250-60 µm, a classification is established - in depending on the resulting performance - of the experimental inoculants (see *Fig. 4.38.*).

Table 4.39. Microstructural characteristics of graphite in the experimental cast irons

Nr. Crt	Inoculant type	Forms of graphite identified in samples						Surface of Graphite	Nodularity of graphite	Dimension of graphite lamellae**						Total no. of particles*
		I	II	III	IV	V	VI	[%]		Size 3	Size 4	Size 5	Size 6	Size 7	Size 8	
		Distribuţie procentuală, [%]								max. 500µ	max. 250µ	max. 120µ	max. 60µm	max. 30µm	max. 15µm	
1	La	36.25	36.77	14.63	3.13	8.00	1.23	11.64	29.06	0	5	24	55	98	255	437
2	LaZr	42.97	19.69	23.47	7.00	6.09	0.77	11.71	23.21	0	6	34	70	100	195	405
3	LaBa	24.29	41.90	25.98	2.43	4.89	0.51	13.78	15.70	0	6	18	71	166	306	567
4	LaBaZr	48.55	36.68	9.84	1.59	2.48	0.86	17.13	18.20	0	13	39	57	96	339	544
5	LaZrTi	30.90	41.49	20.73	3.12	3.34	0.43	14.66	20.85	1	5	29	59	83	178	355
6	LaBaZrTi	36.35	36.27	18.54	4.83	3.72	0.30	13.16	14.39	0	11	16	74	138	296	535

* the average number of particles determined on the analyzed fields (on 3 fields analyzed, in each sample)
** - number of particles detected within each group of dimensional classes

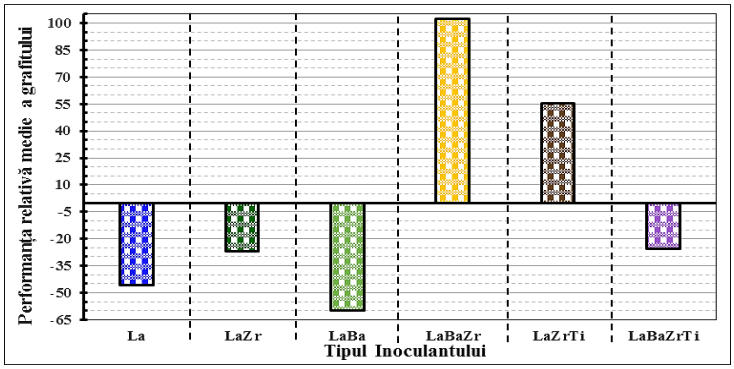

Fig. 4.38. The average relative performance of inoculants according to the metallographic analysis of the graphite

According to these results, the most well-positioned is the LaBaZr inoculating system, which is followed by the LaZrTi system. The system made from the LaBa mixture is most unfavorable, followed by the one without any other active elements added (the reference one, only with La). The following can be noted: that for La in combination with Zr the results obtained are better (as reference being the La and LaBa systems), but the combination of the active elements La, Ba and Zr, gives superior optimal results. Thus, it seems that the addition of Zr has a positive effect in all the inoculating systems in which it is introduced. In addition, it is observet that the additional addition of Ti (in the LaZrTi and LaBaZrTi system) reduces the performance obtained, "in steps": a) more strongly for the LaBaZrTi mixture (greatly reducing the efficiency of the inoculating system) and respectively, lower for the LaZrTi mixture, for the type of samples analyzed.

4.2.6.3. The base metal matrix

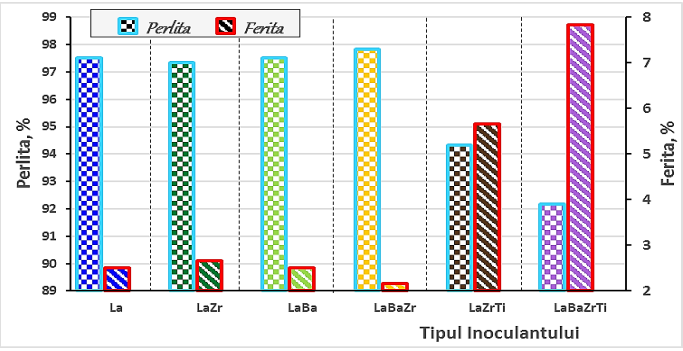

Fig. 4.39. Variations in ferrite and perlite proportions, as determined in the samples analyzed, relative to the type of inoculant used

Analyzing the results obtained for the base metal matrix, the first remark that can be made is that the results of the thermal analysis are confirmed by the fact that the formation of carbides in any experimental inoculant system has not been detected. A second observation, expected by the way, is that a large amount of perlite has been detected in all the samples, a notable difference, however, is the appearance of ferrite in a larger quantity, for the LaZrTi and LaBaZrTi systems (5.67% for the first system and 7.83% for the second). The best positioned system is LaBaZr, followed by the LaBa and La, on a tie, and then by the LaZr system, which confirms the results obtained in the analyzes performed for the graphite structure.

4.2.6.4. Eutectic cells

In order to achieve better accuracy of the results, analysis of the solidified eutectic cells was carried out - using the acquired metallographic images - by automatic image analysis using 2 lines of interception (horizontal) arranged at a distance of 1700 µm between them. The numerical results obtained in this analysis are presented in **Table 4.43**. According to these, the number of eutectic cells formed is relatively small, the variation in the number of grains, depending on the inoculating system, being situated in a range between 10 − 22 grains, 1/cm. In the most favorable position is the LaZrTi inoculant system, which formed the most numerous eutectic cells (of the smallest size), followed by LaBaZr (confirming the results of previous positive analyzes) and then by the LaBa and La systems. The systems in which the conditions most unfavorable to grain formation were created - by the formation of larger eutectic cells - are LaZr and LaBaZrTi (with the weakest position), respectively.

Table 4.43. Microstructural characteristics of eutectic cells of inoculated cast irons

Nr. Crt	Inoculant type	Totale size (length) of the analysis line, [µm]*	No. of eutectic cells, [1/cm]	Average dimension of cells, [µm]
1	***La***	8868.45	16	554,3
2	***LaZr***		14	633,48
3	***LaBa***		17	521,69
4	***LaBaZr***		20	443,44
5	***LaZrTi***		22	403,13
6	***LaBaZrTi***		10	886,88

4.2.7 Analysis of mechanical properties: Brinell hardness

The determination of the hardness of HB was performed over the entire height of the samples and an analysis of the average results on the sample was subsequently carried out and compared to the result obtained in the area closest to 10mm to the center of the thermocouple. The results of the transformation of impressions, produced on the surface of the samples, into Brinell hardness values are shown graphically in *Fig. 4.41*.

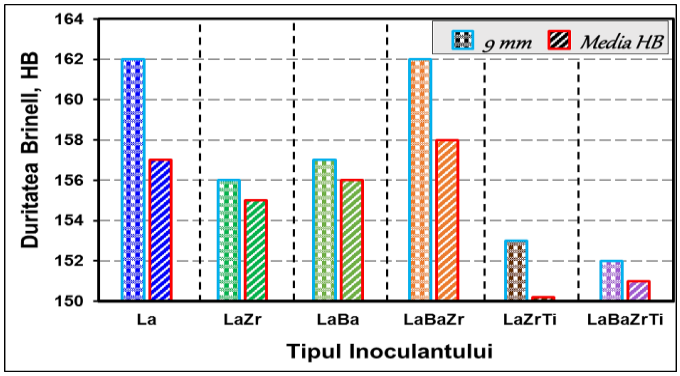

Fig. 4.41. Variația durității Brinell în zona înălțimii de 9 mm a probelor și valoarea medie a durității pe înălțimea probelor (determinată pentru fiecare probă) pentru fontele experimentale inoculate

According to the results obtained for the HB hardness throughout the sample - by analyzing the mean value of all traces obtained, on the sample - the worst positioned, having the same hardness value, are the samples inoculated with LaZrTi and LaBaZrTi respectively, then (also on equality) those treated with the La and LaZr systems, which confirms the results obtained in the analysis of the ferrite and perlite. The most effective inoculating system, from the point of view of hardness, seems to be the LaBaZr system followed by the LaBa system. By comparing the average hardness value determined over the whole sample with the hardness value obtained at a distance of ~10 mm from the thermocouple it is noted that the positioning – in terms of performance – of the castings analyzed, in relation to the inoculant used, are equal in the case of systems with La and LaBaZr respectively.

4.2.8 Analysis of the performance obtained according to the different types of analyzes performed

Correlations between the results obtained for the analyzes carried out under the experimental program are shown in *Figure 4.42.* in order to establish the inoculant system with an optimal effect on the treated castings.

The correlations, made between the results obtained for the different types of analyzes performed, show in the best position the inoculant LaBaZr system, because it has a high hardness, a

number (not the highest) of eutectic cells, the least ferrite formed, and also balanced characteristics of the formed graphite (in terms of the surface and the type of graphite). Well positioned is the LaZr inoculant system, followed by the reference system (La) and LaZrTi. Poorly positioned is located the inoculant LaBa, due to the undercooled graphite formed in large quantities and a smaller grains number (which creates premises for low hardness) while the weakest positioned is the LaBaZrTi system (especially due to the excess ferrite and of the low number of eutectic cells).

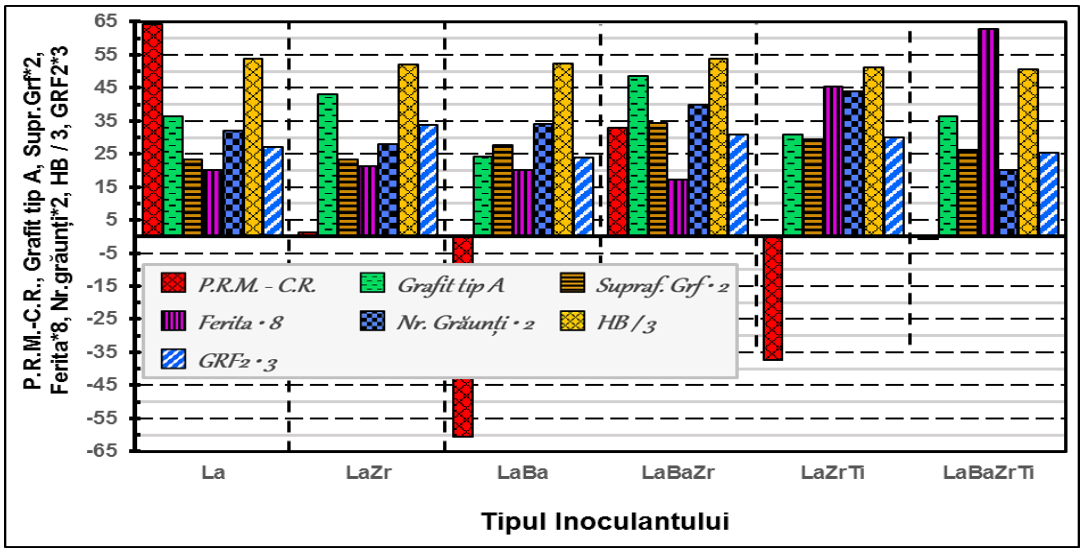

Fig. 4.42. Correlations between: the average relative performance of the main parameters of the cooling curves (P.R.M.-C.R.); the amount of graphite type A; the surface of the graphite (Surf.grf. * 2), ferrite, (ferrite *8), number of grains (Grains No.*5), hardness (HB /3) and factor GRF2 (GRF2 *3) for inoculated castings

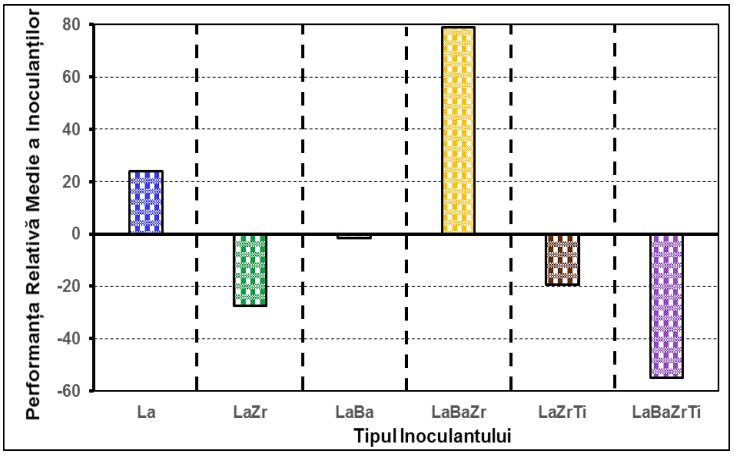

Fig. 4.43. Performanța Relativă Medie a sistemelor inoculante experimentale, pentru Programul Experimental II

Figure 4.43. shows the positioning of the inoculants in relation to the calculation of the average relative performance of inoculants using the results of the various analyzes performed: the average relative performance of the cooling curves of the primary parameters (TAL, TSEF, TEU, TER, TES); parameter GRF2; characteristic analyzes of graphite (type and surface of graphite formed); base metal matrix and eutectic cells.

It is mentioned that, in order to establish the optimal inoculant, parameters with different types and degrees of influence (each acting specifically in cast iron on quality characteristics) have been used in evaluation of the cast iron, and from this point of view cannot be realistic (for all conditions of practical use of cast iron) compare only by associating and quantitatively observing the results. However, this presentation has only an overall qualitative assessment value of the treated cast irons obtained. In this regard, from the results of the average relative performance obtained, it is noted that the LaBaZr inoculant system has a maximum efficiency on the process of solidification of inoculated cast irons, which is followed by the inoculating system La. The LaBaZrTi inoculant system has the lowest capacity of action on the melting, followed by LaZr and then by the LaZrTi system. Well positioned – having only a small negative value (-1.61) compared to LaBaZr and La systems – is also the LaBa system, fact which confirms the combined beneficial action of the two active elements (La and Ba) in the inoculated cast irons.

4.3 In-depth research, using the SEM-EDAX method, about the mode of nucleation and solidification of graphite in overinoculated hypoeutectic gray cast irons, in the case of using different inoculant systems, with and without La, in order to highlight the action of La during the formation of the solidification structure of castings [Experimental Program III]

The experimental program III is centered on the study of commercial gray cast irons – inoculated with various active elements – in order to determine the nature of the graphite nucleation areas, the specific distribution of the elements and the possibility for the existence of a particular compound in the layer at the nucleus-graphite interface, all this with the objective of: assessing the nucleation potential of graphite; examining the place and role of La in the process of solidification of gray cast iron; of identifying additional data and information; and verifying the results obtained in previous research.

4.3.1. Preparation of heats, type of samples and analysis

According to the data – of melt processing and casting – it is generally noted a high temperature of the cast iron at the discharge from the furnace, as well as the fact that the inoculation process was carried out at temperatures around 1420°C. According to the nomograms for determining the casting temperature – used to determine the temperatures required for sample castings[46] – this temperature is not used in industry (typically being used temperatures between 1280-1320°C). The high temperature, selected for use in this experimental program, is used for the purpose of ensuring the most efficient assimilation of the inoculant.

4.3.2. Physical characteristics of castings

The data of the characteristics of the castings reveal that, compared to the theoretical weight (500g), the casted samples obtained had larger dimensions, which would normally have created an underinoculation of the cast irons, ranging from 3-7% wt. In this case, however - due to the fact that the inoculant was introduced in large quantities, in order to achieve overinculation - the overinoculating phenomenon cannot be removed by the relatively small weight variations of the samples.

4.3.3. The chemical composition of the elaborated cast irons and control parameters

After establishing the chemical composition of the casted samples, the specific chemical parameters of the cast iron were determined, with the help of which a characterization of the properties that cast iron possesses is performed, before inoculation treatment and casting into mould (see **Table 4.49.**).

According to the chemical composition data, it is observed that the castings have close chemical characteristics, including equivalent carbon (CE = 4.00−4.10%) and specific control factors regarding the pearlitization factor (Px = 3.97−4.74) and the graphitization constant (K'gr = 5.17−5.53). From the point of view of the graphitization capacity, the relations between the elements that influence the graphitization - respectively S (in relatively low quantity, 0.0307−0.0449%S) and Mn (~0.159−0.428%Mn) - and respectively corelations Mn/S <12, (%Mn) x (%S) <0.02 and ΔMn <0.7, produce medium to low conditions, relative to the potential of nucleation of the graphite when solidifying the experimental castings.

Table 4.49. The specific parameters of the chemical composition for the Experimental program III

Heat	Perlitization Factor	Feritization Factor	Corelations between Mn and S			Constants of grafitization		Eutecticity degree		
	Px	*F/%*	*Mn/S*	*(%Mn) × (%S)*	*ΔMn*	*K'gr*	*K"gr*	*CE [%]*	*Sc*	*Cc*
I	4.57	9.98	11.19	0.0139	0.635	5.53	1.399	4.00	0.94	3,71
II	3.97	18.08	4.66	0.0044	0.391	5.21	1.135	4.05	0.95	3,66
III	4.74	8.10	9.54	0.0192	0.652	5.17	1.136	4.10	0.96	3,67

4.3.4. Characteristics of the experimental program in terms of added inoculant

Considering that the whole inoculant mixture was theoretically assimilated (which did not happen, as seen in **Table 4.53** - which shows the macrostructural images of the samples - but we cannot quantify the unassimilated inoculant) and using the weight data of the casted samples - was performed the calculations to determine the actual amount of inoculant added. From these data, compared to the quantities of inoculants designed to be added, it is noticeable that the differences between the calculated and the real values are not very large, which gives the premises for obtaining viable structures (according to the proposed objectives).

Due the composition, the added inoculant has the ability to bind a large amount of sulfur, which is why additional amounts of sulphur (between 0.099−0.303 gr.) are additionally added into the inoculants (regardless of the amount of sulphur coming from the base cast iron). This is to enhance the possibility of obtaining higher amounts of compounds of the active elements with sulfur and to make them more likely to be detected during SEM analyzes. Even by accumulating the amounts of sulphur introduced into the sample (~ 0.154−0,500 gr) - by means of the processed charge and the inoculant - they do not exceed the total amount of sulphur that the active elements present in the melt can bind (~ 1.85−3.32 gr) metallic. This creates favorable conditions for the possibility of detecting these compounds during SEM analyzes.

4.3.5. SEM - EDAX structural analysis

Following the SEM determinations and inclusions analyzes in the selected samples, the data obtained were centralized, organized and tabulated.

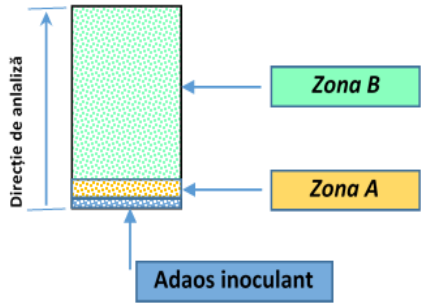

Fig. 4.44. Distinct areas, theoretically identified, in the surface of the samples treated with the experimental inoculant systems

4.3.5.1. Structural analysis parameters

In order to perform the macroscopic analysis of the samples, macrostructural images of the experimental samples were purchased (see **Tab. 4.53.**), after the metallographic preparation. Thus, dimensionaly analyzing the quality of the cast samples, it can be noticed that - despite the high casting temperatures of the samples, for all cast samples, in the area corresponding to the surfaces where the inoculants were deposited are identified large dimensional irregularities. This means that the inoculants were not fully assimilated, which also suggests that the diffusion of the inoculants did not occur uniformly in the body of samples. This fact produces the situation in which there could be 2 distinct areas in the surface of the samples: a) an oversaturated area, with inoculant that did not diffuse towards the upper area of the samples and b) and an area with molten inoculant, and diffused in the structure of the samples. cast iron (see Fig. 4.44.).

Numerous elements were detected in the analyzed samples, therefore, in order to facilitate the understanding of the influences exerted by them, an attempt was made to systematize the combinations of elements possible to form in the cast samples, in the 2 areas mentioned. In order to make it easier to follow the results obtained, they are presented centrally, for all the samples studied, in **Table 4.54.**

Table 4.53. The morphological-macroscopic aspect of the samples after casting and preparation for SEM analysis

	Samples casted and prepared for SEM-EDAX analysis			
The general macroscopic morphological aspect of the analyzed samples	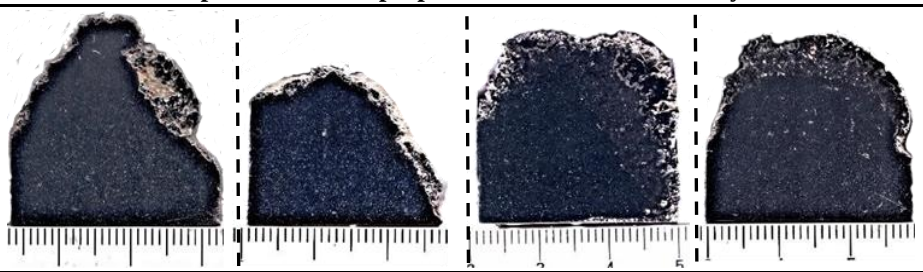			
	Cil. 4	**Cil. 6**	**Cil. 7**	**Cil. 12**

Tablul 4.54. Combinations of elements identified in the analysis of the results obtained, for the determinations performed by the SEM-EDAX method

Inoculant / *Analyzed samples*											
SZrLaBaCaAlSiFe /			**SSrLaBaCaAlSiFe /**			**SrZrLaBaCaAlSiFe /**			**SSrZrMgBaCaAlSiFe /**		
Sample 4			***Sample 6***			***Sample 7***			***Proba 12***		
Inoculant-sample contact area (area A)											
									Mn–O		
Ca–O			Ca–O						Ca–O	Ca–S	
						Ba–O			Ba–O	Ba–S	Ba-O-S
						La–O					
									Mg–O		
						Zr–O					
			Sr–O			Sr–O			Sr–O	Sr–S	
			Al–Si–O								
Fe-Si-Al-O									Fe-Si-Al-O		
									Al-Si-Fe-O		
						Fe-Si-Mn-Al-O					
			Fe-Al-Sr-Si-O	Fe-Si-X							
			Fe-Si-Sr-Al-O	Fe–Si–Al							
Cast iron sample body area (Zone B)											
	Mn-S			Mn–S		Mn-O	Mn-S		Mn-O	Mn-S	Mn-O-S
		Mn-S-O			Mn–S–O			Mn-S-O			Mn-S-O
	Ca-S	Ca-O-S		Ca-S	Ca-O-S	Ca-O	Ca-S	Ca-S-O		Ca-S	Ca-O-S
					Ca-S-O						Ca-S-O
	Ba-S	Ba-O-S	Ba-O	Ba-S	Ba-S-O	Ba-O	Ba-S	Ba-S-O		Ba-S	Ba-O-S
											Ba-S-O
	La-S	La-S-O	La-O	La–S	La–O–S	La-O	La-S	La-S-O			
						Mg-O*	Mg-S*			Mg-S	Mg-O-S
								Mg-S-O*			Mg-S-O
				Sr – S	Sr–O–S	Sr-O	Sr-S	Sr-O-S		Sr-S	Sr-O-S
					Sr–S–O						Sr-S-O
	Zr –S	Zr-S-O				Zr-O	Zr-S	Zr-O-S			
			Fe-O						Fe-Al-O		
			F-Al-O								
Fe-Si-O			Fe–Si–O			Fe-Si-O			Fe-Si-O		
Fe-Si-Al-O			Fe-Si-Al-O			Fe-Si-Al-O			Fe-Si-Al-O		
									Fe-Al-Si-O		

* only 3 Mg inclusions were identified, one of which was in a graphite strip

Subsequently, when the SEM structural determinations were carried out, the above aspects were taken into account and, where appropriate (in the samples showing particular aspects within the meaning of the above), a presentation of the undiffused inoculant area was also made.

As a general observation, two types of compounds were identified in the matrix of the cast experimental samples: oxide type and sulphide type compounds, respectively. Oxidic compounds, of undetermined form, with a high oxygen content in which several elements are identified, but mainly Fe and Si. In the case of sulphide compounds, the Mn-S relationship predominates with a ratio that oscillates in the area of the stoichiometric ratio (Mn / S ≈ 1.7), depending on the presence of other elements with an appetite for sulphur.

4.3.5.2. *Assessment of inoculated samples with experimental inoculant systems according to the analytical criteria established for the SEM analysis*

Next will be presented, the studies and observations made for each inoculating system used - for some of the analyzed surfaces, which have special characteristics - in order to determine the nature of the graphite germination areas, the specific distribution of the elements and, respectively, to trace the potential presence of a certain compound, formed in the layer of graphite-compound interface.

Evaluation of the types of inclusions that could be formed as a result of the interactions between the inoculating elements (Ca, Ba, La, Zr, Sr, Mg) together with Mn, Si and Al from cast iron, with the two main reactive elements (O and S) - existing and / or introduced into the inoculant mixture (the case of addition of

S) - was made based on the associations of the determined elements (by SEM analysis) in the detected inclusions, both in the contact area between the inoculant mixture and cast iron and in the cast iron sample.

A. The sample inoculated with SZrLaBaCaAlSiFe alloy system (*Sample 4*)

A.1 Zone A - surface with inoculant (SzrLaBaCaAlSiFe) not diffused (***Sample 4***)

In this sample, 3 points of interest were identified, in the three mentioned areas: a) at the assimilation limit of the inoculant (see *Fig. 4.45.*, The analyzed surface S.A.1), b) the assimilation area of the inoculant (see *Fig. 4.45.*, the analyzed surface S.A.2) and c) the limit between the assimilation area of the inoculant and the matrix of the cast iron sample in which the graphite appears (see *Fig. 4.45.*, the analyzed surface S.A.3).

Analyzing the composition data at the limit of assimilation of the inoculant (see Analyzed Area 1, in *Fig. 4.45.*) we observe high concentrations of oxygen that are associated with active elements such as Na, Ca, Al but also Si and Mn. The high Si content indicates the presence of Fe-Si solid solution phases. The presence of active elements such as La, Ba, Zr, which can be located in isolated oxides, has not been reported.

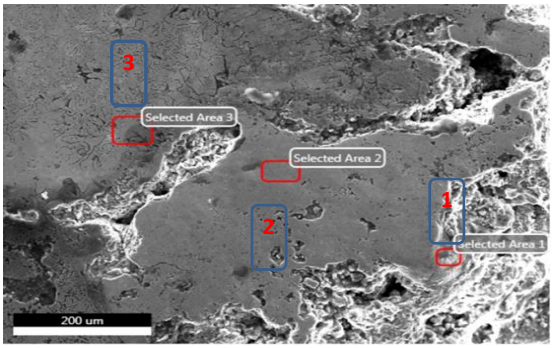

Fig. 4.45. The analyzed points of interest, corresponding to the 3 subzones in the area with undiffused inoculant (see Fig. 4.44., *Area A*), from Structural image A 1)

Regarding the assimilation area of the inoculant (see the analyzed surface S.A.2 in *Fig. 4.45.*) The dominant elements are Fe and Si from the inoculant while the slag (oxidized) elements were pushed to the limit of the solidification front.

At the limit of the inoculant assimilation area, at the contact surface of the inoculum with the cast iron matrix (see the analyzed surface S.A.3 in *Fig. 4.45.*) the oxygen content increases again, which may indicate an contact between the slag film of the melted cast iron and the liquid inoculant. Oxygen is associated with Si, Na, Mn and Fe, the last being the dominant element. Next, there is an increase of %S which can be associated mainly with Mn and Fe. The presence of Na in quite high concentrations is considered accidental, however, because this element was not reported in any other analysis on the height of the sample.

As a general observation, in this area there are favorable conditions for the appearance of the associations of Ca-O and Fe-Si-Al-O elements (see **Tab. 54**). In the cast iron treated with alloy from the inoculating system SZrLaBaCaAlSiFe (Smpl. 4) the O content from the inclusions varies between ~ 6−21%, O being identified in agglomerated inclusions of the type Fe-Si-O and Fe-Si-Al-O.

A.2 Zone B - Analysis of the chemical elements in the inclusions detected in the ***sample 4***.

Two types of compounds were identified in the cast iron sample structure. Oxidic compounds, of undetermined form, with high oxygen content (~ 6−15.7% O) in which are identified mainly Fe and Si but also small amounts of Ca, Al, P and even Na. These compounds form slag films at the interface of the solid inoculant – molten area of the inoculant as well as in the assimilation area of the inoculant – and respectively cast iron matrix. The second type of compounds are of a sulphidic nature, in which the Mn-S relationship dominates, the ratio of which oscillates around the stoichiometric ratio (Mn / S ≈ 1.7) (see *Fig. 4.46. a-e* and paragraph A.2.4. *Structural image I*) depending on the presence of other elements with higher affinity for sulfur such as: Ca, Ba, La, Zr, etc.

A.2.2. Analysis of the **Structural image F**, with 2 analyzed surfaces (v. ***Annex I***, **Table 1**, *position F*)

Elements with a high affinity for sulfur can form specific sulfides in the manganese sulfide matrix (including in its germination zone), or they can even be dissolved. For example, in the *Structural image F*, in *Figure 4.49. a, b*, it can be seen that the particle embedded in the metal matrix (apparently without contact with graphite) stand out to be a manganese sulfide, and it contains a microparticle of La_2S_3 (in its central area) which contains a significant amount of La (3.4 % gr. La, see *Fig. 4.49 d*), and in which the presence of oxygen was not identified.

The compounds of (Mn, X) S, identified between the sulfide body and the sulphure-graphite interface area - an area where Mn is partially replaced by Ca, Ba, La, Zr (according to *Fig. 4.49. d*) - are characterized by different values of the Mn / S ratio (see *Fig. 4.49. c*). Compounds of type (Mn, X) S, which generally have polygonal morphology, formed regular polygons in the presence of these active elements (Ca, Ba, La, Zr). But these elements could form specific compounds that themselves constitute nucleation zones for MnS compounds, as suggested in *Figs. 4.49. c, d*: the detected compound contains in its nucleus La, Zr, Ca, Ba but does not contain Al and O.

A.2.3. Analysis of the **Structural image G**, with 2 analyzed surfaces (v. ***Annex I***, **Table 1**, *position G*)

The *Structural image G* (see *Figure 4.50. a*) shows a complex compound (Mn, X)S, in contact with a graphite lamella - which has a size of ~ 3 µm and an irregular polygonal shape - with a ratio Mn / S, on the body surface of the compound, close to the stoichiometric one. According to *Fig. 4.50. b, c* the body of the compound contains active elements such Ca, Ba, La, Zr. But in the interface of the compound - at its contact surface with graphite - the amount of Mn and S decreases, decreasing the amount of active elements but also their number, being detected only La.

A.2.4. Analysis of the **Structural image I**, with 4 analyzed surfaces (v. ***Annex I***, **Table 1**, *position I*)

A special case, from the *Structural image I*, is inclusion (see *Fig. 4.51., a, b*) which is of quasi-regular hexagonal shape, with a nucleus - a primary microcomposite, with a size of ~ 1.7⌀m, which is arranged in the center of the secondary inclusion - with high concentrations of O and Al (*Fig. 4.51., c-f*) suggesting an Al2O3 compound and which has direct contact with a graphite lamella. The body of this inclusion - subsequently formed on the support particle, and having dimensions (averages) of ~ 6.5⌀m - clearly suggests a compound MnS (S = 19.41% wt; Mn = 38.14% wt; at a ratio Mn/S≈2) which also contains significant amounts of Ca (0.21%) and La (0.27%), so it belongs to the system (Mn, Ca, La)S. The inclusion does not contain Ba and Zr - nor O - and the reporting (detection by the analysis tool a) Al, Fe, Mn and Si may also be due to signals from the cast iron matrix or even from the core.

In the case of the Analyzed Surface 4 (S.A.4) (*Fig.4.51., c-f*), located at the compound interface [complex compound of type (Mn, X)S] –graphite, a thin layer of alumino-silicate is observed (O-Al-Si-Ca-La) more favorable to graphite germination because it has: a) a better crystallographic compatibility (the hexagonal system of graphite versus the typical cubic system of sulphide) and b) a lower deviation of the crystallographic network of the compound compared to the facet (0001) of the graphite network. This situation, which has also been reported by other researchers [75,152,153], is a verification (and, implicitly, confirmation) of the theory that supports the possibility of forming intermediate layers of silicates (with hexagonal lattice) which make the hexagonal graphite lattice more compatible with the cubic lattice of MnS.

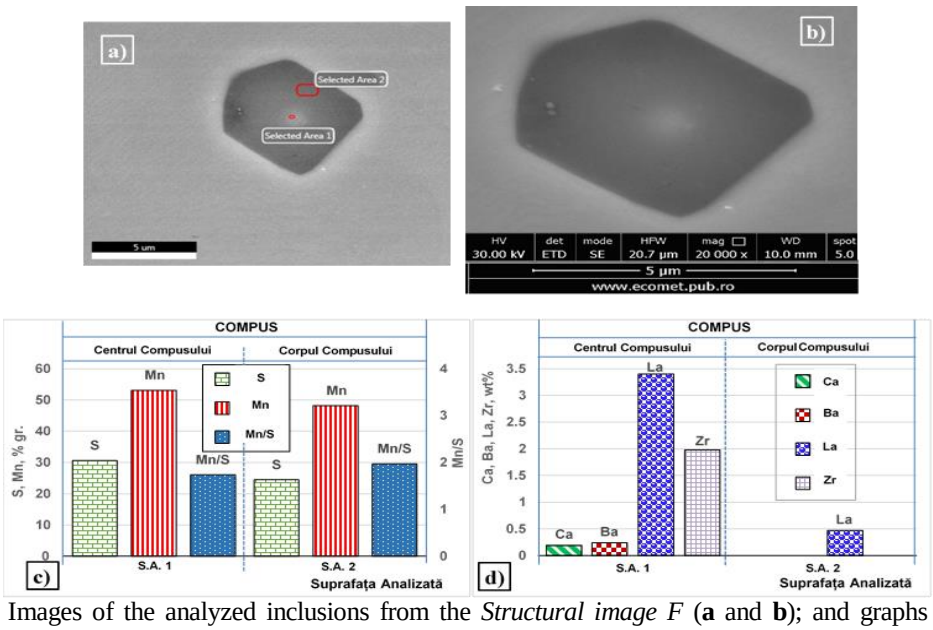

Fig. 4.49. Images of the analyzed inclusions from the *Structural image F* (**a** and **b**); and graphs of the chemical composition in the analyzed areas of the compounds in the structural image F, [**c**) S, Mn, Mn / S; **d**) Ca, Ba, La, Zr]

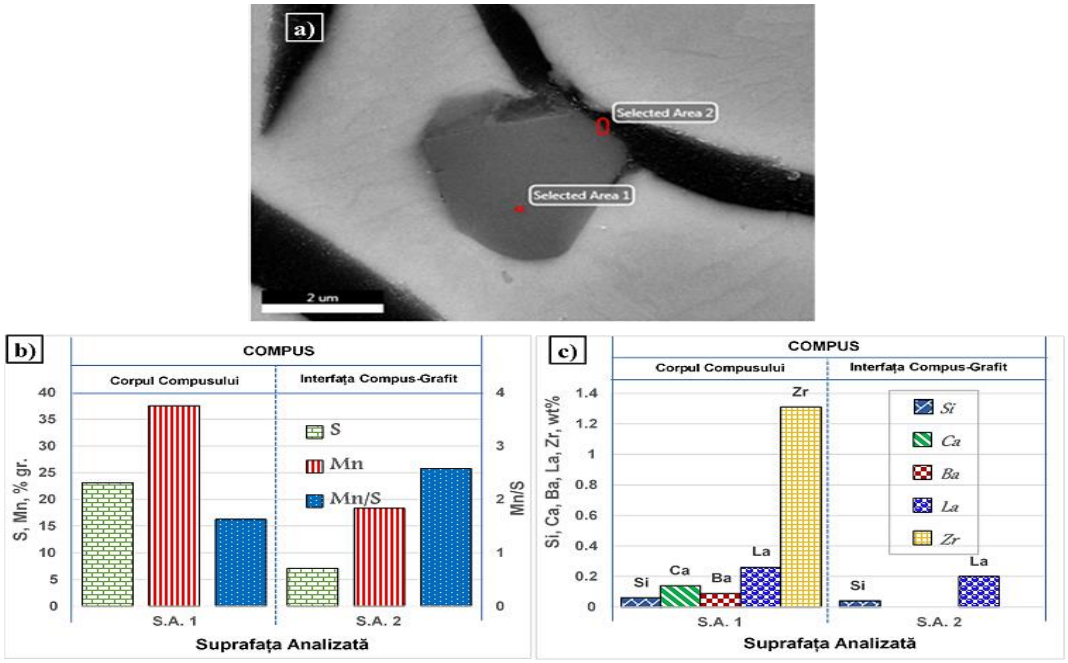

Fig. 4.50. Image of the analyzed inclusions **a**); and chemical composition in the analyzed areas of the *Structural image G* [**b**) S, Mn, Mn/S; **c**) and, Si, Ca, Ba, La, Zr]

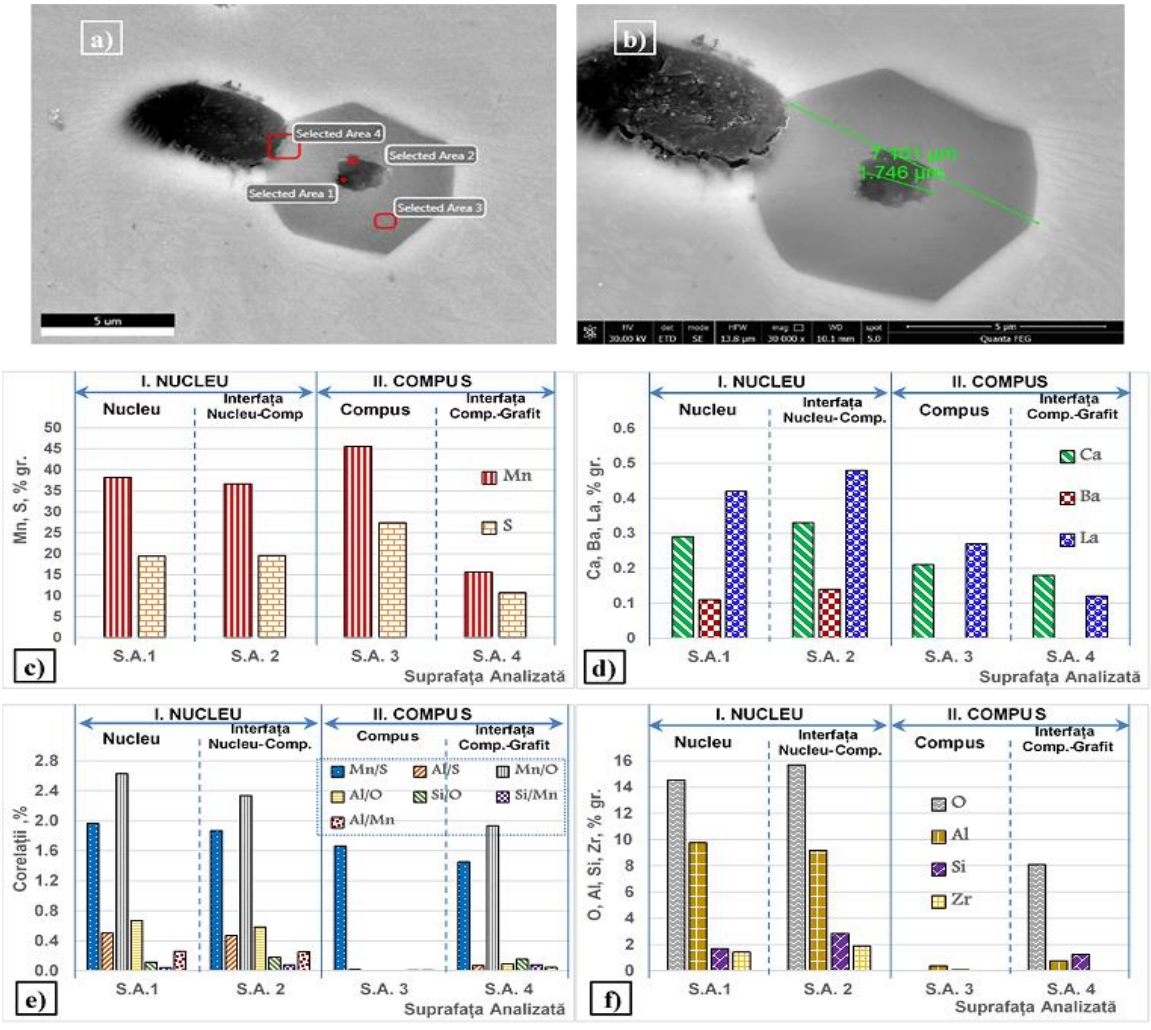

Fig. 4.51. Images of the analyzed inclusions **a**) and **b**); Graphs of chemical compositions in the analyzed areas of the structural image I, [c) S, Mn; d) Ca, Ba, La; e) Mn/S, Al/S, Mn/O, Al/O, Si/O, Si/Mn, Al/Mn]; f) O, Al, Si, Zr

B. The sample inoculated with inoculant from the SSrLaBaCaAlSiFe alloy system (*Sample 6*)

Evaluation of the types of inclusions that could be formed as a result of the interactions between the inoculating elements (Ca, Ba, La, Sr) together with Mn, Si and Al in cast iron, with the two main reactive elements (O and S) existing and / or introduced into the inoculant mixture (case of S) was performed based on the associations of the elements determined by SEM analysis in the inclusions detected both a) in the contact area between the inoculant mixture and cast iron and also b) in the cast iron sample (see **Table 4.54.**).

B.1 Zone A - surface with inoculant, SSrLaBaCaAlSiFe, not diffused (in ***sample 6*)**

The sample treated with the SSrLaBaCaAlSiFe inoculant system contains La, Ca as well as S (which was added), but also Sr and Ba. It should be noted that probably the residual Mg detected comes from the SrFeSi inoculant and from iron sulfide (FeS_2) which brings Mg in the form of MgO.

In the inoculant-body contact area of the inoculated cast iron sample, neither the incipient presence of O nor S is found, although the latter was introduced in the composition of the inoculant. Probably the absence of agitation (sometimes caused by the introduction of cast iron or another active element, eg Mg) resulted in a) a non-bubbling reaction in the contact area and b) a low reaction capacity between the liquid cast iron and inoculating elements. The absence of Mn in the composition of the inclusions in this area and the high values of Si indicate that we are in an area of molten and resolidified inoculant, not yet assimilated in the cast iron sample.

In the composition of the inclusions analyzed in the contact area are found all the elements brought by the inoculant, in different concentrations. The structure in the contact area contains siliceous phases, with polygonal or solid solution aspect, in which Si varies in very wide limits (10–98% Si) which suggests an composition with inoculant not assimilated [with associations of the type: Fe-Si-Al ; Si-Fe; Fe-Si-X; Fe-Al-Sr-Si-O; Fe-Si-Sr-Al-O] (see **Table 4.54**).

B.2 Zone B - Analysis of the chemical elements in the inclusions detected in the ***sample 6***

În zona B, a suprafeței efective a probei de fontă, au fost identificate mai multe incluziuni care par a fi de o diversitate mai mare decât celelalte probe analizate.

B.2.1 Analysis of the **Structural image F**, with 3 analyzed surfaces (see ***Annex I***, **Table 2**, *position F*)

The inclusion in *Fig. 4.54. a, b* is a compound of type (Mn, X) S, - in which X = Sr, Ba, - and with traces of La, Ca and Al, but without oxygen. And in this case the known evolution of the S and Mn content is confirmed:

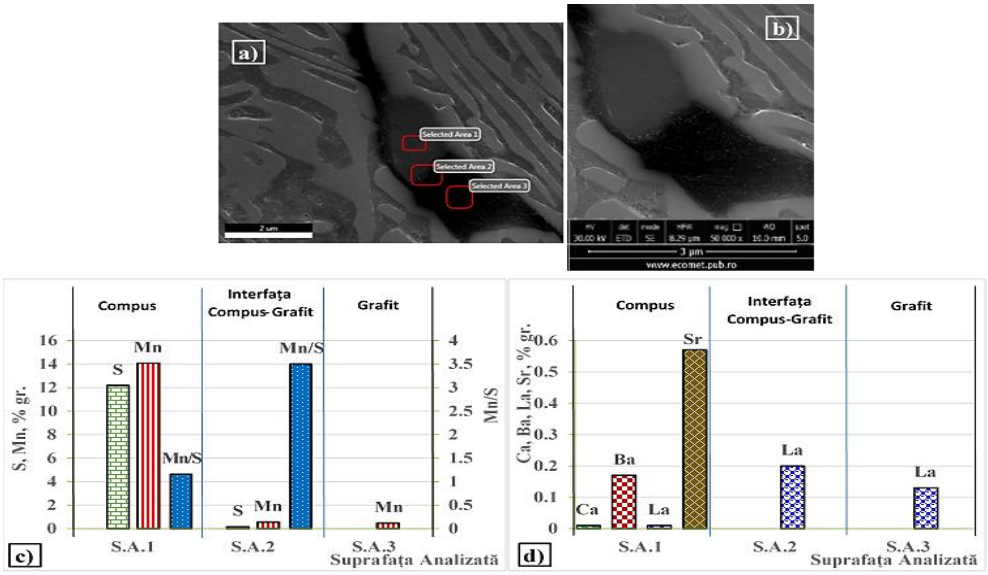

Fig. 4.54. Images of the analyzed inclusions in the *Structural image F* (**a** and **b**); and graphs of the chemical composition of the inclusions in the structural image [**c**) S, Mn, Mn/S; **d**) Si, Ca, Ba, La, Zr]

a) large amounts in the compound (with stoichiometric ratio Mn/S), b) at the interface smaller (but higher Mn/S ratio) and c) in graphite inclusion appearing only Mn. The contents of the active elements

introduced into the inoculant system (Ca, Ba, La, Sr) are found in the complex compound of (Mn, X) S, with the difference that (at the compound-graphite interface and in the graphite inclusion) only La is found (in larger quantities at the compound-graphite interface), which could be a distinctive signal.

The inclusion is partially embedded in graphite and at the compound-graphite interface (see Analyzed Area no. 3) has a higher concentration of La (0.2%, compared to 0.01% in the compound) which suggest (and in this case) a beneficial of La on the relation between complex compound (Mn, X)S and graphite (in this case X being even La).

B.2.2. Analysis of the **Structural image G**, with 4 analyzed surfaces (***Annex I***, **Table 2**, *position G*)

In the *Structural image G*, *Fig. 4.55. a, b* was detected an conglomerate of inclusions in the form of oxy-sulfides (*Fig. 4.55. c-e*, *S.A.1* and *S.A.2*) and sulphides (*Fig. 4.55. c-e*, *S.A.3* and *S.A.4*) which is practically embedded in a graphite separation. Of these S.A. 2 is the most complex containing (in addition to S and Mn, at a ratio Mn/S ≈ 1) in descending order: P, Sr, Ti, La and Ca together with oxygen and graphite (free carbon). The inclusion in *S.A.1* is poorer in S and Mn (at a ratio Mn/S = 1.3) but contains more P and Ti, along with O and C. The inclusion in *S.A.3* has a very high content of Ti (~ 8, 3%wt.) but it is not supported by other reactive elements, the S content being very low. It is possible that it is a oxy-sulfide of Ti, although O does not appear in the composition, but the presence of Al in large quantities (at a %wt.Si<) could support this hypothesis. The presence of P in this conglomerate is attributed to the fact that, as shown in the picture, the graphite is placed in an area with phosphorous eutectic.

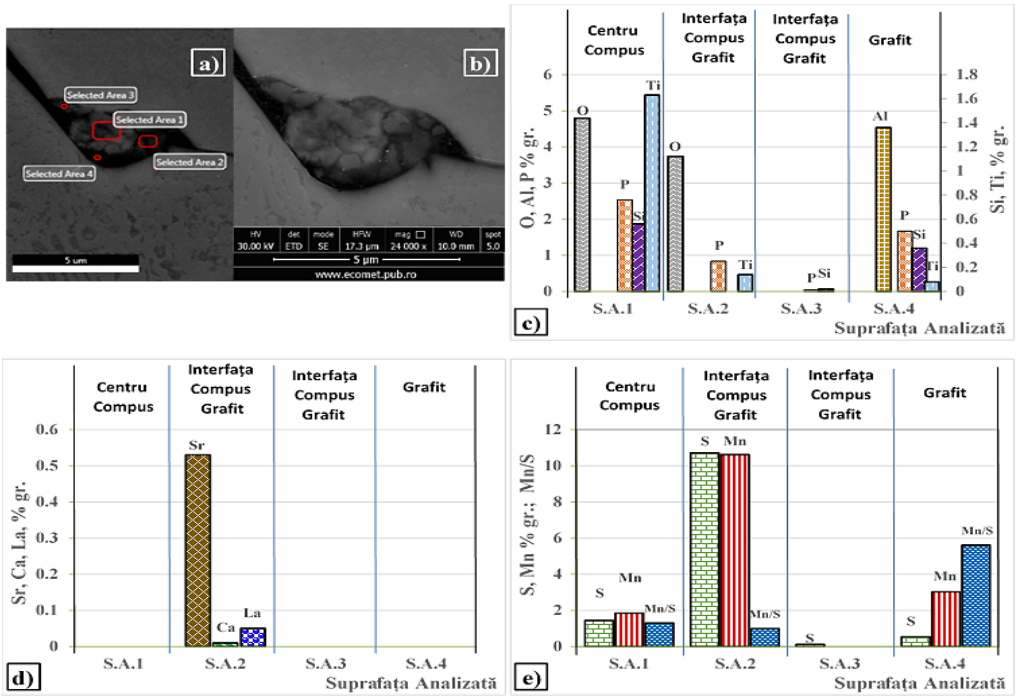

Fig. 4.55. Images of the analyzed inclusions in the structural image G (**a** and **b**); and graphs of the chemical composition of the compounds in the structural image [**c**) O, Al, Si, Ti, **d**) Sr, Ca, La, Ba; **e**) S, Mn, Mn / S]

B.2.3. Analysis of the **Structural image K**, with 4 analyzed surfaces (***Annex I***, **Table 2**, *position K*)

Structural image K, from *Fig. 4.56. a, b*, is a particular case, in the sense that it is in fact a gas bubble embedded at the interface between the matrix and a phosphorous eutectic island [which is accompanied by a conglomeration of oxido-sulphidic inclusions (see *Fig. 4.56. c-e*) of type (Mn,O,X)S where X = La, Sr, Ca, Ba, Al (*S.A.1*) or X = Sr, Ca, Al (*S.A.3*); and sulfides where X = La , Ca, Al, Ti (*S.A. 2*)]. The corresponding composition of *S.A.4* (adjacent to this bubble) is specific to a phosphorous eutectic but also contains small amounts of La. Hence the questions: a) if there is any connection between La and P or b) if La acts in the last phase of solidification [when it is concentrated towards the intercellular areas (where it also meets the phosphorous eutectic, the last solidified)]. This is reminiscent of the theory (Skaland [201,202]) that La provides a secondary germination of nodular graphite (in the

last phase of solidification) generating a finer graphite structure that counteracts the tendency to form retasure. It could, therefore, be an indirect test of this theory.

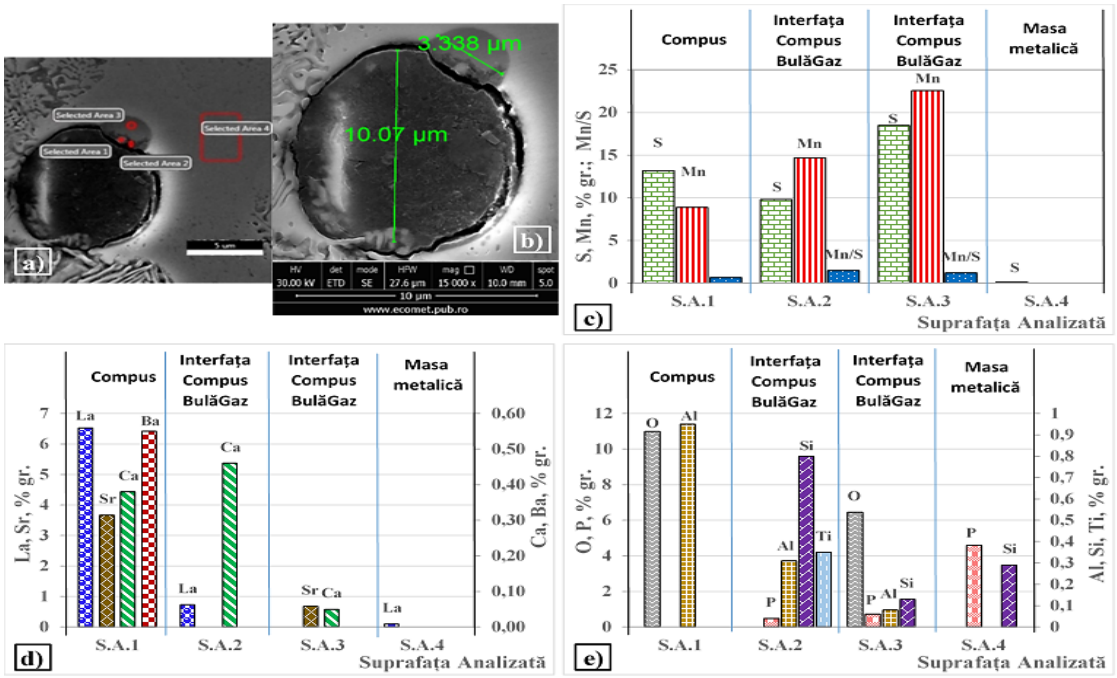

Fig. 4.56. Images of the analyzed areas from the structural image K (**a** and **b**); and graphs of analysis of the chemical composition from the analyzed surfaces [**c**) O, P, Al, Si, Ti; **d**) La, Sr, Ba, Ca]; **e**) S, Mn, Mn/S]

C. The sample inoculated with inoculant from the SrZrLaBaCaAlSiFe system, (*Sample 7*)

Based on the associations between the elements detected by SEM analysis in the determined compounds – both a) in the contact area between the inoculant system - cast iron and b) in the body of the cast iron sample – analyzes were made to allow establishing the place of the types of the inclusions possible to form [folowing the interactions between the active elements (Ca, Ba, La, Zr, Sr) - together with the component elements usually in gray cast iron (Mn, Si and Al) - with the two main reactive elements (O and S) (see *Fig. 4.57. a-e* and *Fig. 4.58 a-h*)].

C.1. Zone A – surface with inoculant, SrZrLaBaCaAlSiFe, undiffused (***Sample 7***)

The sample treated with the *SrZrLaBaCaAlSiFe* inoculant system (*Sample 7*) has a slightly wider transition zone between the inoculant and the cast iron sample, probably due to the violent (bubbling) reaction of Mg (present in small amount and in the inoculant ~ 0.0167%wt. and cast iron elaborated 0.0001%wt.) which dispersed the inoculant granules through the liquid cast iron and increased the inoculant-melt contact surface. In the concomitant absence of O and S from the composition of the analyzed areas, this it is dominated by Fe and Si, in which traces of the other elements are present, which indicates that, in the analyzed areas, melted inoculants predominate but they are in undissolved state, in cast iron.

An important feature of the complex of inclusions identified in the contact area of the sample treated with the *SrZrLaBaCaAlSiFe* inoculant system (*Smpl. 7*) is the fact that they have practically no S and Mn in composition, which excludes the possibility of formation MnS compounds, as well as the fact that in these inclusions are present high amounts of Ba (22%wt.), Ca (2.4%wt.) and La (2.8%wt.) but also significant proportions of Sr (0.7%wt.) and Zr (~0.4%wt.) which, in the absence of S can only be in relation to oxygen (no S was added into the inoculant mixture).

C.2 Zone B - Analysis of the chemical elements in the inclusions detected in the ***Sample 7***

C.2.4. Analysis of the **Structural image K**, with 2 analyzed surfaces (v. ***Annex I***, **Table 3**, *position K*)

For this inoculated cast iron sample, the analysis of *Structural Image K* (see *Fig. 4.64.a,b*), reveals a complex oxy-sulfide inclusion (of ~ 1µm), embedded in a lamellar

graphite separation. It contains mainly La (3.8%wt.), Mg (1.6% wt.) and Ca (0.35% wt.) but does not contain Zr, Sr and Ba (see *Fig. 4.64. c, d*, in analyzed area *S.A.1*).

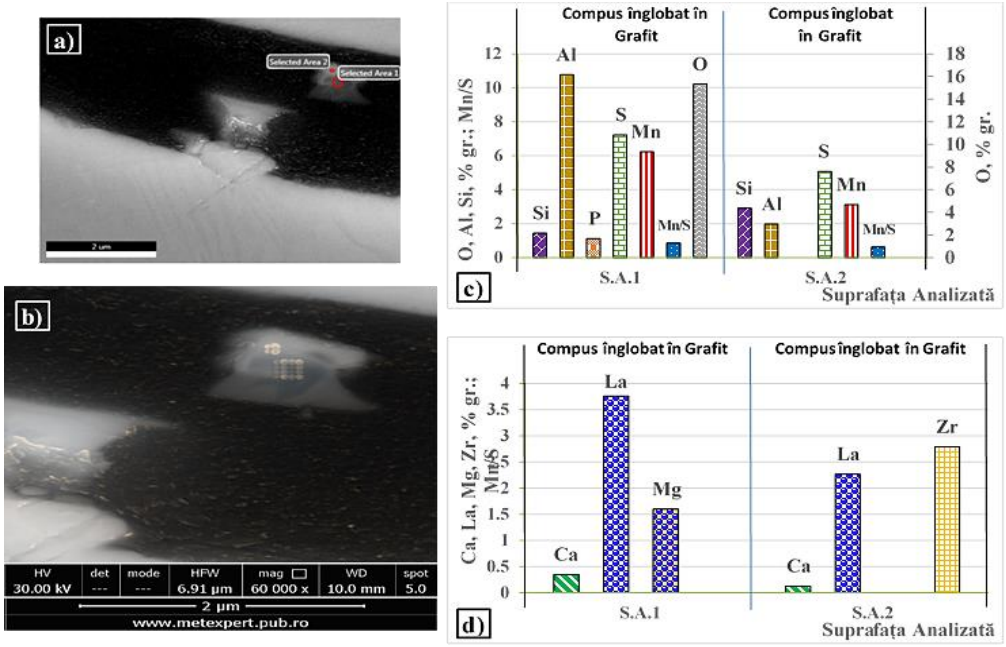

Fig. 4.64. Images of the analyzed areas in the *Structural image H* (**a** and **b**); and chemical composition graphs in the analyzed areas of the structural image [**c**) and, Al,P,S,Mn,Mn/S,O; **d**) Ca, La, Mg, Zr]

The fact that inclusion contains a large amount of O (15,3% wt.) and Al (~10,8% wt.) suggests that it also has a nucleus that can be of the type Al_2O_3. The inclusion is embedded in a graphite lamella and upon contact with it presents a lighter (whitish) color characterized by lower contents of Ca, La and Al but with a significant Zr content that is completely missing in the body of inclusion (*Surface analyzed 1* and *S.A.2*, respectively, in *Fig. 4.64. c,d*). In this area no Ba, Sr and O have been identified, suggesting that it is a sulphidic area of type (MnX)S, in which X = Zr, La, Ca are dissolved elements or in complex chemical relation to MnS. The presence of P, in the body of the oxy-sulfidic inclusion – its presence being identified in other researches[203], in all the analyzed inclusions from 4 studied samples – which is embedded in the graphite lamella, requires greater attention to investigate this phenomenon further.

As a general observation of sample 7:

In the lamellar graphite area of the sample, the inclusions are mainly of the type (Mn,X)S in which the role of X is mainly played by Zr, whose weight varies (between 1,06 − 2,8% wt.), and at a smaller extent (in descending order) by Sr, La, Ca and Ba; they however are present in almost all inclusions, with the exception of Sr and Ba, which have been identified in 3 cases out of 9.

The presence of phosphorus in the inclusions analyzed (in 8 out of 23 cases) cannot be overlooked, situations where it is mainly associated with Ca and O, and (in the absence of Ca) with La. The presence of P has been reported particularly in the case of oxidic inclusions, where it is in higher concentrations (1,8-6% wt.), but also in sulfidic inclusions (at lower concentrations). It is not known, however, whether P has any role in the nucleation of graphite or comes from the separation of phosphorous eutectic present in intercellular areas. Since it is not a single case, being mentioned in other researches [124,203,204], it is worthting to considering conducting more in-depth investigations in the future.

D. The sample inoculated with inoculant from the SSrMgBaCaAlSiFe system, (*Sample 12*)

D.1. Zone A – surface with inoculant, SSrMgBaCaAlSiFe, undiffused (***Sample 12***)

Inclusions detected, in the case of sample 12, in the contact area are generally of oxidic type but are also found associations with S, of the type (Ca, Ba, Sr)S or even more complex, of the type of Ba-O-S.

In the case of cast iron inoculated with the *SSRZrMgBaCaAlSiFe* system, S is present in the composition of the inclusions from the contact area, which suggests a rapid

decomposition of FeS_2 as well as the S input in reaction with the active elements (Ca,Ba,Sr,Mg). In addition to inclusions, different constitutional phases reflect different stages of assimilation of the inoculant: Fe-Si; Fe-Si-Al; Fe-Si-Mg-Al; Fe-Si-Al-Mg-X (X= Ca,Ba,Sr,O). The Fe-Si-X phases have different morphologies and dimensions, depending on the concentration of Si, which vary in very wide limits (15−99%wt.Si); the Si-rich phases have polygonal or stripe shape and the %wt.Si< have an appearance of solid solution. In the composition of the inclosing phases, the presence of Mg is noted, in varying quantities, containing between 0−3,86%wt.Mg. It is worth noting that in both the contact area and the transition area (to the lamellar structure of graphite) the sulfur content of the analyzed inclusions, with one exception, is less than 0,10%wt. and the Mn content is less than 0,35%wt. (at a Mn/S ratio < 13). In this case the inclusions are generally of the oxidic and/or oxido-sulphidic type with a very low sulphur content. Most inclusions in the contact area are phases or siliceous compounds that have dissolved other elements. *It follows that in this case Mn sulphide has no important role in the nucleation of graphite, being annihilated (decomposed) by the inoculant elements present in high concentrations.*

D.2.2. Analysis of the **Structural image K**, with 2 surfaces of analysis (v. ***Annex 1***, **Table 4**, *position K*)

In *Fig. 4.69. a, b*, of the Structural image K, a representative pattern of formation of graphite in gray cast iron is shown. According to its chemical composition (see **Table 4.54**, *Fig. 4.69. c, d*), is a compound of the type (Mn,Mg,Ca,Sr)S, which has these active elements distributed throughout the particle. An early (and thin) graphite layer is formed on the entire surface of the compound, but it has variable thicknesses (between 0.05−1.0µm). The graphite lamellae that have developed are in two specific areas: both of them are on surfaces a) characterized by a thickness of the graphite layer greater than 0.5µm, and b) not on the opposite side of the compound (which has a thickness of the graphite layer lesser than 0.3µm). This situation can be determined by (and suggests that) the graphite germination is favored by specific structure of the compound (Mn,X)S, more compatible with the structural parameters of the graphite.

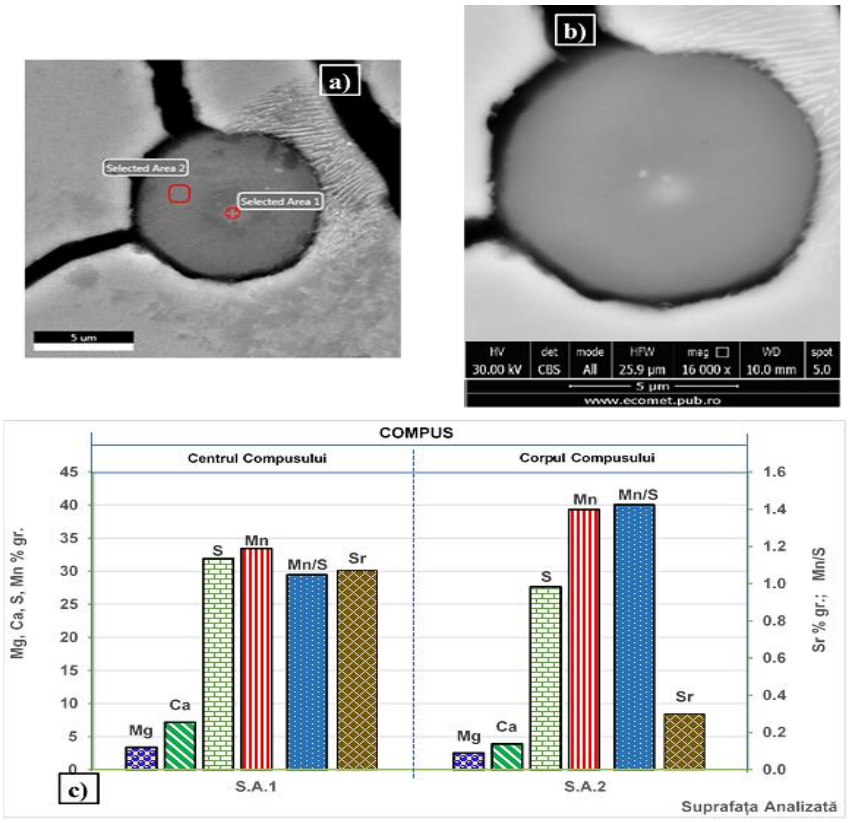

Fig. 4.69. Images of analyzed areas in the *Structural image K* (**a** and **b**); and chemical composition graph in the analyzed areas of the structural image **c**) [Mg,Ca,Sr,S,Mn/S]

D.2.3. Analysis of the **Structural image L**, with 5 surfaces of analysis (v. ***Annex I***, **Table 4**, *position L*)

A specific feature, which illustrates the complexity of the process of forming the graphite, was observed in the case of the compound - from the *Structural image L* - presented in *Fig. 4.70. a-c* that reveals a model of growth of the compound in the incipient phase. It has a relatively ovoid shape with

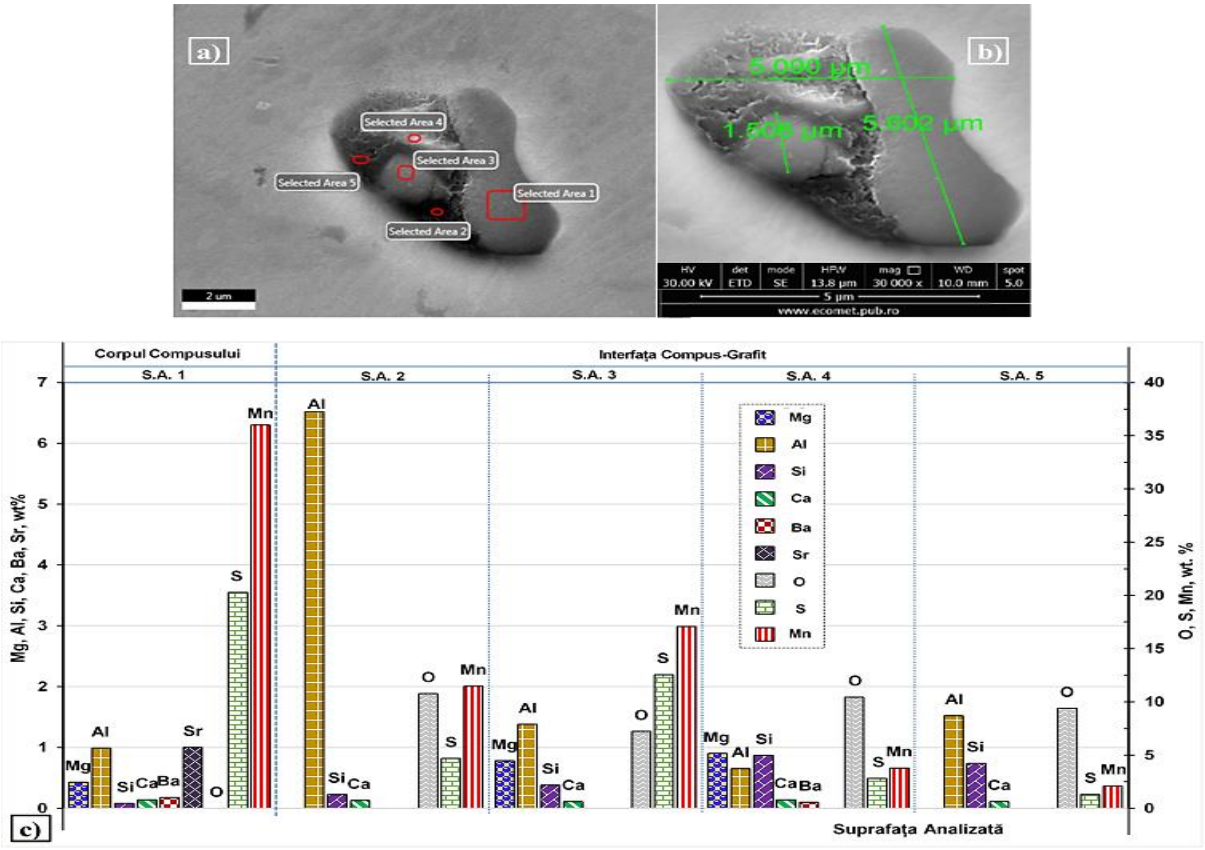

Fig. 4.70. Imaginile zonelor analizate din *Imaginea structurală L* (**a** și **b**) și graficul compoziției chimice în zonele analizate ale imaginii structurale [**c**) Mg, Al, Si, Ca, Ba, Sr, S, Mn]

dimensions of ~ 6x5µm - and contains two distinct areas, one relatively circular (of ~ 1.5µm) and the second ovoid (of ~ 5x2µm) - being in contact with the graphite. The analyzed surface 1 (*S.A.1*) is located on the compound side that has no contact with the graphite. In this area, the chemical composition is typical for the system (Mn,Sr,Mg,Al,Ba,Ca)S, not being identified the presence of oxygen. Other analyzed areas (*S.A.2*-*S.A.5*, see *Fig. 4.70. c*), located at the compound-graphite interface are characterized by a lower content in Mn and S (Mn/S ratio between 1.35-2.45), however, all these analyzed areas contain oxygen as well as, in variable quantities, elements of type Al, Mg, Ca, Ba and Si.

As a general observation, the presence of the Mg in the composition of the inclusive phases – ranging from 0-3.86 %wt. Mg in the contact area with the inoculant (zone A) and between 0-7.4 %wt. Mg into the structural area of the cast iron sample (zone B) – although the graphite is lamellar. This happened, probably due to the high sulphur content (in the composition of the mechanical mixture of the inoculants was also added S, in the form of FeS2, according to the experimental program).

Generally, at high concentrations, Mg is also accompanied by oxygen. It turns out that - although there are also situations where (even at a content of ~ 7%wt. Mg) the oxygen was not registered in the composition of the inclusion - the Mg enters, as component, into (Mn,X)S type compounds, in the form of (Mn-Mg,Ca,Sr,Ba)S (see **Table 4.46**).

The transition to the lamellar form of graphite is made by quasi-compacte morphologies, but with a high degree of branching, tending to unidirectional growth (lamellar graphite formation).

V. General conclusions, Personal contributions and Research directions

V.1. General conclusions

V.1.1. The Experimental program I

- As a result of the information finded in the specialized literature, it was established that there is an important contribution of the active elements of the RE category, present in the inoculating systems used for the treatment of cast irons, in obtaining quality castings. The presence of La, in the inoculation systems, not being mentioned in the case of treatments performed to obtain of grey iron castings with lamellar graphite, an experimental program was made - by achieving average conditions of germination of graphite - in order to establish the opportunity for the introduction of La, as an additional active element, in the classical industrial inoculant systems (based on FeSi).
- Under the conditions presented, chemical composition, thermal, structural and mechanical properties (HB) analysis, and also of carbide formation trend, have been conducted to examine the effects of La and Ca on the ability to act on hypoeutectic grey cast iron (with lamellae graphite) castings a) with lower content of Al, Zr and Ti (which act in the first stage of graphite nucleation), but b) with a good ratio of Mn and S content (which creates average conditions for graphite germination).
- The influence exerted by the inoculant La-FeSi by the formation of austenite dendrites (also indicated by the higher values of the parameter TAL and lower for ΔT_1) which is confirmed by the dendritic microstructure (with graphite type E and D) observed, compared to the Ca-FeSi system.
- Under the experimental conditions presented, the behavior of the gray cast iron during solidification – at the minimum point of the eutectic temperature (corresponding to undercooling ΔT_1, which is refered at Tmst) – is strongly dependent on the state of the molten cast iron (inoculated or uninoculated) and the presence of antigraphitization action after inoculation, but it is less dependent on the inoculant system used.
- From the point of view of the inoculant treatment, the most significant beneficial effect has been manifested especially in the last part of the solidification process (corresponding to the $\Delta T3$, respectively the TES point related to Tmst), considerably more in the case of the castings inoculated with Ca-FeSi system alloy.
- Addition of Te – as antigraphitization treatment, of molten iron, made after inoculation treatment – brings the undercooling parameter ΔT_1 to an intermediate level (close to or just below zero), but restores the undercooling value at the end (of process) of the solidification ΔT_3 to the high level (previously held), equivalent to that corresponding to the uninoculated grey cast irons.
- High values – due to inoculating treatment – of ΔT_1 (a lower undercooling at the beginning of the eutectic reaction), produce lower undercooling at the end of the solidification ΔT_3 (with less negative values), in the case of both inoculant systems, between these parameters existing a good correlation.
- Inoculation with La-FeSi system alloy produces lower values of eutectic recalescence, ($\Delta Tr=3\div5\ ^oC$) – compared to those produced by the commercial inoculant in the Ca-FeSi system ($5\div6\ ^oC$) – on average by 25 %, which produces a favorable context especially for the use of soft moulds.
- For all the ten measurements made, the inoculation with laca-phesi leads to higher values of the graphitization factor GRF1 than that obtained in the case of Ca-FeSi alloy system (on average, a value of 47.4 compared to 43.7), which proves a greater capacity to form graphite immediately after the moment when the maximum (recalescence) temperature was reached.
- Inoculation descends the value of the graphitization factor GRF2 (from 31 to values between 16 -20) as well as the value of the end of solidification FDES – of first derivative cooling curve – (from -2.3 to values between $3.3 \div 3.6\ ^oC/s$), in the case of both inoculating alloy systems used, the inoculant La-FeSi having the best performance in improving the quality of the cast iron.

- Thus, according to the thermal analysis, in the cast iron with an optimal sulphur content (0.05-0.06%wt.S) the La addition has limited but specific benefits – this: it a) decreases the value of the eutectic recalescence gradient (ΔTr) as well as the maximum degree of eutectic realescence (TEM); b) the values of GRF1's graphitization factors increase and GRF2's decrease; c) while the value of the first derived at the end of solidification decreases it (FDES) – which creates favorable conditions for reducing the incidence of microretasures formation.
- The complementary analyzes carried out also reveal a general positive behavior of La in the experimental castings, thus, the decrease in the cooling rate during the solidification process - achieved by increasing the cooling module - causes the possibility of carbide formation to decrease in both inoculation systems, the La-FeSi system proving a more efficient beneficial effect (being about 20% more efficient). The superior inoculating power of the La-FeSi alloy is more clearly perceptible in the case of moulded wedge samples (especially those of type W_1), respectively in the case of solidification carried out with a higher cooling speed.
- A high level of correlation was obtained between the values specific to the analysis of the chilling tendency of the grey cast irons and those of the eutectic undercooling ΔT_1 (respectively of the thermal analysis) - the parameter of the undercooling being determined by its reporting to the lower threshold of the eutectic temperature (TEU) taking as a reference the metastable eutectic temperature (Tmst).
- The structural analyzes confirm - and through the method of calculating the average relative performance of the experimental castings - the favorable action of La in the experimental cast iron by: a) increasing the number of eutectic cells formed; b) improving the characteristics of the germinated graphite (regarding the type, the surface, and the number of germinated graphite particles) relative to the uninoculated cast iron; but also c) by optimization (having as reference the uninoculated cast iron and the one treated with the classic inoculant) of the Ferrite/Pearlite correlation, which has as effect of d) obtaining a higher hardness, despite the smaller number of eutectic cells (relative to the treatment with Ca-FeSi).

V.1.2. The Experimental program II

- The positive results obtained under the first (preliminary) experimental program led to the design and conduct of further studies (through chemical, thermal, microstructural and HB hardness research) to examine the effects of Al, Zr, Ti, Ca, Ba and La on treated experimental cast iron, being know to have a key role in the process of nucleation of lamellar graphite, in gray hypoeutectic cast iron with a low sulfur content (< 0.02%wt. S) and very low aluminum (<0.002%wt. Al), but with a high carbon equivalent (CE = 4.1).
- The thermal analyzes performed reconfirm that the inoculant system LaCaAl-FeSi act effectively, from the point of view of the inoculant treatment, in the analyzed experimental castings, producing - from a thermodynamic point of view - a reduced eutectic undercooling throughout the eutectic reaction but, specifically , at the end of the solidification process.
- According to the results of the thermal analyzes, supported by those of the complementary analyzes performed, the representative elements of sulphidic and oxidic compounds - such as Zr, Ba or Ti, in association (simpler or more complex) with La (for the same content of Ca and Al) - have produced the modification (in different ways and with a different capacity) of the pattern of solidification of the gray iron castings with lamellar graphite, on: a) the course of the onset of solidification (respectively in the formation of the austenite dendrites, TAL, as well as at the time of initiating the transformation eutectic, TSEF), b) during the eutectic reaction (at the beginning and end of this stage, TEU and TER) as well as c) at the time of the solidification process (TES and FDES). For the effects produced, under these conditions, no information in the specialized literature is found on the solidification process.
- The relative performance of the inoculants, relative to thermal analysis, has been assessed in view of the extent to which they have the ability to promote a) the increase in temperatures corresponding to the formation of austenite (TAL) and the initiation of eutectic solidification (TSEF); b) the increase in the minimum temperature of the eutectic undercooling (TEU, which will determine the existence of a lower level of undercooling ΔTm, relative to the value of the eutectic temperature in the stable range, while the parameter ΔT_1 - which refers to the temperature value in the metastable range - increases); respectively, an increase c) of the temperature at the end of solidification (TES, with negative values less low for the parameter of undercooling ΔT_3, relative to the metastatic

eutectic temperature), but also a d) decreases the value of the eutectic realescence (defined as the difference ΔTR = TER – TEU).

- From the point of view of the formation of primary austenite – at the beginning stage of solidification – research has revealed that effective action is, in ascending order, the systems of inoculants LaZrTi, LaBaZr and (optimally) LaBaZrTi, [because austenite germinated at a higher temperature (TAL) than with other inoculant systems].
- The inoculant reference system, containing only La (as an additional active element), is shown to be effective throughout the duration of the eutectic reaction, by having an effect – of producing higher thermal parameters – on both: a) the start temperature of eutectic solidification (TSEF) and; b) the minimum temperature of the eutectic reaction (TEU). A higher value range between TEU and Tmst (with TEU above Tmst, which means lower values of the undercooling level ΔTm and/or increased values of ΔT_1) it translates not only by creating a low potential for free carburising capacity, but also by reducing the possibility of producing undercooling graphite (type D, according to ASTM).
- The maximum temperature of the eutectic reaction – expressed by the parameters TER and ΔT_2 – illustrates two antagonistic effects: a) one concerning the decrease in the amount of the undercooling graphite formed (this effect is favored by the increased values of the parameters TER and ΔT_2); and b) the other regarding the decrease of the formation of shrinkage trend (this result being favored by the low values of the parameters TER, ΔT_2 and ΔTr). In order to reduce the conditions of formation of the undercooling graphite an effective solution is the reference inoculant system, with La, while – from the point of view of shrinkage – the inoculant in the LaBaZr alloy system is presented to be as the most efficient.
- For the end of solidification, the most favorable conditions (TES with increased values, and respectively lower negative values of ΔT_3) were obtained in the case of the inoculant mixture with La, a second option being the complex LaBaZrTi inoculant mixture.
- The microstructural analysis confirms the relative position of the tested inoculants as their influence on representative temperatures (cooling curves) and eutectic undercooling parameters (on first derivative of cooling curves). The lowest amount of under-cooling graphite (type D and E), and consequently the smallest amount of ferrite formed, characterize the inoculated cast iron in simpler (La and LaZr) and more complex (LaBaZr) systems, which are also characterized by high values of TEU and ΔT_1 and low values of Δtm parameters, respectively. On the contrary, solidification at a higher level of undercooling, typical of the LaZrTi and LaBaZrTi inoculants, results in a higher amount of graphite morphologies of type D and E (ASTM), and an increased ferrite/perlite ratio (confirmed by structural and hardness HB analyzes).
- Following the evaluation performed, by means of the method of calculating the average relative performance (using results obtained in all types of analyzes carried out) of the inoculants, it was found that – for the case of a general use of gray cast irons, under normal conditions – the inoculant La-FeSi has a high efficiency when used in gray cast irons with lamellar graphite (melted in electric furnaces) with: a) low in S and Al content; b) high-value of equivalent carbon; and c) where no additional intake of other active elements pre-exists. In this context, the most effective inoculant is the LaBaZr-FeSi alloy system. Favorable but more reduced results, compared to the La-FeSi system, are also obtained with the use of the LaBa-FeSi alloy system.
- In the case of the use of gray iron with lamellar graphite in specific applications – requiring the promotion of a higher amount of austenitic dendrite or lower values of eutectic recalescence, respectively – it is recommended to use more complex (with La base) inoculant systems, such as the inoculant LaBaZrTi-FeSi (for the first requirement) or the inoculant LaBaZr-FeSi (to satisfy the second requirement).

V.1.3. The Experimental program III

- Designing and carrying out the proposed experimental programs and the positive results obtained, respectively - which resulted in identifying the positive role exercised by La in the intensification of the inoculant effects (in certain condition) of the classical industrial system (from the CaAl-FeSi system) as well as the creation of new inoculant systems (by adding new elements active, such as: Ba, Zr, Ti) with increased inoculating effects on the treated experimental castings - certifies the need to carry out new researches that can contribute to the detection of the mechanisms by which the new elements become able to produce the desired

changes in the inoculated castings. For this purpose, an experimental program was carried out through which was performed an overinoculating treatment with inoculating alloy systems (created experimentally).

- The results reconfirm the role of complex compounds (Mn,X)S – micronically sized (1-10μm), which exhibit visibly (or not exhibit) a nucleus of oxidative origin (0,1-3 μm) – as major graphite nucleation sites.
- For treatment with an inoculant from the La,Ca,Ba,Al,Zr,S-FeSi system (of a base iron with 0.035%S), SEM analysis shows that the first microcompound formed is a complex Al silicate (containing Zr, La, Ca, Ba) that enhances the nucleation capacity of the second compound formed [of type (Mn,Ca,La)S].
- By adding inoculant elements the nucleation capacity of the MnS compound increases, acting on the first oxidic compound formed (favoring the formation of MnS) and by replacing the Mn from the Mn-S compound, thus reducing the lattice differences between this substance and the facet (0001) of the graphite lattice.
- In addition, the possibility of the existence of a thin layer (of nanometric dimensions) was identified at the sulfur-graphite interface, which contains elements that form oxides (O-Al-Si-Ca-La), able to increase the ability (Mn,X) for graphite nucleation (having a better crystallographic compatibility).
- In all three important nucleant action zones it was identified La (a) in the first nuclei of a oxidic nature, b) then in the Mn-S combination which subsequently germinated to include it, c) and at the sulphure-graphite interface, which later forms on the compound Mn-S, to enclose it) which increased the efficiency of the inoculating elements.
- Mn and S are the elements present in all the micro-inclusions analyzed, and they are in an obvious relationship: the increase in Mn content with the increase in S content results in a relative decrease in the Mn/S ratio
- Silicon has a lower frequency of occurrence compared to Mn and S, while some active elements (such as Ca, Mg, Ba) have replaced Mn in this reaction with S or O.
- It has been identified, as the body of a compound, a system of type (Mn,X)S containing elements that form sulphur (X = Mg, Ca, Sr, Al), and in which it can be present - sometimes - and oxygen.
- Analysis of the areas at the interface between the MNs-type compound and graphite particles revealed a possible particular situation. Mn and S elements were found to be still present at the compound-graphite interface, but the main feature is the presence of oxygen in these regions.
- Oxygen is identified in particular in the first micro-compound formed – visible in the form of the nucleus (core) of the complex compound (Mn,X)S – and often in a thiner layer (of nanometer size) at the sulfide-graphite interface containing both O and also Si, Al, Ca, Ba, Sr, La, Mg.
- The findings support the possibility of forming compounds from a wider range of chemical systems (such as Fe-Si-Al-O, Mn-O-S, Ca-O-S, Ba-O-S, SR-O-S, Mg-O-S) most often in the form of particles of silicates or of classical oxy-sulfides.
- It is noted that Mg, the newly identified active element – over the entire section of compounds (Mn,X)S [oxides + sulphides] – also appears to have a potentially important role in the formation of graphite in gray cast iron with lamellar graphite (not only in nodular graphite cast iron).
- The results indicate that the elements that form oxy-sulphides - elements that are included in the interface layer, achieving an increase of the amount of MnS formed and/or the formation of a superficial layer (thin, of nanometric sizes) of oxides or oxisulphures - improves the capacity of micro-inclusions of (Mn,X)S to germinate the graphite due to a better compatibility (between the hexagonal system and cubic sulphur system) and a diminished deviation of the crystalline network, compared to the facet (0001) of the graphite.

V.2. Personal contributions

I believe that through this doctoral paper, based on the suggestions of a extensive literature (specialized, and not only), on the experimental programs designed and on the results of their development, contribute to the completion of the scientific knowledge in the field through the following personal contributions:

- Worldwide referral and highlighting the production of a cleavage in the consumer market – from large-scale products used by large groups of people to small-scale products (miniaturized in some areas) used individually – which also produce (commit) a shift of needs to the industrial level, by

decreasing the interest in the manufacture of classic products and thus diminishing (sometimes almost to extinction) some industries. This phenomenon, also produced in the field of cast iron industry, motivated – in order to support industry – the need to increase competitiveness, which materialized (in the present paper) by selecting and focusing on the issues covered by this broad spectrum of scientific research.

- The needs of a) the production of low-weight castings and the development of the performances obtained by their production - parts made with the new specifications (imposed by the consumer market) and using cast iron as a raw material - determined the identification (made by performing an analysis in a particular style of the literature) of the negative effects generated in the structure of the cast iron as well as the specific aspects regarding the way of action of La in the process of solidification of the gray lamellar cast iron, identifying that La acts, in specific modes, on the graphitization process during the period of solidification of the cast iron. The specific aspects of the action include: a) the ability to interact with the main elements with a role in the germination of graphite; b) the moments when it interacts with other elements (mainly O and S but also with other, numerous, elements) during the cooling of liquid cast iron and its solidification; c) the way it acts in the germination and growth processes of lamellar graphite; d) the influence of La on the parameters of the cooling curve of gray lamellar cast iron under conditions in which it acts alone or in association with other inoculating elements (Ca, Ba, Sr, Zr, etc.); e) how it can be substituted for other elements, taking into account its increasing cost and existing supply difficulties.
- Once they identified, studies were started, focused on the treatment method with inoculants (respectively on the graphitizing action exercised by La - element typical of the nodular gray iron castings - for which, however, relevant information was identified about its graphitizing capacity, in exteded literature) of experimental gray lamellar cast irons.
- Due not finding in the literature any eloquent data regarding the use of la in the process of inoculation, a complex research project was developed – carried out in three phases, which favored the conduct of complex investigations on the entire process of producing the gray cast (production, processing and analysis of samples) – which included studies a) with view to establishing the viability of adding La in classical inoculating systems and b) assessing the possibility of improving its effects (by adding additional active elements), and subsequently starting c) studies using the SEM method for contouring (by analyzing the formed graphite nuclei) the mechanism of action of the elements introduced into the inoculants.
- Efforts made to obtain the most truthful data and results of the studies (on data obtained), by a) selecting as rigorous as possible the experimental parameters, as well as b) controlling (and respectively checks) of them and of the findings – including by repeating, under the same conditions, several times of the samples casted (10 times, in the thermal analysis; 2 times, in the case of chilling trend analyzes, etc.) and of analyzes (with the intention of applying statistical processing) - carried out within the experimental program.
- Attempts to extend the area of knowledge and application of traditional methods of analysis in the field by applying, in the extended study of cooling curves, their derivative. The new resulting data, being related to the parameters of the chilling tendency as well as to the structural parameters, can contribute to the achievement of a rapid process of classifying the quality of cast iron castings, before the casting itself of them.
- The experiments carried out provided arguments that support the advantages of adding La also in inoculating systems used to treat lamellar graphite cast elements, in case of specific conditions: a) critical solidification conditions, b) high cooling speeds when solidifying or moulds made from materials with high thermal conductivity. The direct consequence of these experiments is to create the conditions for producing an inoculating system with increased efficiency, based on the LaCa-FeSi alloy system.
- Experimental realization of complex systems of synthetic inoculants that have been tested to identify how to associate La in the formation of compounds with role in lamellar graphite germination (LaCaAl-FeSi, ZrLaCaAl-FeSi, LaBaCaAl-FeSi, ZrLaBaCaAl-FeSi, TiZrLaCaAl-FeSi and TiZrFeAl-BaAl), useful in obtaining positive results in the case of requirements to increase the proportion of primary austenite in the structure of cast iron (in order to increase mechanical

properties) or potentiation of the graphitization activity, but produced to a less high degree of recalescence, in order to avoid the formation of shrinkages.

- A novel technique has been provided to investigate the inoculant's mode of action during the solidification of the cast iron, which allowed to obtain a wide range of variation in the concentration of the inoculating element in liquid cast iron – from zero saturation to oversaturation – in this range the evolution of the solidification structure of the cast iron, especially the microinclusions and graphite that precipitated on them, was analyzed. The SEM EDAX analysis has generated a series of new data, which complements or confirms previous knowledge, of which may include:
  - the mechanism (in 3 steps) for the formation of the graphite - S_1 = formation of the oxidic compound; S_2 = formation of the sulfide type compound: (Mn,X)S; and S_3 = graphite formation - is confirmed;
  - within this mechanism, is reaffirmed the major role played by the inclusions of (Mn,X) - of very small dimensions (1-10µ) - in which the primary oxidic nucleus (identified or unidentified) has dimensions between 0.1-3µm;
  - identification, following SEM analyzes, of the distribution of La in the compounds formed during the solidification of the treated cast iron - with the emphasis on how to associate La with other elements of the inoculant and/or cast iron composition - so that (due to the existing relationship between the compositions of the inoculant and the nucleated particles) was determined the wide combining capacity of a multitude of active elements (such as La, Mg, Mn, Si, Al, Zr, Sr, Ca, Ba, O or S);
  - the identification of Mg in the complex sulfidic compound (Mn,X)S – in the center (of an oxidic nature) but also in the body of the compound (so, practically, it can be formed throughout the surface of the compound) – poses (and requires a solution to) the problem of detecting the role that Mg plays in the case of lamellar graphite nucleation (in addition to the similar problem studied – clasicaly – only for nodular graphite cast iron;
  - the detection of arguments that: **1**) demonstrates that La participates in the process of germination of the graphite in all its stages - being detected in all 3 component areas - respectively: *a*) S_1 - formation of oxidic nuclei, *b*) S_2 -precipitation of sulfidic compounds and *c*) S_3 -formation intermediate layers of silicates, on which finally precipit the graphite; **2**) attests the important contribution, in the gray cast iron, of La in the formation process of the lamellar graphite;
  - Confirmation of the formation capacity of compounds of an oxidic nature (aluminosilicates) by detecting – for the first time – a thin layer of alumino-silicate located at the interface between the compound [complex of type (Mn,X)S] and the particle (with nanometer size) of graphite formed, which increases the ability to form the graphite particle (because this compound has a crystallization system identical to graphite), and which contains: O, Si, Al, Ca, Ba, Sr and Mg.

This last observation, respectively the presence at the sulfidic compound-graphite interface, together with O and Si, is the last link of the lamellar graphite germination model proposed following the research conducted by the cast iron team within the Department of Metal Materials Processing and Ecometalurgy. Moreover, it was assumed that there would be an intermediate layer of silicates (having a hexagonal crystallographic lattice) that would facilitate the germination of graphite - with has hexagonal lattice - on the sulfidic (with cubic lattice) supports, but until now it could not be highlighted, perhaps, due to the very small thickness of this layer and therefore the very low concentration of elements. It is possible that the use of the technique of supersaturation in the inoculating element allows the concentration of the elements to increase beyond the detection limit of the SEM, thus managing to highlight such compounds.

V.3. Further research directions

I believe that the complex research program addressed should be continued, first of all, by: A) carrying out the full SEM analyzes, on the whole height of the samples (they are already cut - including the portion located in the sample feeding area - and ready for analysis) In order to study the effect of the inoculant addition at various heights from its source (at the base of the mould) and up to the maximum distance from the inoculating source; and, respectively, b) to carry out analyzes for the rest of the samples, from experimental program III (treated with 7 other inoculant systems).

In addition – and perhaps with a greater potential for achieving more outstanding results – a deepening of SEM-type analyzes could be achieved by using additional investigative techniques which could not be used at this level – due to high costs –, such as: *a*) TEM analysis, to determine the changes in the parameters of the crystalline lattice under the influence of inoculation with different elements; *b*) analysis of the melts in the process of cooling and solidification, using the THERMOCALC software system, to identify the types of compounds that form in the melt but also the moments when they form; *c*) the use of special techniques for extracting microparticles from the structure matrix in order to carry out an individual analysis of them, thus eliminating the disruptive effects of adjacent areas, etc.

SCIENTIFIC WORKS ELABORATED - Eduard-Marius ŞTEFAN

I. DISSEMINATION OF RESULTS OBTAINED IN THE DOCTORAL THESIS

I.1. – Results included in papers published in Journals and Procedings

I.1. I. Riposan, M. Chisamera, S. Stan, **E. Stefan**, C. Hartung. Role of Lanthanum in Graphite Nucleation in Grey Cast Iron. *9th International Symposium on Science and Processing of Cast Iron (SPCI-9)*, November 09-13, 2010, Luxor, Egypt. *Key Engineering Materials-KEM*, Vol 457 [Science and Processing of Cast Iron IX] (2011), pp. 19-24. **Accession Number:**WOS:000291962900003 Trans. Techn. Publications, Switzerland, Editor(s): Nofal A; Waly M, DOI: **10.4028/www.scientific.net/KEM.457.19,** ISSN 1013-9826, online available since 2010/Dec/30 at http:// www.scientific.net/kem [ISSN 1662-9795]. **Indexări: ISI Proceedings**; ISI-Materials Science Citation Index, SCOPUS; INSPEC; Compendex.

I.2. E.M. Stefan, M. Chisamera. Solidification Control by Thermal Analysis of La/Ba Inoculated Grey Cast Iron, *The 9th International Conference on Materials Science and Engineering – BraMat2015*, 4-7 march 2015, Brasov, Romania, *Advanced Materials Research* Vol. 1128, "Advanced Technologies of Materials Processing", (2015) pp 35-43, Trans Tech Publications, Switzerland, doi:10.4028/www.scientific.net/AMR.1128.72. ISBN-13: 978-3-03835-637-0; ISSN: 1662-8985; http://www.ttp.net/978-3-03835-637-0.html; **Recenzii/Indexări:** Index Copernicus Journals Master List www.indexcopernicus.com; Google Scholar scholar.google.com; Inspec (IET, Institution of Engineering Technology) www.theiet.org. SCImago Journal &Country Rank (SJR) www.scimagojr.com; EBSCO www.ebsco.com.

I.3. E. Stefan, I. Riposan**,** M. Chisamera. Application of Thermal Analysis in Solidification Pattern Control of La-Inoculated Grey Cast Irons. *12th European Symposium on Thermal Analysis and Calorimetry (ESTAC12)*, Brasov, Romania, August 2018; *Journal of Thermal Analysis and Calorimetry*, **2019**, Volume 138, Issue 4, pp. 2491-2503. DOI: 10.1007/s10973-019-08714-7; First Online 28 August 2019; Publisher Name Springer International Publishing; Print ISSN 1388-6150; Online ISSN 1588-2926; **Accession Number:** WOS:000499703500013. **IF=2.731 (2019, publicat June 2020)-la publicare. Q2 cotare (**CHEMISTRY, ANALYTICAL/THERMODYNAMICS)

I.4. E. Stefan, M. Chisamera, I. Riposan**.** Chill sensitiveness and thermal analysis parameters relationship in hypo-eutectic, Ca and Ca-La inoculated commercial grey cast irons. *CEEC-TAC5 & Medicta2019 Conference*, August 2019, Roma, Italia. Paper Code IL15; *Journal of Mining and Metallurgy, Section B: Metallurgy*, special issue entitled TPTPMIAC2019, 2020. **Online First** *J. Min. Metall. Sect. B-Metall. DOI: 10.2298/JMMB200108020S*. Vol. 56, Issue 3, 2020, pp. 387-396. **Impact Factor** IF=1.382 (2020) (JCR, 2021), **Accession Number**: WOS: 000603579100012, **Indexări: ISI-WOS Clarivate Analytics** [Metallurgy and Metallurgical Engineering].

I.5. E. Stefan, M. Chisamera, I. Riposan**,** S. Stan. Graphite nucleation sites in commercial grey cast irons. *Materials Today Proceedings*, Article reference MATPR19627, DOI: https://doi.org/10.1016/j.matpr.2020.11.09, Received 3 Sep 2020, Accepted 2 Nov 2020, On-line 15 Dec 2020, https://www.elsevier.com/locate/issn/2214-7853, ISSN: 2214-7853. Published 2021, Volume 45, pp.4091-4095, Special Issue 51 Part 5. **Accession Number:** WOS: 000655645500001. **Indexări: ISI-WOS-Conference Proceedings Citation Index**, Scopus, INSPEC. Selection and peer-review under responsibility of the scientific committee of the 8th International Conference on Advanced Materials and Structures - AMS 2020.

I.6. E. Stefan, I. Riposan, M. Chisamera, S. Stan. Lanthanum Role in the Graphite Formation in Gray Cast Irons. *Minerals***2020**, *10*, 1146 (15 pages); doi:10.3390/min10121146. Received: 14.10.2020; Accepted: 17.12.2020. Published: 21 December 2020. **Section:** Crystallography and Physical Chemistry of Minerals (https://www.mdpi.com/journal/minerals/sections/Crystallography_Physical_Chemistry), eISSN 2075-163X, **Special Issue:** ***Crystallization and Growth of Graphite (https://www.mdpi.com/journal/minerals/special_issues/CGG).*** **Web of Science Core Collection**: Science

Citation Index Expanded, **Accesion Number:** WOS:000602431100001. **Additional Web of Science Indexes**: Current Contents Physical, Chemical & Earth Sciences | Essential Science Indicators. **IF=2.38** (2019, publicat June 2020)-la publicare**. JCR** category rank: 11/30 **(Q2)** in 'Mineralogy'; 6/21 **(Q2)** in 'Mining & Mineral Processing'

I.2. Results included in presentations at international conferences

I.7. I. Riposan, M. Chisamera, **E. Stefan**, S. Stan. Lamellar Graphite versus Nodular Graphite Formation in Commercial Cast Irons - new data, *7th International Conference on Materials Science and Technologies-RoMat 2020*, 26-27 November 2020, Bucharest, Romania, [Invited Lecture I.1].

I.8. I. Riposan, M. Chisamera, **E. Stefan**, S. Stan. Graphite formation in commercial grey cast iron – new data. The 12th ECI (European Cast Iron) Meeting, Kraków, Poland, April 2021. [CD-Proceedings].

I.9. M. Chisamera, **E. Stefan**, I. Riposan, S. Stan. New data on the graphite nucleation sites in commercial grey cast irons. The 61th Internationl Foundry Conference, 15th – 17th of September 2021, Portoroz, Slovenia. Plenary Invited Lecture. [CD-Proceedings]

I.10. I. Riposan, M. Chisamera, **E. Stefan**, S. Stan. Lamellar Graphite versus Nodular Graphite Formation in Commercial Cast Irons. SPCI-XII – International Symposium on the Science and Processsing of Cast Iron, Muroran-Hokaido, Japan, 09-12.11.2021, Paper No. 21. [CD-Proceedings]

II. WORKS / ACTIVITIES THAT HAVE CONTRIBUTED TO THE DESIGN AND FINALIZATION OF THE EXPERIMENTAL PROGRAM

II.1. Thermal analysis – drawing and interpreting cooling curves when solidifying

II.1. M. Chisamera, S. Stan, I. Riposan, **E. Stefan**, G. Costache, Thermal Analysis of Inoculated Grey Cast Irons, *International Scientific Conference UgalMat 2007 Advanced Materials and Technologies*, "Dunarea de Jos" University of Galati, 19-20 october 2007; in *The annals of "Dunarea de Jos" University of Galati*, Fascicle IX, Metallurgy and Materials Science, year XXVI (XXXI), No. 2 , ISSN 1453 – 083X, Galati University Press, november 2008, p. 11-16.

II.2. M. Chisamera, I. Riposan, S. Stan, **E. Stefan**, G. Costache. Thermal analysis control of in-mould and ladle inoculated grey cast irons. *CHINA FOUNDRY*, Vol. 6, No. 2, pp. 145-151, 2009. **Accession Number:**WOS:000266666800010ISSN 1672-6421 [**ISI-Web of Science/Science Citation Index Expanded]. Recenzii/Indexări**: SCOPUS

II.3. S. Stan, M. Chisamera, I. Riposan, **E. Stefan**, L. Neacsu, A. M. Cojocaru, I. Stan, Integrated System of Thermal / Dimensional Analysis for Quality Control of Gray and Ductile Iron Castings Solidification. "Keith Millis" International Ductile Iron Symposium, 23-26 October, 2018, Hilton Head Island, SC, USA, Paper No. 12. *International Journal of Metalcasting* [Inter Metalcast]. DOI: https://doi.org/10.1007/s40962-018-0285-5, First Online 29 November 2018, Publisher Name: Springer International Publishing, Print ISSN1939-5981, Online ISSN 2163-3193; **2019**, Volume 13, Issue 3, pp. 653-665. **Accession Number:** WOS:000471614400020. **IF=1.347 (2019, publicat June 2020)-la publicare**

II.4. S. Stan, M. Chisamera, I. Riposan**, E. Stefan**, L. Neacsu, A. M. Cojocaru, I. Stan. Simultaneous thermal and contraction / expansion analyses of cast iron solidification process. *Journal of Thermal Analysis and Calorimetry*, **2019.** Vol. 138, Issue 4, pp. 2529-2540. DOI: 10.1007/s10973-019-08595-w; Published online: 29 July 2019. **Accession Number**: WOS:000499703500016; ISSN: 1388-6150 ; eISSN: 1588-2926. **IF=2.731 (2019, publicat June 2020)-la publicare. Q2 cotare**

II.5. I. Riposan, S. Stan, M. Chisamera, L. Neacsu, A.M. Cojocaru, **E. Stefan**, I. Stan. Simultaneous thermal and contraction / expansion curves analysis for solidification control of cast irons. *China Foundry*, Vol.17 No.2, March 2020, pp. 96-110. DOI: 10.1007/s41230-020-9147-x, **Published:** MAR 2020, **Document Type:** Review, **Accession Number:** WOS:000529360400003. **IF=0.947** (JCR, published June 2020)

II.6. I Riposan, S Stan, M Chisamera, L Neacsu, A M Cojocaru, **E Stefan** and I Stan. Control of Solidification Pattern of Cast Irons by Simultaneous Thermal and Contraction / Expansion Analysis. *IOP Conference Series: Materials Science, and Engineering* 529 (2019) 012016 (6 pagini) DOI: 10.1088/1757-899x/1/012016. To cite this article: I Riposan et al. 2019 IOP Conf. Ser.: Mater. Sci. Eng. 529 012016. **Accession Number:** WOS: 000561759900016

II.7. I. Riposan, S. Stan, M. Chisamera, A. M. Cojocaru, L. Neacsu, **E. Stefan**, I. Stan. Connection of the shrinkage sensitiveness of iron castings with solidification expansion/contraction and cooling curves data. *59th International Foundry Conference & World Foundry Technical Forum*, 17.09-20.09.2019, Portoroz, Slovenia, Invited Lecture [CD-ProceedingsBook]

II.8. I. Riposan, S. Stan, M. Chisamera, A.M. Cojocaru, L. Neacsu, **E. Stefan**, I. Stan, "Thermal & Expansion-Contraction Curves specific parameters: connection to the shrinkage sensitiveness of iron castings," presented at the *9th International Conference on Materials Science & Engineering – UGALMAT-2020*, 08.12-09.12.2020,

Galati, Romania, Invited Plenary Lecture (IPL2). Accessed: May 27, 2021. [Online]. Available at: https://ugalmat.ugal.ro/index.php/en/

II.2. Inoculation [graphitization modification] of cast irons with graphite in the structure

II.9. I. Riposan, **E. Stefan**, S. Stan, N. R. Pana, M. Chisamera. Effects of Inoculation on Structure Characteristics of High Silicon Ductile Cast Irons in Thin Wall Castings. *Metals* 2020, *10*(8), 1091 (15 pages); https://doi.org/10.3390/met10081091 (registering DOI) - 12 Aug 2020. **Impact Factor IF=2.117** (2019) (JCR, June 2020), **Q1 (5/78), Metallurgy and Metallurgical Engineering** (JCR, published June 2020).Received: 23 June 2020 / Revised: 6 August 2020 / Accepted: 9 August 2020 / Published: 12 August 2020. (This article belongs to the Special Issue Thin Wall Iron Castings). **Accession Number:** WOS: 000567267200001

II.3. Use of technological samples to control the solidification of cast irons

II.10. S. Stan, M. Chisamera, I. Riposan, **E. Stefan**, M. Barstow. Solidification Pattern of Un-inoculated and Inoculated Gray Cast Irons in Wedge Test Samples. *AFS Casting Congress*, Orlando, Florida, USA, March 2010, Paper 10-010, ***Transactions of the American Foundry Association (AFS),*** **Vol. 118, pp 295-309, 2010. Accession Number:**WOS:000292750800028[IDS Number: BMA20; ISBN: 978-0-87433-340-4]; **Indexări: ISI Proceedings;** AFS (American Foundry Society) Library, 20100178, SCOPUS.

II.11. I.V. Anton, C. Militaru, **E.M. Stefan**, N. Ivan, M. Chisamera, I. Riposan. Wall Thickness-Solidification Features Correlation of Ductile Iron Castings under Mould Type Influence. UPB Sci. Bull., Series B, Volume 71, No. 4, 2009, pp. 115-126. ISSN 1454-2331 **Recenzii/Indexări: INSPEC; SCOPUS**

II.12. Cristina Militaru, Irina Varvara Anton, **Eduard Stefan**, Nicoleta Ivan. Ductile Iron solidification under mould type and wall thickness influence. *World Technical Forum, International PhD Foundry Conference*, 3rd June 2009, Brno, Czech Republic.

II.13. Cristina Militaru, Irina Varvara Anton, Nicoleta Ivan, Stelian Stan, **Eduard Stefan**, Bogdan Albu, Mihai Chisamera, Iulian Riposan. Graphite shape degeneration under the solidification conditions influence. *Conferința Națională de Turnătorie și Expoziție*, ediția a 20-a, Brașov, 9 – 10 iunie 2010.

II.4. Works presented at workshops

II.14. Eduard-Marius Stefan - Investigations on hypoeutectic grey cast irons inoculated with Lanthanum and Barium – WORKSHOP TEMATIC „Tendințe noi în procesarea materialelor metalice”, Editia a 2-a, 21-22 Martie 2019. București, Romania

II.5. Participation in International Scientific Research Projects/Contracts

II.15. I. Ripoșan, M. Chișamera, S.Stan, P.Toboc, I.V.Anton, **E.M. Ștefan.** RE Inoculants in Low Sulphur Grey Iron. Contract International, Project ELKEM 52155, 2006-2007, UPB/CEMS-ELKEM ASA Foundry Products/Research, Norvegia.

II.16. I. Ripoșan, M. Chișamera, S.Stan, P.Toboc, I.V.Anton, **E.M. Ștefan.** (Ca + Ba) Inoculants in Low Sulphur Grey Iron. Contract International, Project ELKEM 52157, 2006-2007, UPB/CEMS-ELKEM ASA Foundry Products/Research, Norvegia.

II.17. I. Ripoșan, M. Chișamera, S.Stan, P.Toboc, I.V.Anton, **E.M. Ștefan.** SiSiCAR80 Application in Cast Iron Industry. Contract International, Nr.807, 2007, UPB/CEMS - Metalkraft AS, Norvegia.

II.18. I. Ripoșan, M. Chișamera, S.Stan, P.Toboc, I.V.Anton, **E.M. Ștefan.** Representative Inoculants Comparison-Low and Medium Sulphur Grey Irons. Contract International, Project ELKEM 5215552127/2008-1, 2008-2010, UPB/CEMS-ELKEM ASA Foundry Products/Research, Norvegia.

II.6. Participation in National Scientific Research Projects/Contracts

II.19. I. Riposan, M. Chisamera, S. Stan, **E.M. Stefan**. PN-II-IN-CI-2012-1-0067, Optimizarea procesului de prelevare a probelor de fontă în vederea analizei spectrale, SC SPECTRO SERVICE ROMANIA SRL / UNIVERSITATEA POLITEHNICA DIN BUCUREȘTI -CENTRUL DE CERCETARE ȘI EXPERTIZARE MATERIALE SPECIALE (CEMS)

II.20. S. Stan, I. Riposan, M. Chisamera, **E.M. Stefan** et all. “Sistem Integrat de Analiză termică / Dimensională (ISTAQ) destinat controlului topiturilor metalice și solidificării pieselor turnate” ” (cod PN-III-P2-2.1-PED-2016-1793, acronim ISTAQ),18 luni (2017-2018), Contract 115PED/2017

BIBLIOGRAPHY

[14] S.C. Stan, M. Chisamera, I. Riposan, High Performance Cast Iron Matrix Composite - Solidification Pattern Control by Thermal Analysis, in Proceedings M2D2017, presented at the 7th International Conference Mechanics and materials in design, Albufeira, Portugal: INEGI/FEUP, 2017. pg. 2

[20] About Elkem, accesed online la 2022.04.15, https://www.elkem.com/about-elkem/

[22] B. Simpson, History of the metal casting industry, American Foundrymen's Society, 2nd Edition, 1969.

[23] L. Sofroni, I. Riposan, V. Brabie, M. Chişamera, Turnarea Fontei, Editura Didactică şi Pedagogică, Bucureşti, 1981. pg. 364

[24] T.E. Prucha, D. Twarog, R.W. Monroe, "History and Trends of Metal Casting", în Casting, ASM Handbook, Volume 15, 2nd ed, 2008. pg. 3

[27] D.M. Ştefănescu, Ştiinţa şi ingineria solidificării piesei turnate, Ed. AGIR, Bucureşti, 2007.

[28] I. Baker, Fifty Materials That Make the World, Springer International Publishing, 2018

[29] G. Bhutada, All the Metals We Mine Each Year, in One Visualization', World Economic Forum, 2021.10.14, accesat online la 2022.04.14, https://www.weforum.org/agenda/2021/10/all-tonnes-metals-ores-mined-in-one-year/

[30] N. LePan, All the World's Metals and Minerals in One Visualization, Visual Capitalist, 2020.03.01, accesat online la 2022.04.14 https://www.visualcapitalist.com/all-the-worlds-metals-and-minerals-in-one-visualization

[31] Census of World Casting Production, în rev. Modern Casting, no. 12, Dec. 2021. accesat online la 2021.12.27 https://www.qgdigitalpublishing.com/publication/?i=730025&view=issueViewer&pp=1

[32] A.M. Musledin, Industry report from Romania, în WFO Global Foundry Report, 2020. https://www.thewfo.com/wfo-global-foundry-report-2020

[33] D.M. Ştefănescu, The Meritocratic Ascendance of Cast Iron: From Magic to Virtual Cast Iron (Hoyt Lecture at the 123rd Metalcasting Congress and Published in 2019 AFS Transactions), International Journal of Metalcasting, vol. 13, no. 4, 2019.

[34] D. M. Ştefănescu, R. Ruxanda, Lightweight Iron Castings – Can they Replace Aluminum Castings?, în Proceedings of the 65th World Foundry Congress, Gyeongju, Korea, Oct. 2002. pg. 71–77.

[35] D. Oman, "Hoyt Memorial Lecture—Changing Perceptions: The Need for an 'Unbalanced Force,' International Journal of Metalcasting vol. 12, 2018

[46] M. Chişamera, I. Ripoşan, L. Sofroni, S. Stan, Fabricarea pieselor din fontă prin turnare, în Tratat de Ştiinţa şi Ingineria Materialelor Metalice, vol. 4, Ed. Tehnică, 2010. pg. 587

[47] I.Riposan, M. Chisamera, S. Stan, Enhanced Quality in Electric Melt Grey Cast Irons. ISIJ Int., vol. 53, 2013. pg. 1683–1695

[48] K. Rathod, A. Sharma, S. Prakash, Energy-Efficient Melting Technologies in Foundry Industry. Indian foundry journal, no 62, 2016. pg. 39–46.

[49] E.M. Stefan, I. Riposan, M. Chisamera, Application of thermal analysis in solidification pattern control of La-inoculated grey cast irons, Journal of Thermal Analysis and Calorimetry, vol. 138, no. 4, aug.2019. pg. 2491–2503.

[55] S. Katz, Foundry Processes: Their Chemistry and Physics, Springer Science & Business Media, 2012.

[64] C. Hartung, D. White, K. Copi, M. Liptak, R. Logan, The Continuing Evolution of MgFeSi Treatments for Ductile and CG Irons. Inter Metalcast, no. 8, 2014. pg. 7–15

[65] C.S., Kanetkar, H.H. Cornell, D.M. Stefanescu, The Influence of Some Rare Earth (Ce-La-Pr-Nd) and Yttrium in the Magnesium Ferrosilicon Alloy on the Structure of Spheroidal Graphite Cast Iron, AFS Proceedings 1984, AFS Transactions, Paper 84-92.

[66] Y. Zhang, G. Han, M. Jürisoo, The geopolitics of China's rare earths: a glimpse of things to come in a resource-scarce world?, Stockholm Environment Institute, 2014.

[67] D. Sheng, J. Liu, Cast Irons Containing Rare Earths, Tsinghua University Academic Press, China, 2009.

[68] I. Ripoşan, M. Chişamera, S.Stan, P.Toboc, I.V.Anton, E.M. Ştefan. (Ca + Ba) Inoculants in Low Sulphur Grey Iron. Contract International, Project ELKEM 52157, 2006-2007, UPB/CEMS-ELKEM ASA Foundry Products/Research, Norvegia.

[69] I. Ripoşan, M. Chişamera, S.Stan, P.Toboc, I.V.Anton, E.M. Ştefan. RE Inoculants in Low Sulphur Grey Iron. Contract International, Project ELKEM 52155, 2006-2007, UPB/CEMS-ELKEM ASA Foundry Products/Research, Norvegia.

[70] I. Ripoşan, M. Chişamera, S.Stan, P.Toboc, I.V.Anton, E.M. Ştefan. SiSiCAR80 Application in Cast Iron Industry. Contract International, Nr.807, 2007, UPB/CEMS - Metalkraft AS, Norvegia.

[71] I. Ripoşan, M. Chişamera, S.Stan, P.Toboc, I.V.Anton, E.M. Ştefan. Representative Inoculants Comparison Low and Medium Sulphur Grey Irons. Contract International, Project ELKEM 5215552127/2008-1, 2008-2010, UPB/CEMS-ELKEM ASA Foundry Products/Research, Norvegia.

[72] I. Ripoşan, M. Chişamera, S.Stan, Effects of Al, Zr and Ti in the nucleation process form grey Iron - Contract International, Project No.1, 2003, ELKEM Norway -UPB/CEMS.

[73] I. Ripoşan, M. Chişamera, S.Stan, Effects of Rare Earth in nucleation of (low sulphur) Grey iron, Contract International, Project No.2, 2005, ELKEM Norway -UPB/CEMS.

[74] I. V. Anton, C. B. Albu, I. Riposan,. Structure Characteristics of Low Sulphur, Ce/Ba/Ca Inoculated Grey Irons, in: International Conference on Advanced Materials and Structures. Advanced Materials and Structures IV, vol. 188, 2012, Diffusion and Defect Data., Pt. B. Solid State Phenomena

[75] I. Riposan, M. Chisamera, S. Stan, E. Stefan, C. Hartung. Role of Lanthanum in Graphite Nucleation in Grey Cast Iron. Key Engineering Materials-KEM, Vol 457, Science and Processing of Cast Iron IX , 2011. pg. 19-24

[77] P. Barrera, Rare Earths Outlook 2021 | INN | REE Magnet Supply to Remain Tight. Investing News Network, accesat online la 2021.05.28, https://investingnews.com/daily/resource-investing/critical-metals-investing/rare-earth-investing/rare-earth-outlook/

[84] *** Rare-Earth-Metals Price Chart,China Rare-Earth-Metals Price Today-Shanghai Metals Market, accesat online la 2022.01.13, https://price.metal.com/Rare-Earth-Metals
[85] Black RE-Friday; US RE-Dependency; EU-Commission Goes Nuclear; Apple Buy Rare Earths; Critical Materials Corner; E-Tech De-Risked?; Deposit Flipping; Bitcoin meets Rare Earths?; Ucore, DEFN, et al. The Rare Earth Observer, accesat online la 2022.03.11, https://treo.substack.com/p/black-re-friday-us-re-dependency
[86] I. Ripoşan, M. Chişamera, L. Sofroni, S. Stan, Fonte cu grafit în structură, în Tratat de Ştiinta şi Ingineria Materialelor Metalice, vol. 3, Editura AGIR, 2009. pg. 463-580
[87] O. Rilwan, High Strength Solution-Strengthened Ferritic Ductile Cast Iron, Master Thesis, Aalto University School of Engineering, Espoo, Finland, 2015.
[90] *** Total Media, acc online la 2022.04.01 https://www.totalmateria.com/page.aspx?ID=Physical&LN=RO
[91] Cast Metals Handbook, American Foundrymen's Society, Des Plaines, Illinois, SUA, ed. 4, 1957
[93] J.R. Davis, ASM Specialty Handbook - Cast Irons, ASM International, 1996
[95] J. P. Scholes, The Selection and use of Cast Irons - Engineering Design Guides, Oxford University Press, vol.31, 1979
[96] E. Plénard, The Elastic Behavior of Cast Iron, în Recent Research on Cast Iron, H.D. Merchant, Ed., Gordon and Breach Sci. Publ., New York, 1968, pg. 707–792
[98] I. Stan, D. Anca, S. Stan, I. Riposan, Solidification Pattern of Si-Alloyed, Inoculated Ductile Cast Irons, Evaluated by Thermal Analysis. Metals, issue 11, 2021. pg. 846.
[99] F. Neumann, The Influence of Additional Elements on the Physico-Chemical Behavior of Carbon in Carbon Saturated Molten Iron, Recent Research on Cast Iron, H.D. Merchant, Ed., Gordon and Breach, 1968. pg. 659
[102] I. Riposan, M. Chisamera. Tehnologia Elaborării şi Turnării Fontei. Ed. Did. şi Ped., Bucureşti, 1981
[103] T. D. West, Metallurgy Of Cast Iron - A complete exposition of the processes involved in its treatment, chemically and physically, from the blast furnace through the foundry to the testing machine., 7th ed., 1902. The Cleveland Printing and Publishing Co., Publishers, Cleveland, Ohio, U.S.A.
[104] O. F. Hudson, Guy D. Bengough, Iron and Steel. An introductory text-book for engineers and metalurgists. With a section on corrosion. Constable & Company Limited, London, 10 & 12 Orange Street Leicester Square WC 2, 1921.
[105] A. Muumbo, H. Nomura, M. Takita, Casting of semi-solid cast iron slurry using combination of cooling slope and pressurisation. International Journal of Cast Metals Research, vol. 17, 2004. pg. 39-46
[107] M. Srinivasan, Science and technology of casting processes. IntechOpen Limited, London, 2012, p. 364
[108] J. Campbell, Complete Casting Handbook, Second Edition, 2nd ed.; Elsevier, 2015.
[109] J. Walker, E. Harris, C. Lynagh, et al. 3D Printed Smart Molds for Sand Casting. Inter Metalcast vol. 12, 2018, pg. 785–796
[110] D.M. Stefanescu, Production of Gray Iron Castings, in: Cast Iron Science and Technology. ASM International, 2017.
[111] *** Best Available Techniques in the Smitheries and Foundries Industry, în Integrated Pollution Prevention and Control Report Reference Document, 2005, accesat online la 2019.10.10 https://eippcb.jrc.ec.europa.eu/sites/default/files/2019-11/sf_bref_0505_1.pdf.
[114] C.S. Stan, Studii şi cercetări privind influenţa aluminiului rezidual asupra grafitizării fontelor cenuşii, Teza doctorat, UPB, 2014.
[115] I. Riposan, M. Chisamera, S. Stan, D. White, I. Complex (Mn, X) S compounds-major sites for graphite nucleation in grey cast iron. China Foundry, vol. 6, 2009. pg. 352–358.
[116] S. Vacu, E. Berceanu, P.S. Niţă, M. Nicolae; Metalurgia Feroaliajelor, EDP, Bucureşti, 1980
[117] M. Chisamera, I. Riposan, S. Stan, C. Ecob, G. Grasmo, D. Wilkinson, Preconditioning of Electrically Melted Grey Cast Irons. Presented at the AFS 2009 International Iron Melting Conference, Orlando, Florida, USA, 2009. p. 35.
[120] I. Ripoşan, M. Chişamera, S. Stan, T. Skaland. A New Approach on the Graphite Nucleation Mechanism in Grey Irons. Proceedings of the American Foundry Society Cast Iron Inoculation Conference, Sept. 29-30, 2005, Schaumburg, IL, USA,
[121] I. Riposan, M.Chisamera, S. Stan, Inoculation Project –Gray Iron– ELKEM Norvegia, project no. 99743/1999
[123] L.F. Mondolfo, Grain Refinement in Casting and Welds, The Metallurgical Society, 1983, p.3
[127] I. Riposan M. Chisamera, S. Stan, White, D. and Hartung, C. How to Control Graphite Nucleation and Type-A Graphite Formation in Gray Cast Iron. 115th AFS Casting Congress, Schaumburg, IL, USA, April 2011, Panel Paper 11-131.
[130] I. Riposan, T. Skaland, Modification and Inoculation of Cast Iron, ASM Handbook Cast Iron Science and Technology, ASM International, 2017. pg. 160–176
[131] S.O. Olsen, T. Skaland, Inoculation of grey and ductile iron - a comparison of nucleation sites and some pratical advises, 66th World Foundry Congress Proceedings, Ed. TÜDÖKSAD, Istanbul, Turkey, 2004. pg. 891–902.
[133] I. Riposan, M. Chisamera, S. Stan, P. Toboc, C. Ecob, G. Grasmo, D. Wilkinson, Complex Treatment of Electrically Melted Grey Cast Irons. Presented at the 7th Arab Foundry Symposium - ARABCAST-2008, Arabian Foundry Congress, Sharm El-Sheikh, Egypt.
[136] I. Riposan, M. Chisamera, S. Stan, T. Skaland, Graphite Nucleants (Microinclusions) Characterization in Ca/Sr Inoculated Grey Irons. International Journal of Cast Metal Research, Vol. 16, No. 1-3, 2003. pg.105-111.
[137] M. Chisamera, I. Riposan, S. Stan, T. Skaland, Effects of Calcium and Strontium Inoculation on Undercooling, Chill and Microstructure in Grey Irons of Varying Sulphur and Oxygen Contents. 64th World Foundry Congress, Paris, France, 2000.
[138] I. Riposan, M. Chisamera, S. Stan, T. Skaland, M.I. Onsoien, Analyses of Possible Nucleation Sites in Ca/Sr Overinoculated Grey Irons. AFS Transactions, Vol. 109, 2001. pg. 1151-1162.
[139] M. Chisamera, I. Riposan, S. Stan, White, D. and Grasmo, G. Graphite Nucleation Control in Grey Cast Iron. International Journal of Cast Metals Research, Vol. 21, Issues 1-4, 2008. pg. 39-44
[140] I. Riposan, M. Chisamera, S. Stan, C. Hartung, D. White, Three-Stage Model for the Nucleation of Graphite in Grey Cast Iron. Materials Science &Technology, Vol. 26, Issue 12, 2010. pg. 1439-1447.

[179] D.E. Krause, "Gray Iron—A Unique Engineering Material", în Gray, Ductile, and Malleable Iron Castings—Current Capabilities, H.J. Heine (ed.), ASTM STP 455, American Society for Testing and Materials, Philadelphia, 1969, pp. 3–28

[180] I. Riposan, V. Uta, S. Stan, R.L. Naro, D.C. Williams, The effect of minimizing Rare Earth Elements during nodulizing treatments and the inoculation of ductile iron, AFS Proceedings, Paper 14-004, 2014. pg.1-18

[181] I. Riposan, M. Chisamera, V. Uta, S. Stan, R. Naro, D. Williams, The importance of Rare Earth contribution from nodulizing alloys and their subsequent effect on the inoculation of Ductile Iron, International Journal of Metalcasting, vol. 8, no. 2, 2014.

[183] *** - DigiLance IV Memory - user manual, 2006

[184] K. Toedter; H.-G. Joosten, Improved Determination of Carbon in Cast Iron, at 71st World Foundry Congress (WFC 2014) Advanced Sustainable Foundry; Curran Associates, Inc. 2015, Bilbao, Spain

[185] *** Echivalența inoculanților utilizați la tratarea fontelor; în Note de curs: Elaborarea și turnarea aliajelor feroase. Fontele, 2005

[186] F.M. Ciprian, Fonte modificate cu grafit vermicular/compact, Teză doctorat, UPB, 2015

[187] L. Harcea, Cercetări privind influența sistemului inoculant asupra eficienței modificării fontelor cu grafit lamelar, Teza doctorat, UPB, 2013

[188] E.M. Stefan, M. Chisamera, Solidification Control by Thermal Analysis of La/Ba Inoculated Grey Cast Iron, Advanced Material Research, vol. 1128, 2015. pg. 35–43

[189] D.M. Stefanescu, R. Suarez, S.B. Kim, 90 years of thermal analysis as a control tool in the melting of cast iron, China Foundry, vol. 17, no. 2, 2020. pg. 69–84

[192] I. Ripoșan, M.Chișamera, S.Stan, P. Toboc, G.Grasmo, D.White, C. Ecob, C.Hartung, Benefits of residual aluminum in ductile iron, Journal of Materials Engineering and performance, vol. 20, no. 1, 2011. pg. 57-64 <DOI: 10.1007/s11665-010-9640-2>

[194] *** ATAS - Users Guide v5: Chapter 6. Adapting ATAS

[197] ECOMET, accesat online la 2022.02.11 http://www.ecomet.pub.ro/infrastructura/expertize-mecano-metalurgice/microscop-electronic-cu-baleiaj/

[200] *** Grey Cast irons - Classification; International Standard ISO 185/2005

[203] I.V. Anton (Balkan), Cercetări privind capacitatea inoculantă a Ceriului în fontele cenușii, Teză doctorat, UPB, 2020

[204] G. Feng, L. Qin, Study on Interaction between Lanthanum and Phosphor in Purity Steel. Journal of Rare Earths, vol. 1, Supplement 1, 2006. pg. 409–412